R-66

ASTROGEOLOGIC STUDIES

ANNUAL PROGRESS REPORT

July 1, 1963 to July 1, 1964

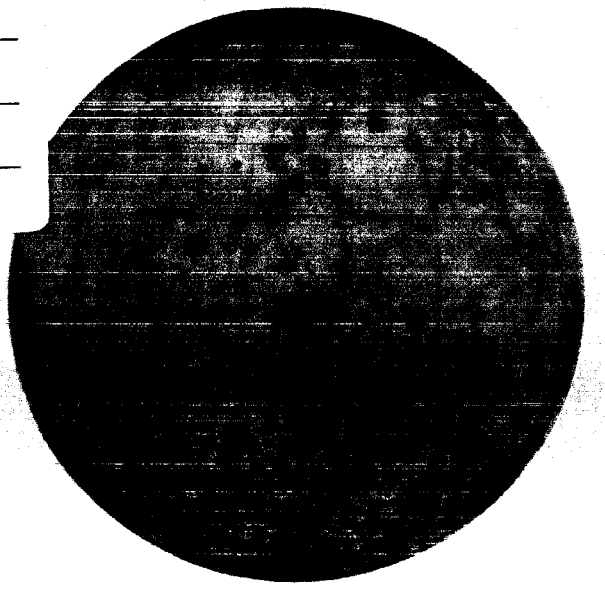

PART A

LUNAR AND PLANETARY INVESTIGATIONS

DEPARTMENT OF THE INTERIOR

UNITED STATES GEOLOGICAL SURVEY

ASTROGEOLOGIC STUDIES

ANNUAL PROGRESS REPORT

July 1, 1963 to

July 1, 1964

PART A: LUNAR AND PLANETARY INVESTIGATIONS

November 1964

This report concerns work done on behalf of the National Aeronautics and Space Administration.

DEPARTMENT OF THE INTERIOR
UNITED STATES GEOLOGICAL SURVEY

CONTENTS

Page

PART A--LUNAR AND PLANETARY INVESTIGATIONS

Introduction

Major structural features of the Mare Vaporum quadrangle, by D. E. Wilhelms---------- 1

Introduction---------- 1

Stratigraphy---------- 2

Structure---------- 6

Conclusions---------- 14

References---------- 15

Stratigraphy of the terra part of the Theophilus quadrangle, by D. J. Milton---------- 17

Introduction---------- 17

Pre-Imbrian materials---------- 18

Fra Mauro Formation(?)---------- 20

Imbrian plains-forming unit---------- 21

Imbrian(?) plateau-forming unit---------- 25

References---------- 27

Progress in geological mapping of the Grimaldi quadrangle, by J. F. McCauley---------- 28

Introduction---------- 28

CONTENTS--Continued

	Page
Stratigraphy	28
Humorum Group and Cordillera Group	28
Procellarum Group and dark mare material	30
Structure	31
References	32
Trajectories of objects producing Copernicus ray material on the crater Eratosthenes, by M. H. Carr	33
References	41
A possible volcanic complex near the Harbinger Mountains of the Moon, by H. J. Moore	42
Introduction	42
Characteristics of the complex	42
Possible terrestrial analogs	48
Conclusions	50
References	51
Impact-induced volcanism, by M. H. Carr	52
Introduction	52
Distribution of heat produced by impact	52
Thermal history of craters after impact	56
Effect of impact on thermal history of Mare Imbrium	63

CONTENTS--Continued

Page

Conclusions---------- 64

References---------- 64

Infrared emission from the illuminated Moon,

by Kenneth Watson---------- 67

Introduction---------- 67

Infrared emission of the illuminated Moon---------- 67

Conclusions---------- 76

References---------- 78

A systematic program of photoelectric and photo-

graphic photometry of the Moon, by H. A. Pohn---------- 79

References---------- 83

Initiation of a program of lunar polarimetry,

by D. E. Wilhelms---------- 84

Description of an extensive hummocky deposit around the Humorum

Basin, by S. R. Titley and R. E. Eggleton---------- 85

References---------- 89

Stratigraphic and structural relationships in the

Pitatus Quadrangle and adjacent parts of the Moon,

by S. R. Titley---------- 90

Introduction---------- 90

Regional setting---------- 90

Stratigraphy---------- 91

Pre-Humorum Group strata---------- 91

CONTENTS--Continued

Page

Humorum Group---------- 92

Imbrian System---------- 94

Eratosthenian and Copernican Systems---------- 97

Stucture---------- 98

Summary---------- 100

References---------- 101

A preliminary report on the role of isostatic rebound in the geologic development of the lunar crater Ptolemaeus, by Harold Masursky---------- 102

Introduction---------- 102

Geology of Ptolemaeus---------- 105

Origin of craters of the Copernicus type---------- 106

Forms of large terrestrial impact craters---------- 109

Forms of large lunar craters---------- 114

Comparison of Ptolemaeus with other craters---------- 120

Theory of viscous flow and isostatic rebound of craters---------- 125

Geologic history of Ptolemaeus---------- 128

References---------- 131

INTRODUCTION

This Annual Report is the fifth of a series describing the results of research conducted by the U.S. Geological Survey on behalf of the National Aeronautics and Space Administration. This report, which covers the period July 1, 1963 to July 1, 1964, is in three volumes corresponding to three main areas of research: Part A, Lunar and Planetary Investigations; Part B, Crater and Solid State Investigations; and Part C, Cosmic Chemistry and Petrology; and a map supplement. An additional volume presents in abstract form summaries of the papers in Parts A, B, and C.

The major long-range objectives of the astrogeologic studies program are to determine and map the stratigraphy and structure of the Moon's crust, to work out from these the sequence of events that led to the present condition of the Moon's surface, and to determine the processes by which these events took place. Work being carried out that leads toward these objectives includes a program of lunar geologic mapping; studies on the discrimination of geologic materials on the lunar surface by their photometric, polarimetric, and infrared properties; field studies of structures of impact, explosive, and volcanic origin; laboratory studies on the behavior of rocks and minerals subjected to shock; and study of the chemical, petrographic and physical properties of materials of possible lunar origin and the development of special techniques for their analysis.

16265

Part A: Lunar and Planetary Investigations contains (with the map supplement), the preliminary results of detailed geologic mapping on a 1:1,000,000 scale of five new quadrangles in the equatorial belt of the Moon. Several major stratigraphic units in the Imbrian and pre-Imbrian systems are described by the authors who have studied these quadrangles. Four papers discuss problems of origin and evolution of various types of craters and features associated with the craters such as rilles and rays. As a part of the lunar geologic investigations, detailed studies of the infrared emission and reflected visible radiation from the Moon are in progress; a description of a systematic program of photoelectric and photographic photometry and the relation of the visible lunar photometric function to the infrared emission are given in this report. Author

Part B: Crater Investigations contains the results of field and laboratory studies of shock and crater phenomenology. The effect of shock on rock materials forms the subject of four reports: (1) the shock wave synthesis of stishovite, (2) the physical properties of shock-formed plagioclase from a meteorite, (3) some characteristics of natural glasses and high pressure phases that serve as evidence for their origin by meteorite impact, and (4) the effect of shock on the radiogenic argon content of granite. One report concerns the shock equation of state on two rocks from Meteor Crater, Arizona. Two reports deal with experimental craters: one is concerned with a field study of craters formed by missile

impact and the other with a study of craters formed in porous-cohesive targets by hypervelocity projectiles. Work on three naturally formed craters is reported. This includes a new topographic map of Meteor Crater, Arizona, made to serve as a base for the geologic work; a geologic study of a meteorite crater and associated rays of ejecta at Henbury, Australia; and field and laboratory studies of the Flynn Creek structure, Tennessee.

Part C: Cosmic Chemistry and Petrology includes reports on aerodynamic features, geologic occurrences, chemical composition and metallic spherules of tektites, methods of chemical analysis of tektites and other extraterrestrial material, and the luminescence of achondritic meteorites.

MAJOR STRUCTURAL FEATURES OF THE MARE VAPORUM QUADRANGLE

by D. E. Wilhelms

Introduction

This paper describes the major structural elements of the Mare Vaporum quadrangle and outlines their relation to the Mare Imbrium basin. Some stratigraphic problems are pointed out, but the stratigraphy is discussed only as it bears upon structure. To date, only a limited amount of telescope time has been available for study of the geology of the Mare Vaporum quadrangle, and this preliminary report suggests lines to be followed in further work. The gross structural pattern in the vicinity of the Mare Imbrium basin has been recognized by Hartman and Kuiper (1962) and other workers.

In the Mare Vaporum quadrangle the maria and low terra areas occupy shallow circum-Imbrium troughs; the position and details of form of the maria are also partially controlled by Imbrian sculpture and by older structures associated with the Mare Serenitatis basin. Other structural features appear to be unrelated to either the Mare Imbrium or Mare Serenitatis basins.

Stratigraphy

All stratigraphic units mapped so far in the Mare Vaporum quadrangle have been previously recognized and described in other nearby quadrangles (Shoemaker, 1962; Hackman, 1963 and 1964; Eggleton, 1964). The Imbrian, Eratosthenian, and Copernican systems are all represented in the quadrangle (see Map Supplement). Only problems in mapping the Fra Mauro Formation of Imbrian age and in identification of certain smooth materials on the terra area, however, are discussed in this report.

Fra Mauro Formation.--Most of the terra area of the Mare Vaporum quadrangle has been mapped as Fra Mauro Formation, the name given to a regional deposit that partly surrounds the Mare Imbrium basin. The Fra Mauro Formation is the oldest unit recognized in the quadrangle. The formation has been divided by Eggleton (1964, p. 51) into a hummocky and a smooth facies in the type area in the Montes Riphaeus quadrangle, about 200 km west of the nearest exposures in the Mare Vaporum quadrangle. Although the exposures are not continuous between the type area and the Mare Vaporum quadrangle, close similarity in the topographic characteristics of the formation in the type area and the quadrangle studied leaves little doubt that the unit mapped is the Fra Mauro Formation. Most of the description of the Fra Mauro given by Eggleton applies to the exposures in the Mare Vaporum quadrangle, and only highlights and observations peculiar to this area are given here.

In the Mare Vaporum quadrangle, both the hummocky and the smooth facies have been recognized--the hummocky facies in the northwest part and the smooth facies in the southeast. The contact between the two facies is a fairly abrupt transition in most places. Northwest of the contact, hummocks intrinsic to the Fra Mauro are resolved on good photographs[1/], while southeast of it most of the surface on the Fra Mauro is smooth in detail even when observed telescopically. The hummocky facies is subdivided into dark and light units; the dark hummocky facies is more extensive and more prominent in the Mare Vaporum quadrangle than in any other region of the Moon.

Much of the topography of the hummocky facies of the Fra Mauro, except in the Apennine Mountains, consists of subdued, rounded hummocks or hills which overlap and coalesce in somewhat sinuous, low, crudely braided ridges 1 to 3 km broad and 3 to 30 km long. These ridges lie roughly radial to Mare Imbrium. The braided topography is better developed over much of the Mare Vaporum quadrangle, especially in the dark hummocky facies, than in the type area. There, it has been interpreted

---

1/ Since the compilation of the map, several areas 10 to 20 km across within the mapped hummocky Fra Mauro have been observed telescopically to be smooth. These may be related to the Fra Mauro, or may be a separate younger unit.

as being partially due to scarps and ridges on the surface on which the Fra Mauro is deposited (Eggleton, 1964, p. 52), but I interpret the sinuosity of the braids to indicate that the ridges in the Mare Vaporum quadrangle are intrinsic to the Fra Mauro; the braided topography is a scaled-up analog of the outer subradial-ridge topography of crater-rim material around large craters of Eratosthenian and Copernican age. It is difficult, however, to discriminate intrinsic depositional topography of the Fra Mauro from topographic relief due to Imbrian sculpture which everywhere underlies the Fra Mauro. Deposition of the hummocky Fra Mauro apparently smoothed out initially rough terrain by filling depressions and roughened initially smooth terrain by the superposition of the hummocky material. The result is a muted, fairly uniform terrain.

The intrinsic topography of the Fra Mauro is most easily recognized on the relatively gentle terra surfaces south and east of Sinus Aestuum; it can also be observed in the structurally complex and rugged Apennine Mountains. Here, however, it consists of nearly equidimensional clumps of hummocks rather than strung-out braids. Fra Mauro and the underlying structure together give the mountains a blocky appearance with fewer linear ridges and grooves than the terrain farther from the center of the Mare Imbrium basin. This also appears analogous with typical crater rim material.

The topography of the smooth Fra Mauro facies is muted in the same

manner as that of the hummocky facies: ridges in this facies typically have a smooth whale-back or drumloid form, and troughs are shallow and smooth. Pre-Imbrian craters overlain by smooth Fra Mauro, such as Pallas and Murchison, have neither sharp topographic forms like Copernican and Eratosthenian craters nor large numbers of superimposed small craters like pre-Imbrian craters far distant from Mare Imbrium. The smoothing effect of the Fra Mauro is less pronounced southeast of Sinus Medii than in the terra adjacent to the hummocky facies.

I believe that the hypothesis that the hummocky facies of the Fra Mauro Formation is a thick and extensive depositional blanket of material ejected from the Mare Imbrium basin in general fits the observed texture and distribution of the formation so well that it need no longer be doubted. The nature of the smooth facies of the Fra Mauro, however, is still in doubt. It is possible that pre-Imbrian rocks are exposed in some areas now mapped as Fra Mauro.

Smooth materials of terra areas.--Several patches within the terra areas have been labeled Ipm? on the geologic map. On photographs, the patches appear smooth and dark, but not all of them have been carefully studied telescopically and it is possible that at least some of these patches are not mare material of the Procellarum Group of Imbrian age. Smooth materials of probable pre-Procellarum age have been observed in nearly every terra area of the Moon that has been carefully studied.

Like Procellarum mare material, these other mare-like materials fill depressions, especially old craters and troughs concentric with the larger basins. A band of such smooth material southeast of the Mare Vaporum quadrangle has been observed by Milton (1964) and Masursky (oral communication, 1964). Further study is necessary to determine the origin and stratigraphic position of these smooth materials, and pending such study, the questionable units in the Mare Vaporum quadrangle have been only tentatively assigned to the Procellarum Group.

Structure

Much of the structure of the Moon's surface, including many irregular mare depressions, shows a geometrical relation to the large mare basins; both radial and concentric structures have been recognized about most of the basins and about many large craters (Hartmann and Kuiper, 1962; Baldwin, 1963, chap. 16). Radial structures are dominantly expressed by ridges and valleys with abrupt local relief, whereas the concentric structures are principally broad depressions and highs. The Imbrian sculpture, recognized by Gilbert (1893) and discussed by Hartmann (1963) and others, is the best known example of a prominent pattern of ridges and valleys radial to the center of a large basin. This sculpture is an important feature of the terra area of the Mare Vaporum quadrangle (see Map Supplement), but little more can be contributed at this time to its

description and interpretation. Broader major structures arrayed concentrically about the Mare Imbrium basin are also present in the Mare Vaporum quadrangle; these are stressed in the following discussion.

Structures related to the Mare Imbrium basin.--The Mare Imbrium basin, part of which appears in the upper left-hand corner of figure 1, is nearly circular. Its deep inner part lies within an arcuate garland of mountains of pre-mare material protruding through the mare surface (Straight Range, Mt. Pico, etc., and the nameless peaks shown in figure 1), and its outer boundary is a circular arc formed by the inner front of the Apennine and Carpathian Mountains (Hartmann and Kuiper, 1962, plate 12.24). As references for the subsequent discussion, concentric arcs (small circles on the lunar surface) are drawn in figure 1 at 200 km intervals from the center, and radials (great circles on the lunar surface) are drawn at 20° intervals.

The mare material exposed in the Mare Vaporum quadrangle occupies parts of the broad depressions concentric about the Mare Imbrium basin. Major segments of the Procellarum-Group contact in the three principal maria present in the quadrangle--Sinus Medii, Sinus Aestuum, and Mare Vaporum--are roughly parallel either to one of the radials or one of the concentric arcs about the Mare Imbrium basin. I interpret these three depressions which the mare material occupies as shallow troughs with gently sloping flanks; they are unlike the deep circular mare basins. In

Figure 1. Major structures of the Mare Vaporum quadrangle (within heavy outline) and its surroundings.

Rim crest of craters mentioned in text and other main craters. Crater rim materials not shown.

Mare material (Ipm) and Ipm(?)

Non-mare smooth material.

Radials and concentrics to Mare Imbrium basin.

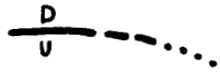

Fault

Crest of anticline

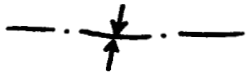

Trough of syncline

Grid from Air Force Aeronautical Chart and Information Center (ACIC) mosaic LEM-1.

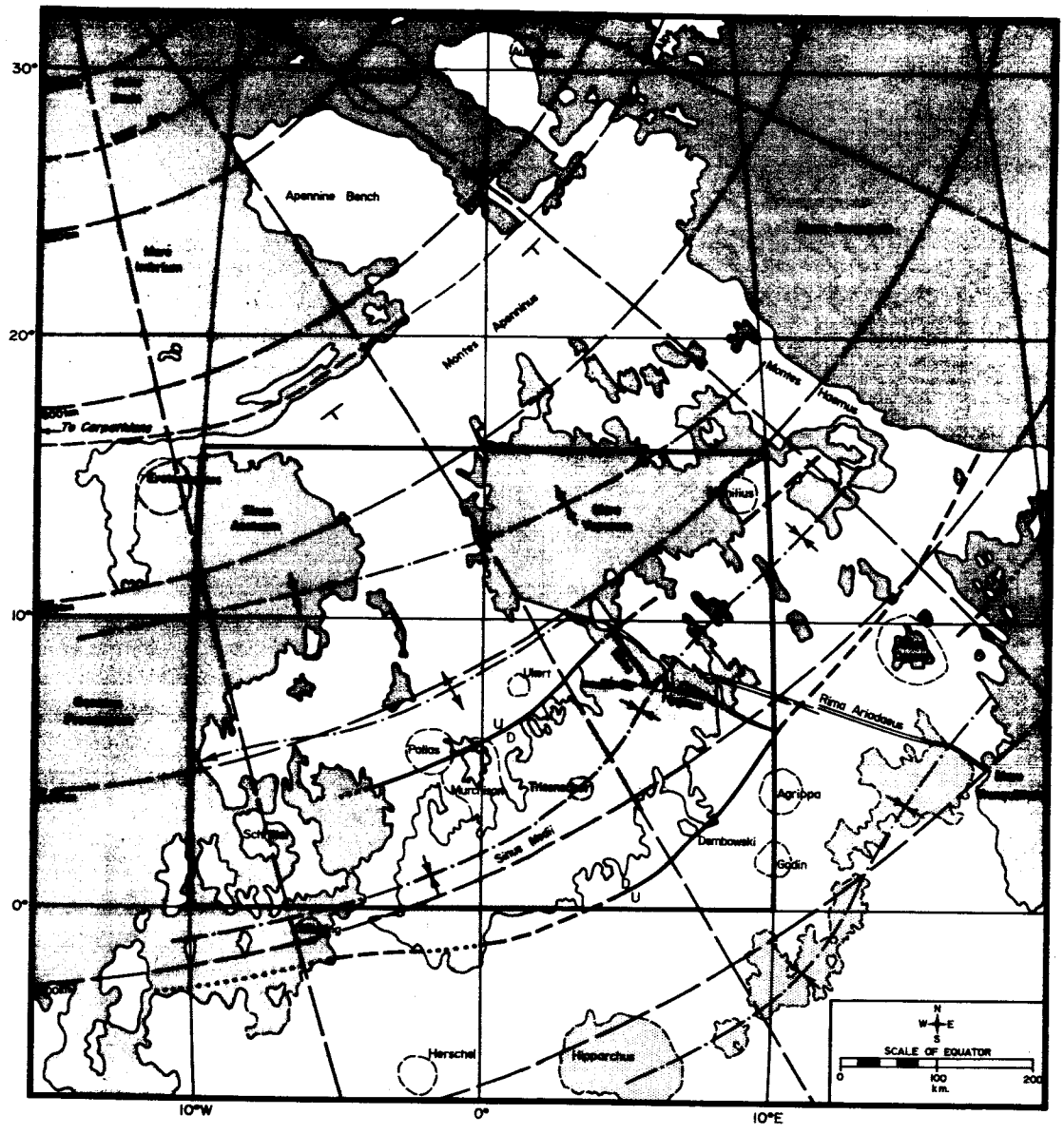
30°
20°
10°
0°
10°W
0°
10°E
Apennine Bench
Mare Imbrium
Montes Apenninus
Montes Haemus
To Carpentaria
Rima Ariadaeus
Agrippa
Dembowski
Goldin
Sinus Medii
Herschel
Hipparchus
N
W
E
S
SCALE OF EQUATOR
0
100
km.
200

detail, the margins of the maria are considerably embayed; complexly outlined peninsulas of the terra extending into the maria are broad near their base and become narrower at the tip, commonly ending in a series of isolated outcrops of Fra Mauro surrounded by mare material. This pattern indicates gradual deepening of the depression toward the center of each mare. The pre-Procellarum Group surface is irregular in detail rather than a smooth contact as commonly found in familiar terrestrial synclines, but I believe these broad troughs have been formed by folding or downwarping of the lunar surface. The axes of the synclinal troughs are marked by syncline symbols and the crests of the intervening broad anticlinal highs by anticline symbols on figure 1.

Along their axes, which are concentric to the Mare Imbrium basin, the troughs rise and plunge; the troughs are modified and their depth accentuated in places by the cross-cutting Imbrian sculpture. The mare material occupies only the lower parts of the troughs. Alternating highs and lows along a given concentric trough are typical of the circum-Imbrium region. These appear to form a pattern of broad cross folds. The Apennine Bench and a similar bench northeast of it alternate with mare-filled depressions which appear to be part of a radial system of broad folds.

Three concentric troughs are recognized on the southeast side of the Mare Imbrium basin. In order of increasing distance from the basin,

these are (1) the Mare Vaporum-Sinus Aestuum trough, (2) the Sinus Medii trough, and (3) an unnamed trough extending from Hipparchus to Mare Tranquilitatis.

The main part of Mare Vaporum is crudely circular and has been interpreted by some authors as occupying a circular mare basin. A large mare embayment to the east, however, must be considered part of Mare Vaporum although the connection is obscured by the post-Imbrian crater Manilius. In addition, the remainder of the terra area to the northeast, except for the Haemus Mountains, is low, and isolated depressions are filled with mare material. The entire Mare Vaporum trough, thus outlined, is interpreted here as a broad synclinal fold which plunges from the northeast terra low beneath Mare Vaporum and then rises again to the low, narrow terra area separating Mare Vaporum from Sinus Aestuum.

I interpret the depression occupied by the Sinus Aestuum as part of the synclinal trough containing Mare Vaporum. As is true of Mare Vaporum, there is a possibility that Sinus Aestuum is located in a pre-Imbrian circular basin, but no evidence for this was observed.

Sinus Medii occupies the second concentric trough crossing the Mare Vaporum quadrangle. An embayment of Oceanus Procellarum west of Sinus Medii and separated from it only by a low ridge, together with the relatively low terra area northeast of Sinus Medii and small isolated low areas filled with mare material, are all within the trough. Part of

the depression of the Sinus Medii trough appears to be due to faulting. The main displacement on the northwest side of the trough, mostly within terra material, is a distinct scarp, passing just south of Ukert and through Pallas and Murchison. Its trend is nearly concentric with the Mare Imbrium basin. The fault may bend and continue north of Schröter. The scarp dips south, and the displacement of craters suggests that the scarp is a normal fault with south side down. Low scarps extending as far as Mare Serenitatis may connect with it. On the southeast side of the Sinus Medii depression, a similar scarp passes southeast of the crater Dembowski. Certain lineaments that can be traced as far as the Oceanus Procellarum[1/] may represent its continuation westward. Eastward it may connect with other short scarps that face north. These two main scarps are probably the largest faults contributing to the depression of the basin, but there are numerous smaller parallel scarps, only a few of which are shown on the preliminary geologic map.

The third concentric trough lies outside the quadrangle to the southeast (fig. 1). It is marked by a belt of pre-Procellarum smooth depression-filling material (Milton, oral communication, 1964).

1/ Eggleton (oral communication) notes a distinct scarp in the Montes Riphaeus quadrangle which may be a westward continuation of the same fault.

Structures related to Mare Serenitatis.--In addition to the radial Imbrian sculpture and the broad folds concentric with Mare Imbrium, other structures probably related to Mare Serenitatis, occur in the Mare Vaporum quadrangle. Mare Serenitatis occupies a pre-Imbrian circular basin like that of Mare Imbrium. The Haemus Mountains form part of the rim of the basin and are possibly comparable in origin to the Apennine Mountains, although modified by later Imbrian deformation and deposition of the Fra Mauro Formation. Vaguely defined broad troughs and highs concentric with Mare Serenitatis have been recognized (Baldwin, 1963, p. 320). Probably the gross topography of the Mare Vaporum quadrangle reflects concentric and radial structures related to both Imbrium and Serenitatis. The areas of mare material directly southwest of the Haemus Mountains may mark a Serenitatis synclinal trough modified by Imbrian sculpture. Possibly the alternate rise and plunge of the troughs concentric about the Mare Imbrium basin in the Mare Vaporum quadrangle is due partly to cross folds concentric about the Serenitatis basin.

Structures not related to circular basins.--Many prominent rilles and lineaments of the Mare Vaporum quadrangle are neither radial nor concentric to Mare Imbrium, Mare Serenitatis, or any other known basin. Probably they are not produced directly by basin-forming events. Examples are Rima Ariadaeus, all but one of the principal segments of Rima Hyginus, an en-echelon set of short rilles west of the crater Hyginus, and the

Triesnecker rille system. All these rilles have straight walls. Other rilles with more irregular, rounded walls are present in the terra areas.

Rima Ariadaeus, two segments of Rima Hyginus, and two members of the en-echelon set strike N75-78°W; two other members of the en-echelon set strike N69°W; and the easternmost segment of Hyginus strikes N62°W. Parallel lineaments occur several hundred kilometers south of these rilles (Milton, oral communication, 1964). All these rilles are wide enough for their floors to be distinguishable; the floors appear to be the same material as the surrounding terrain, in most places mare material. Ariadaeus appears to be a graben, and the others are probably graben also.

The rilles of the Triesnecker system are like the other rilles in most respects, but are not as straight; the Triesnecker rilles intersect to form a complex network. In places, the walls of one rille of an intersecting pair seem to continue across the other, as shown on the map. The system as a whole trends north-south, but segments of the rilles also strike parallel with Imbrian concentric circles, parallel with Imbrian sculpture, and parallel with the Hyginus-Ariadaeus set of rilles.

The orientation and appearance of the Triesnecker rilles suggests that they were produced by tension in an east-west direction, and opened up along faults trending both perpendicular to this direction and along pre-existing lines of weakness. The only other lunar features remotely resembling them either in size or form are reticulate systems of rilles

inside large craters, whose floors appear to have been raised (Masursky, written communication, 1964). Possibly the Sinus Medii trough has also been raised after emplacement of the Procellarum Group, which they cut.

Conclusions

The broad structural features in the region of Mare Vaporum are a group of large subdued synclinal troughs and anticlinal rises plunging and rising in undulating fashion along axes roughly concentric with the Mare Imbrium basin. Relief on these folds is augmented by faults parallel with their axes. The concentric structures are intersected by Imbrian sculpture, which is interpreted as reflecting normal faults radial to Mare Imbrium. The broad synclines and anticlines are probably crossed by older similar structures around Mare Serenitatis, which may account in part for the rise and plunge of their axes. Probably these structures were formed by shock waves that proceeded out from large impacts that are believed to have produced the basins (Shoemaker, 1962, p. 349). Such concentric synclines and anticlines appear to be fundamental elements of lunar structure and may account for most of the major topographic features of the Moon's surface. Isostatic readjustment after the formation of the basins and folds may prove to offer an explanation for many structures which do not now appear to be connected with the basins.

References

Baldwin, R. B., 1963, Measure of the Moon: Chicago, Univ. Chicago Press, 590 p.

Eggleton, R. E., 1964, Preliminary geology of the Riphaeus Quadrangle of the Moon and definition of the Fra Mauro Formation: U.S. Geol. Survey, Astrogeologic studies annual progress report, August 25, 1962 to July 1, 1963, pt. A, p. 46-63.

Gilbert, G. K., 1893, The moon's face--a study of the origin of its features: Philos. Soc. Washington Bull., v. 12, p. 241-292.

Hackman, R. J., 1963, Stratigraphy and structure of the Apennine region of the Moon: U.S. Geol. Survey, Astrogeologic studies annual progress report, August 25, 1961 to August 24, 1962, pt. A, p. 2-10.

Hackman, R. J., 1964, Stratigraphy and structure of the Montes Apenninus Quadrangle of the Moon: U.S. Geol. Survey, Astrogeologic studies annual progress report, August 25, 1962 to July 1, 1963, pt. A, p. 1-8.

Hartmann, W. K., 1963, Radial structures surrounding lunar basins, I--The Imbrium System: Arizona Lunar and Planetary Lab. Comm., v. 2, no. 24, p. 1-15, pl. 1-30.

Hartman, W. K., and Kuiper, G. P., 1962, Concentric structures surrounding lunar basins: Arizona Lunar and Planetary Lab. Comm., v. 1, no. 12, p. 51-72, pl. 1-30.

References--Continued

Milton, D. J., this report, Stratigraphic notes from the Theophilus quadrangle.

Shoemaker, E. M., 1962, Interpretation of lunar craters, in Kopal, Zdenek, ed., Physics and astronomy of the Moon: London, Academic Press, p. 283-359.

STRATIGRAPHY OF THE TERRA PART OF THE THEOPHILUS QUADRANGLE

by D. J. Milton

Introduction

This report briefly describes some stratigraphic units mapped in the Theophilus quadrangle of the Moon (see Map Supplement) and discusses their relationships. The abrupt local variations in geology characteristic of the rugged terrae, or highlands, which occupy much of the quadrangle, pose difficult problems in geologic mapping and correlation of units with more distant parts of the Moon.

In previously mapped areas of the Moon, nearer to Mare Imbrium, a principal stratigraphic datum is the base of the Imbrian System. The basal unit in those areas is an easily recognized formation first mapped as Imbrian Regional Material (Hackman, 1962; Marshall, 1963) and assigned to the Apenninian Series by Marshall. More recently, two formations have been recognized in the Apenninian Series, the older Fra Mauro Formation (Eggleton, 1964; and Hackman, 1964) and the younger Apennine Bench Formation (Hackman, 1964). At least the former and perhaps both are believed by these authors to consist of ejecta from the Mare Imbrium basin. The recognition of the Fra Mauro Formation or a correlative unit is the key problem in correlating the stratigraphy of the Theophilus quadrangle with other regions of the Moon.

Pre-Imbrian materials

Certain areas in the Theophilus quadrangle are characterized by sharp ridges and steep scarps with a northwest-southeast alignment. Much of the terrain consists of the broken rim of old craters, for example Taylor A and Taylor B.

The northwest-southeast scarps appear to be part of the Imbrian sculpture of Gilbert (1893), a system of scarps and furrows radial to Mare Imbrium. The Imbrian sculpture is believed to consist largely of faults formed at the time of formation of the Mare Imbrium basin, the initial event of the Imbrian period. The terrain that it affects must therefore be of pre-Imbrian age. Accordingly, terrain with what is believed to be Imbrian sculpture is shown on the geologic map as "pre-Imbrian undifferentiated material."

There are two difficulties in the use of Imbrian sculpture to indicate pre-Imbrian terrain. First, not all lineaments with the appropriate direction are Imbrian sculpture. The direction of the Imbrian sculpture, at least in this area, is a direction of weakness along which faulting recurred more than once during lunar history. Thus, lineaments within the Copernican crater Theophilus, such as the trough-like Theophilus P, have the proper direction but cannot be Imbrian sculpture if the term is restricted to features produced at the time of formation of the Mare Imbrium basin.

A second problem in mapping pre-Imbrian terrain is the difficulty of distinguishing sculpture in outcropping material from thinly buried sculpture. Several of the formations discussed below are widespread blankets and there is little reason to suppose that they would avoid the steep-sloped, rugged areas that show pre-Imbrian sculpture. On this basis, similar areas in the Kepler (Hackman, 1962) and Letronne (Marshall, 1963) quadrangles have been mapped as Apenninian "where the Apenninian layer may be generally very thin and pre-Imbrian material locally exposed." The ruggedness of the terrain, however, precludes the development, or at least the observation, of the fine-grained topography characteristic of the Apenninian of this quadrangle, so that it would seem more objective to correlate these areas on the basis of the latest age assignable to the features actually seen. The albedo, which should depend only on the surficial layer, is of little help. The intrinsic brightnesses of the pre-Imbrian and Imbrian materials are similar and the steep slopes in the pre-Imbrian terrain are characterized by a higher albedo, presumably due to exposure of fresh material by erosion, so that areas bright enough to be mapped as Copernican slope material are commonly associated with the pre-Imbrian terrain.

Imbrian sculpture is not uniformly developed around Mare Imbrium. The craters Abulfeda and Tacitas lie in a region where Imbrian sculpture is obscure and appear fresher than pre-Imbrian craters elsewhere in the

quadrangle. The outer rim of Abulfeda even shows hummocky crater rim topography. The two craters, however, are overlapped by the Fra Mauro(?) Formation described below, and hence must be of pre-Imbrian age.

Fra Mauro Formation(?)

The Fra Mauro Formation of the Apenninian Series, as established by Eggleton (1964), has two facies, hummocky and smooth. The former is characterized by "abundant close-spaced, low, rounded, subequidimensional hills and intervening depressions generally 2 to 4 kilometers across." In addition, there are "fairly common elongate, gently sloping scarps. . . typically 1½ to 2 kilometers wide" as long as 15 or 25 kilometers, aligned toward Mare Imbrium. Terrain of this description occurs in the Theophilus quadrangle. Owing to the rather fine scale of the characteristic texture, the best observing conditions are necessary to see or photograph it satisfactorily. Good examples are in the area west of Theon Senior C as shown on photograph L 24 taken by G. H. Herbig on the 120-inch telescope at Lick Observatory or the area southwest of Taylor as shown on photograph 113 (Kuiper Atlas plate C5B) taken by F. G. Pease on the 100-inch telescope at Mt. Wilson Observatory. The exact distribution of the Fra Mauro Formation(?) as shown on the geologic map is not accurate, as the characteristic features are commonly at or beyond the limit of resolution of the available photography.

The Fra Mauro Formation in the type area has been interpreted as material ejected from the Mare Imbrium basin. This interpretation seems satisfactory for the unit in the Theophilus quadrangle. The topographic pattern suggests the braided hummocks of the outer zones of the rims of large craters. The roughness of texture appears to decrease from north to south, as would be expected of ejecta from the Mare Imbrium basin. Nevertheless, the possibility remains that the characteristic topography of this unit is not the result of deposition, but is a tectonic grain, perhaps a somewhat different manifestation of Imbrian sculpture than the much coarser system of lineaments in the terrain mapped as pre-Imbrian, simulating the texture of the Fra Mauro. For this reason the stratigraphic assignment is queried.

Imbrian plains-forming unit

Extensive, level, low-lying areas in the western part of the Theophilus quadrangle are mapped as underlain by the plains-forming unit. The surface on this unit is as level and smooth as the maria but the albedo is higher and small craters are more frequent. The plains-forming unit proper occupies the floors of old craters and irregular basins. In the higher ground adjacent to the level plains, the land forms commonly appear less angular than elsewhere in the uplands. These areas appear to be covered by a thinner deposit of the same material as fills the basins

and are accordingly mapped as underlain by "thin plains-forming unit." The contact of the plains-forming unit proper and the thin facies can be either distinct or gradational. In places the peaks of older hills emerge as islands from the level plains. The contact of the thin facies with older terrain is everywhere gradational.

Several small areas in the quadrangle, notably Kant D, are smooth plains, but have a multitude of small craters (apparently not satellitic to any primary crater) and some small hills. These areas are distinguished as the pitted plains-forming unit.

A maximum age for the plains-forming unit is indicated by the overlap relation of the unit onto Fra Mauro(?) Formation, for example near Taylor C or east of Dolland. Overlap by mare material at a few places within the Theophilus quadrangle and at other places in the Julius Caesar quadrangle indicates a pre-Procellarum age for at least part of the plains-forming unit. Another unit, mapped as the Theophilus Formation, that forms smooth plains and is superimposed on the rim material of the crater Theophilus of Copernican age, is very similar to the plains-forming unit. The possibility that some of the smooth material on the terra likewise is as young as Copernican cannot be excluded. Nevertheless, it is assumed as a working hypothesis that the plains-forming material constitutes a single unit of one age. Two possible correlations for the plains-forming unit would be with the smooth facies of the Fra Mauro Formation (Eggleton, 1964) or with the Apennine Bench Formation (Hackman, 1964).

The Apennine Bench Formation is regarded as younger than the hummocky facies of the Fra Mauro on which it lies; Eggleton regards the smooth facies of the Fra Mauro as contemporaneous with the hummocky facies, although he recognizes the possibility that it may be younger, perhaps correlative with the Apennine Bench. The plains-forming unit is clearly superimposed on and younger than the Fra Mauro(?) Formation in the Theophilus quadrangle. The stratigraphic relationships and the appearance of the plains-forming unit and the Apennine Bench Formation are similar, although the plains-forming unit appears to have a lower albedo. A correlation will not be made in this stage of the investigation, however, because the two units are widely separated and lie in different structural environments.

The base of the Archimedian Series is formally defined by the lowest crater rim deposit resting on the Apenninian Series. The lack of a definite example of a crater post-dating the Fra Mauro(?) Formation and predating the plains-forming unit forces the assignment of the latter to the older Apenninian Series. The crater Delambre may, however, have just this relationship to the two units. The rim material of Delambre north and northeast of the crater laps onto Fra Mauro(?); indeed terrain with an apparent Fra Mauro texture appears to be partially concealed by the rim material directly north of the crater, as shown by Herbig photograph L 24. The evidence for the later age of the plains-forming unit is less

direct. There are two belts (mapped as Archimedian crater rim material) running northwest from the vicinities of Theon Junior C and Theon Senior C with small pits, again best seen on L 24. These pits may be secondary impact craters from Delambre. They are absent on the smooth plains and are restricted to the higher ground which, in their absence, would be mapped as Fra Mauro(?). The most reasonable explanation is that the plains-forming unit is later and buries any secondary craters in the lower ground. If these observations can be substantiated at the telescope they will necessitate the reassignment of the plains-forming unit to the Archimedian epoch.

The only landform intrinsic to the plains-forming unit (except the pitted facies) is the level plain. Even the ridges and domes of the maria are absent. This suggests that the unit consists of unconsolidated material. Its origin is not at all obvious. If the Fra Mauro(?) Formation consists of ejecta from an impact in the Mare Imbrium basin, then it is exceedingly difficult to attribute the same origin to the entirely different plains-forming unit. It may consist of fragmental ejecta from a widespread volcanic episode, with the actual centers of eruption concealed or impossible to distinguish.

The pits and hills of the pitted facies may be volcanic features. The thickness of the plains-forming unit in crater floors seems clearly greater than on the adjacent uplands. Either more material was generated

in the low areas or some mechanism operated to transport material downhill. There is no satisfactory hypothesis for either possibility.

Imbrian(?) plateau-forming unit

The eastern part of the terra in the Theophilus quadrangle has a character different from the western. Here are broad smooth-surfaced rolling plateaus, rather than the flat-floored basins and rougher uplands of the western area. Where scarps probably existed in the underlying topography there are now slopes of moderate steepness with the same surface character as the higher level areas. The areas north and south of Kant exemplify this well. Associated with this terrain, which is mapped as the plateau-forming unit, are large irregular depressions, such as those east of Alfraganus, some of which coalesce to form irregular rilles, such as that running from Zollner J to Alfraganus E. The distinction between the plains-forming unit and the plateau-forming unit is not sharp and the two may be gradational facies.

The plateau-forming material is apparently overlapped by mare material and seems to bury Imbrian sculpture; so an Imbrian age seems most likely. There is no compelling reason to believe that all of the material is of one age, however, so the age designation is queried. Similar material occurs in other quadrangles, especially to the south. The Censorinus N material of the Columbo quadrangle (Elston, 1964) to

the east appears very similar.

The plateau-forming unit does not conform to pre-existing topography as does the plains-forming unit. It may consist of volcanic flows that spread more or less evenly within a restricted area. A few volcano-like features can be seen on Herbig photograph L 24. One of these is a smooth dome with a summit crater due east of Alfraganus D and due south of Alfraganus F, and there are similar but less clearly developed features south of the buried highland block south of Delambre.

An area centered on the north rim of Descartes, mapped as hummocky plateau-forming unit, is characterized by an extremely rough but unoriented texture of irregular hills and small rilles and a very high albedo. The material has a considerable thickness, filling the northern half of Descartes to the rim, but has no great areal extent. Eggleton and Marshall (1962) considered this to be an outlying patch of hummocky Apenninian material (which would now be called Fra Mauro), but it clearly overlies what is here considered as Fra Mauro Formation. The age of this material is indeterminate; for convenience it has been considered a facies of the plateau-forming unit. The unit and somewhat similar but darker patches in Andel M and Almanon are probably volcanic fields formed of a material that for some reason, such as lower viscosity if fluid or less violent eruption if fragmental, did not spread as widely and evenly as the plateau-forming unit.

References

Eggleton, R. E., 1964, Preliminary geology of the Riphaeus Quadrangle of the Moon and definition of the Fra Mauro Formation: U.S. Geol. Survey, Astrogeologic studies annual progress report, August 25, 1962 to July 1, 1963, pt. A, p. 46-63.

Eggleton, R. E., and Marshall, C. H., 1962, Notes on the Apenninian Series and pre-Imbrian stratigraphy in the vicinity of Mare Imbrium and Mare Nubium: U.S. Geol. Survey, Astrogeologic studies semi-annual progress report, February 26, 1961 to August 24, 1961, p. 132-137.

Elston, D. P., 1964, Pre-Imbrian stratigraphy of the Colombo Quadrangle: U.S. Geol. Survey, Astrogeologic studies annual progress report, August 25, 1962 to July 1, 1963, pt. A, p. 99-109.

Gilbert, G. K., 1893, The moon's face--a study of the origin of its features: Philos. Soc. Washington Bull., v. 12, p. 241-292.

Hackman, R. J., 1962, Geological map and sections of the Kepler region of the Moon: U.S. Geol. Survey Map I-355.

Hackman, R. J., 1964, Stratigraphy and structure of the Montes Apenninus Quadrangle of the Moon: U.S. Geol. Survey, Astrogeologic studies annual progress report, August 25, 1962 to July 1, 1963, pt. A, p. 1-8.

Marshall, C. H., 1963, Geologic map and sections of the Letronne region of the Moon: U.S. Geol. Survey Map I-385.

PROGRESS IN GEOLOGICAL MAPPING OF THE GRIMALDI QUADRANGLE

by J. F. McCauley

Introduction

The Grimaldi quadrangle lies between latitudes 0° and 16°S, and longitudes 50° and 70°W on the Moon, and is bounded on the north by the Hevelius quadrangle (McCauley, 1964a). It includes the southeastern margin of Oceanus Procellarum; the northeastern one-third of the quadrangle consists predominantly of mare material. The Mare Humorum basin (Titley, 1964) lies about 400 kilometers to the southeast of the area, and the Mare Orientale basin (McCauley, 1964b) lies about 800 kilometers to the southwest. Materials derived from these basins cover the terra in the remaining two-thirds of the quadrangle.

Stratigraphy

Humorum Group and Cordillera Group

A definite relationship observed in the Grimaldi quadrangle establishes the relative ages of the Orientale and Humorum basins. The evidence is obtained from the superposition of rim materials of the Orientale basin on those of the Humorum basin.

Regional material of the Humorum Group of pre-Imbrian or Imbrian age (Titley, 1964), which is present in the southeastern part of the

Grimaldi quadrangle has a moderate albedo, is hummocky, and under low illumination exhibits a very rough surface. This unit is best developed north of the crater Fontana.

Rocks of the Cordillera Group are present in the south and southwestern part of the quadrangle. These are higher in albedo than is the regional material of the Humorum Group, generally free of hummocks, and smoother under low illumination (McCauley, 1964b). The Cordillera Group overlies a complex older topography and partially fills subjacent craters. The average spatial density of craters superimposed on the Cordillera Group is lower by a factor of about two than that on the Humorum Group.

The relationship between the two groups is best seen north of the crater Fontana, where the hummocky, rougher, and darker surface of the Humorum Group is buried by lighter, smoother material of the Cordillera Group that increases in thickness northwestward. Proceeding away from the limit of the Cordillera Group, the change in thickness is gradual so that the hummocks and small craters on the Humorum Group can be observed in outline beneath a thin veneer of the Cordillera Group, at least as far as the vicinity of the crater Sirsalis 50 kilometers northwest of the contact. The Cordillera Group thickens continuously to the west toward Mare Orientale, and in the region north of Cruger, the topographic character of the basal contact can no longer be recognized.

Procellarum Group and dark mare material

Typical mare material of the Procellarum Group is present throughout the northeastern part of the quadrangle, where it overlies older rocks of both the Humorum and Cordillera Groups. Mare material that is distinctly darker than average in albedo is present, however, at a number of localities, particularly in the floor of Grimaldi, along the margin of Oceanus Procellarum near Grimaldi C, and in the floor of the crater Billy.

This dark mare material is distinguished from typical mare material of the Procellarum Group by: (1) measurably lower spatial density of superimposed craters (the dark mare material within the crater Grimaldi exhibits a spatial density of resolvable craters about one-half that of correspondingly large parts of Oceanus Procellarum--$70/10^5$ km^2 versus $150/10^5$ km^2); (2) less measurable roughness based on telescopic observation as well as photometric slope analysis of high resolution photographs (McCauley, unpublished communication); (3) fewer superimposed rays of the type associated with Copernican craters.

It has been mapped separately from material of the Procellarum Group and given the preliminary designation md.

The dark mare material within the Grimaldi quadrangle may be significantly younger than that of the Procellarum Group. The lower density of superimposed craters and rays are the strongest evidence for this. Copernican dark halo craters present elsewhere on the Moon probably

indicate that volcanism occurred late in lunar history. Dark mare material in the Grimaldi quadrangle may range in age from Eratosthenian to Copernican.

Structure

The most significant structural feature within the Grimaldi quadrangle is the pronounced northeast-trending system of lineaments radial to the Mare Orientale basin. The system includes numberous scarps along which displacement appears to have taken place; they are prominent along the eastern flank of Grimaldi. A spectacular series of chain craters north of Damoiseau C is also part of the system. This chain is almost 100 kilometers in length and includes individual craters up to 18 kilometers in diameter. It represents the largest feature of its type recognized to date. The Sirsalis Rille is also generally parallel to the regional Orientale trend. As is also the case for the Damoiseau C chain craters, the Sirsalis Rille structure post-dates deposition of the Cordillera Group, indicating that repeated displacement and probably volcanic activity occurred here after the radial lineament system of the Orientale basin was initially formed.

References

McCauley, J. F., 1964a, A preliminary report on the geology of the Hevelius Quadrangle: U.S. Geol. Survey, Astrogeologic studies annual progress report, August 25, 1962 to July 1, 1963, pt. A, p. 74-85.

McCauley, J. F., 1964b, The stratigraphy of the Mare Orientale region of the Moon: U.S. Geol. Survey, Astrogeologic studies annual progress report, August 25, 1962 to July 1, 1963, pt. A, p. 86-98.

Titley, S. R., 1964, A summary of the geology of the Mare Humorum Quadrangle of the Moon: U.S. Geol. Survey, Astrogeologic studies annual progress report, August 25, 1962 to July 1, 1963, pt. A, p. 64-73.

TRAJECTORIES OF OBJECTS PRODUCING COPERNICUS RAY MATERIAL ON THE CRATER ERATOSTHENES

by M. H. Carr

Under full Moon illumination the lunar surface in the region of Eratosthenes shows a wide range of brightness. The differences in brightness or normal albedo correspond to differences in the materials exposed at the surface. The darkest material is crater rim and floor material of Eratosthenian age. This is exposed in the western part of Eratosthenes on the inner wall, on the eastern flank of the crater, and to the north where the crater rim material is superimposed on the Fra Mauro formation of Imbrian age. Some dark material crops out around three small dark halo craters of Copernican age on the western rim of Eratosthenes. East of Eratosthenes are exposures of mare material of Imbrian age with an albedo slightly higher than the Eratosthenes rim material. Much of the crater is streaked with high albedo ray material which is part of the complex ray pattern surrounding the crater Copernicus.

Ray material is largely absent on slopes facing away from Copernicus. For example, the inner west wall and the outer east wall of Eratosthenes are both almost devoid of ray material (fig. 1). Some ray material is found on the northeast flank of the crater, but here the crater rim is breached and is 1000 feet lower than the rim on either side. The northeastern side of several ridges outside Eratosthenes and the northeastern side of the central peak of Eratosthenes are also devoid of ray

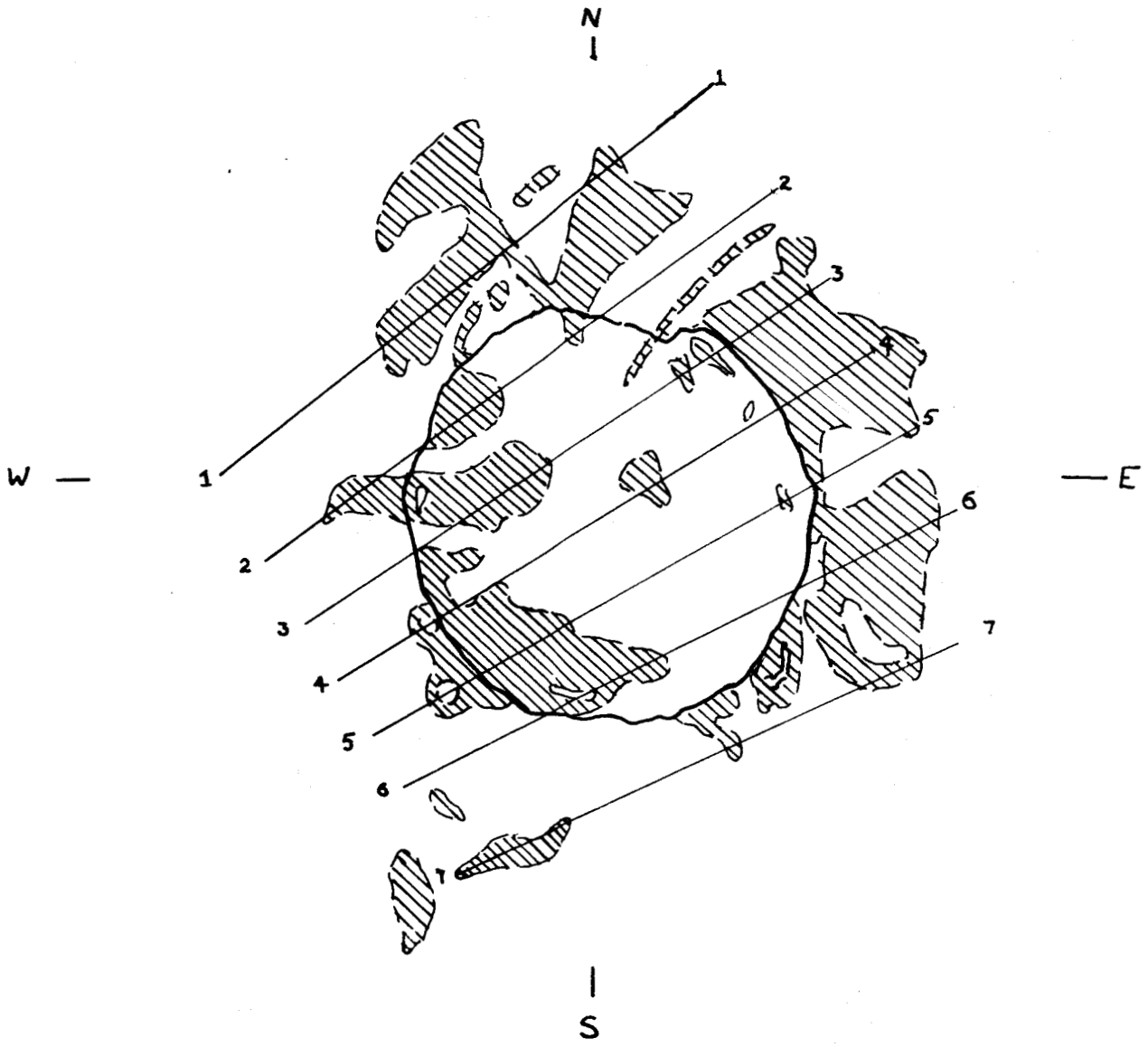

Figure 1. Eratosthenes, showing dark areas and location of cross section. Scale 1:1,000,000.

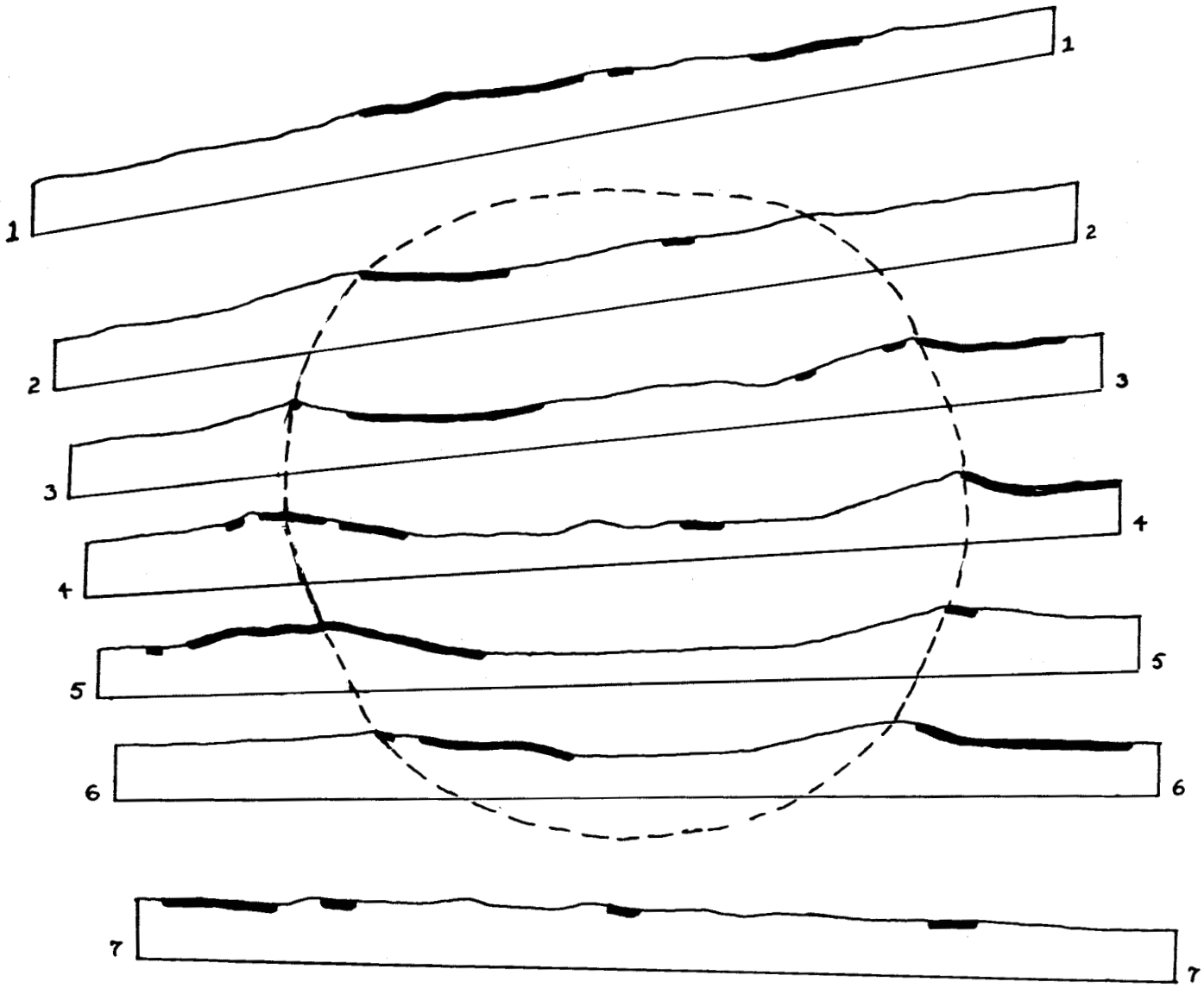

Figure 2. Sections across Eratosthenes radial to Copernicus showing dark areas. Vertical and horizontal scales 1:500,000.

material.

These relations suggest that the ray material is absent in these areas because of topographic barriers in the path of lunar fragments ejected from Copernicus which formed the rays. The absence of ray material in some cases may be due merely to a lack of material in a particular trajectory, but it appears highly likely that the principal cause of lack of ray material in the immediate area of Eratosthenes is topographic shielding.

Knowing the areas of non-deposition of ray material, their elevations and the elevations of the intervening barriers, the minimum angle of incidence of fragments which formed the rays can be found. Minimum angles of incidence were found for several sections across Eratosthenes radial to Copernicus (fig. 2). The profiles are constructed from U.S. Air Force Aeronautical Chart and Information Center, chart LAC 58. From the angle of incidence and the distance from the source, the ejection velocity of the ray material can be computed from the ballistic equation for spherical bodies,

$$R = 2r \tan^{-1}\left(\frac{\bar{V}e^2 \sin\theta \cos\theta}{1 - Ve^2 \cos^2\theta}\right) \qquad (1)$$

where,

R is the range (distance between present position of ray material and its source),

r is the radius of the Moon,

θ is the angle of incidence and

$\bar{V}e^2 = \frac{Ve^2}{rg}$ where Ve is the ejection velocity,

g is the gravitational acceleration at the lunar surface.

Copernicus is thought to have been enlarged by 25 km by slumping after initial opening of the crater by ejection of material (Shoemaker, 1962). The range, R, was obtained assuming that the ray material originated near the edge of the initial opening produced by ejection, about 35 km from the center of the present crater. Velocities calculated on this basis from equation 1 for the measured minimum ejection angles are given in table 1. An ejection velocity of 1.1 km/s and an ejection angle of 7° may be representative of lunar fragments from Copernicus that landed on Eratosthenes.

This ejection velocity and ejection angle may be substituted in the equation

$$v = Ve\sqrt{\frac{2\rho_r}{\rho_m}} \cdot \frac{1}{\sin^{3/2}\theta}\left(\frac{d}{x}\right)^{3/2}, \qquad (2)$$

where

v is the velocity of the impacting bolide,

ρ_m is the density of the bolide and

x is its radius,

ρ_r is the density of the lunar crustal material, and

d is the depth of the center of gravity of energy release, based on a simplified model of cratering by impact (Shoemaker, 1962), to find the velocity of the impacting bolide. Assuming that the ray material was ejected along paths radial to the center of gravity of energy release, d can be derived for various points of ejection of the ray material. Distances of 10, 20, and 30 km from the epicenter of the shock for the ejection point give respectively 1.2, 2.4, and 3.6 km for the depth of the burst point. The depth of 3.6 km is reasonable for an impact crater produced by a dense bolide. With an estimate for d, the energy of the impacting bolide can be calculated for various ratios of d/x, and various values of v and ρ_r (table 2). The velocities computed for the projectile that formed Copernicus, if taken literally, would indicate that the object was a comet; in one case the velocity is clearly too high.

The ejection angles computed for Copernicus ray material are smaller than those anticipated from hypervelocity impact experiments in basalt (Gault, Shoemaker, and Moore, 1963). Recent work by D. E. Gault and H. J. Moore, however, has shown that the ejection angles are much lower if non-cohesive sand is used as a target instead of basalt (Moore, personal communication). The better analogy between Copernicus and non-cohesive sand targets is consistent with the contention of Moore, Gault, and Heitowit (1964) that the effective target strength decreases with increasing size of a hypervelocity impact crater.

Table 1. Ejection velocities and ejection angles computed for various sections across Eratosthenes.

Cross-section	Range (R) (km)	Ejection angle (θ)	Calculated ejection velocity (Ve) (km/sec)
2	274	8°12'	0.99
3	279	6°23'	1.06
	325	6°17'	1.14
4	257	13°36'	0.84
5	262	10°47'	0.91
6	272	5°07'	1.16
	316	6°05'	1.17

Table 2. Velocity and energy of bolide forming Copernicus, computed for various values of ρ_m, $\frac{d}{x}$, and $\frac{\rho_v}{\rho_m}$.

$\frac{\rho_r}{\rho_m}$	$\frac{d}{x}$	ρ_m (gm/cc)	v (km/s)	E (ergs)
1/2	2	4	73	2.8×10^{30}
		3		2.2×10^{30}
		2		1.6×10^{30}
	1.5	4	48	3.0×10^{30}
		3		2.2×10^{30}
		2		1.5×10^{30}
1	2	3	103	2.9×10^{30}
		2		1.9×10^{30}
	1.5	3	68	4.4×10^{30}
		2		3.0×10^{30}

References

Gault, D. E., Shoemaker, E. M., and Moore, H. J., 1963, Spray ejected from the lunar surface by meteoroid impact: U.S. Natl. Aeronautics and Space Adm. Tech. Note D-1767, 39 p.

Moore, H. J., Gault, D. E., and Heitowit, E. D., 1964, Change in effective target strength with increasing size of hypervelocity impact craters: U.S. Geol. Survey, Astrogeologic studies annual progress report, August 25, 1962 to July 1, 1963, pt. D, p. 52-63.

Shoemaker, E. M., 1962, Interpretation of lunar craters, in Kopal, Zdenek, ed., The Moon: New York, Academic Press, p. 283-359.

A POSSIBLE VOLCANIC COMPLEX NEAR THE HARBINGER MOUNTAINS OF THE MOON

by H. J. Moore

Introduction

An unusual group of lunar craters and rimae (rilles) are present just west of the Harbinger Mountains between selenographic coordinates 25°31' and 28°N and 41° and 45°W (astronautical convention). The craters commonly occur on the crests and flanks of small hills, but some are present in flat terrain. Rimae commonly join with the craters, and some rimae are, at least partly, composed of chains of coalesced craterlets. The close association of the craters and rimae suggest that the area is a volcanic complex.

The area just west of the Harbinger Mountains was studied by observations using the 36-inch refractor at Lick Observatory, photographs taken by James Greenacre at Lowell Observatory and other photographs. Crater dimensions were obtained using the U.S. Air Force Aeronautical Chart and Information Center chart of the Aristarchus quadrangle (LAC 39).

Characteristics of the complex

Albedo.--The albedo of the surfaces around the craters and rimae is generally very low—about the same as nearby mare material—with

gradational lateral variations. Bright rays from the crater Aristarchus, however, cross part of the area and form local streaks of high albedo. In addition, the walls of some rimae have a high albedo which makes them easy to trace on full Moon photographs. Local areas of high albedo occur around the crater Prinz B and the crater south of Prinz B (figs. 1 and 2), but the walls and flanks of a similar crater west of Prinz B, at 26°50'N and 44°W do not have a high albedo.

Topographic characteristics.--The topographic forms of the complex include broad hills, craters, chain craters, and rimae (figs. 1-3). Four morphologic associations are present: (1) hills with apical or flank craters, or both, and associated rimae, (2) hills with apical craters without associated rimae, (3) craters in gently sloping to flat terrain with associated rimae, and (4) isolated rimae in flat terrain. The first morphologic association is represented by the crater Prinz B, a flank crater immediately to the south, and Rima Prinz II (fig. 2, craters 2 and 3; and fig. 3). Prinz B is at the apex of a more or less elliptical hill about 15 km wide and 25 km long that rises about 600 m above the surrounding terrain. The crater is about 5 km across, and its floor is about 700 to 800 m below the crest of the crater rim. Two small rimae, 5 and 15 km long, are present on the south and northeast flanks of Prinz B. The crater on the flank of the hill immediately to the south of Prinz B is about 3 km across and about 300 m deep. Rima Prinz II, a sinuous rima associated with Prinz B and the flank crater, may be traced,

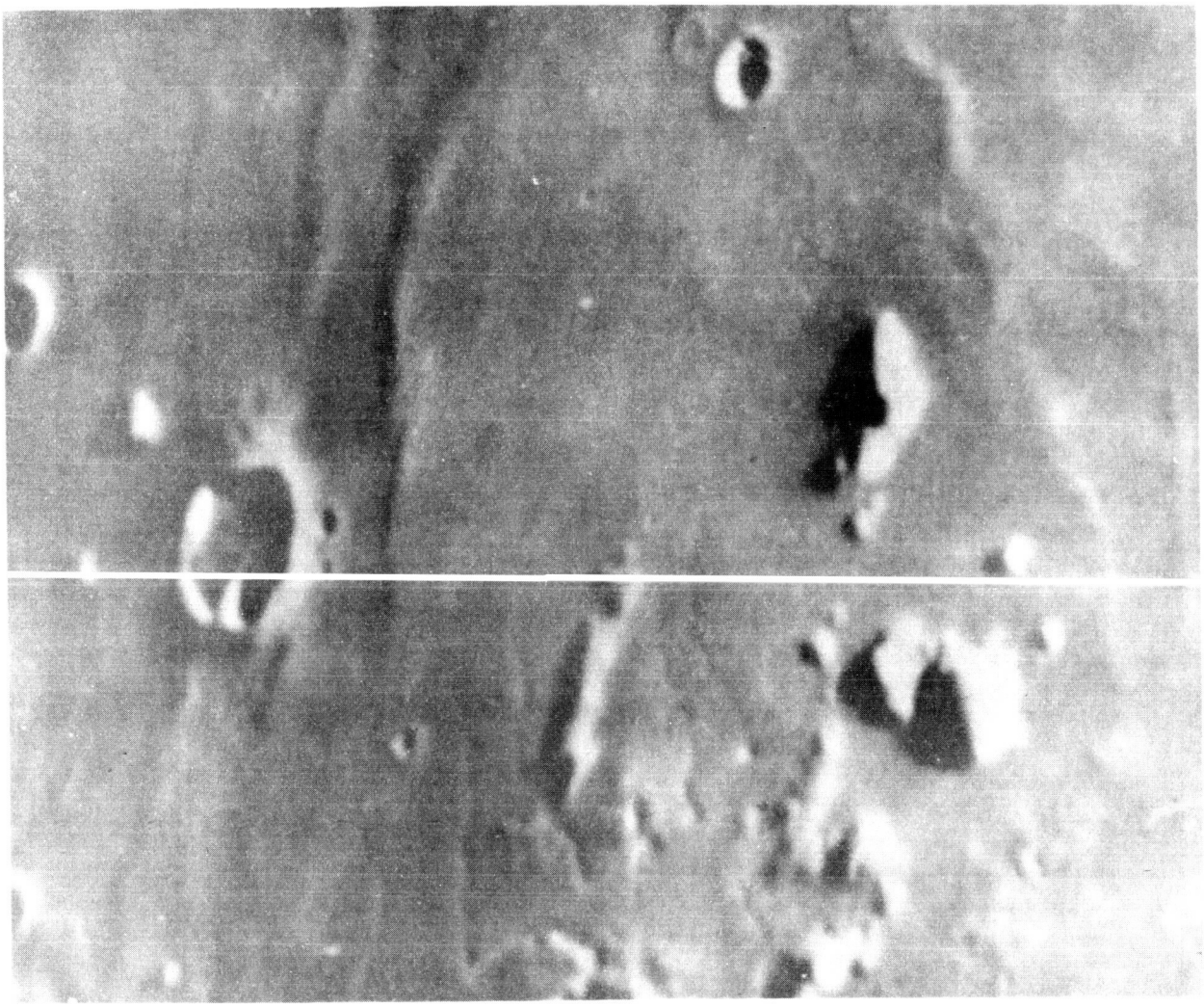

Figure 1. Photograph showing volcanic complex just west of the Harbinger Mountains. Large, partially buried crater left center is Krieger. Photograph taken at the Pic du Midi Observatory 60 cm refractor (courtesy of Zdenek Kopal and T. W. Rackham, see also Kopal and Rackham, 1963).

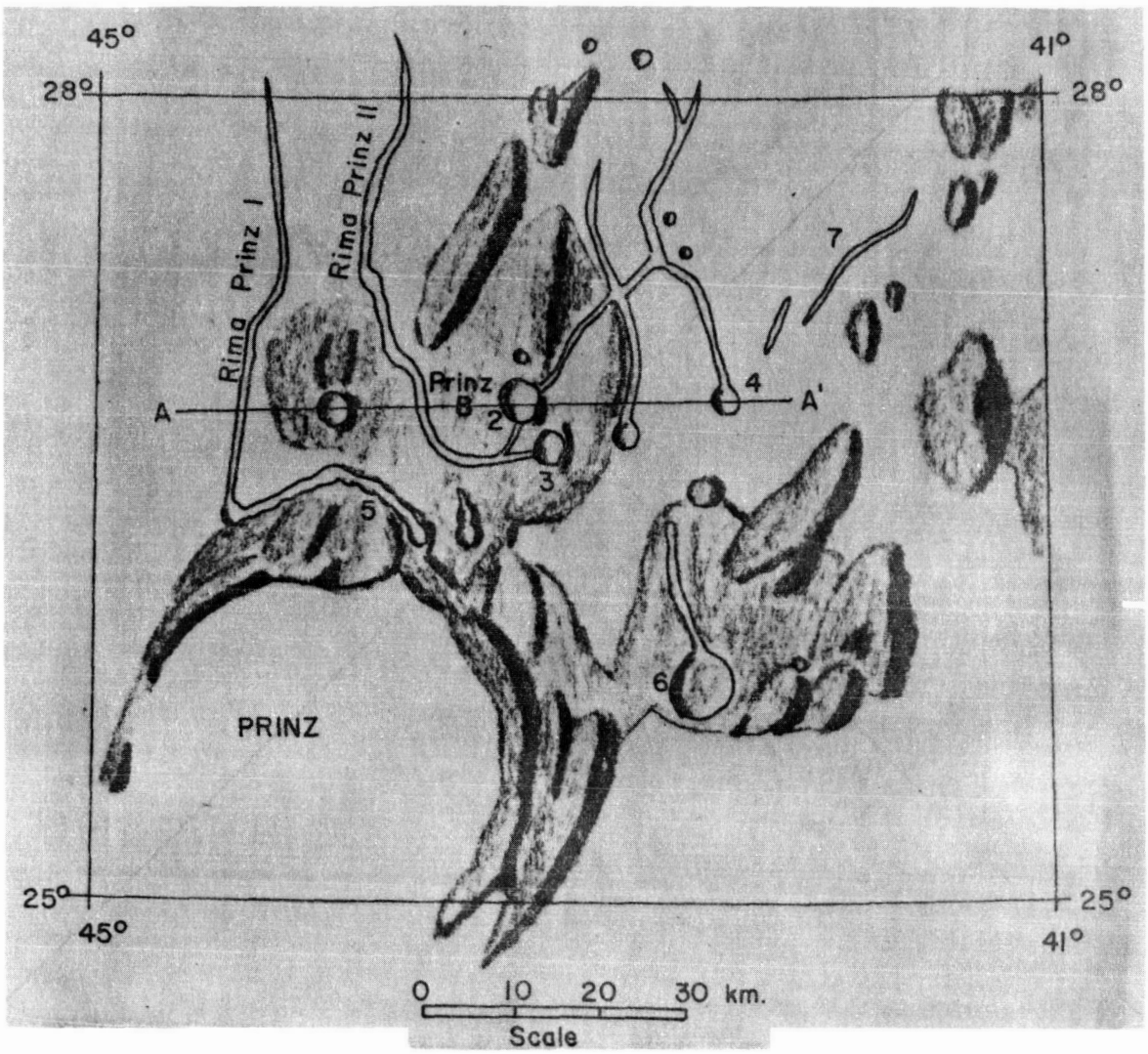

Figure 2. Sketch map of possible volcanic complex just west of the Harbinger Mountains of the Moon showing craters and rimae.

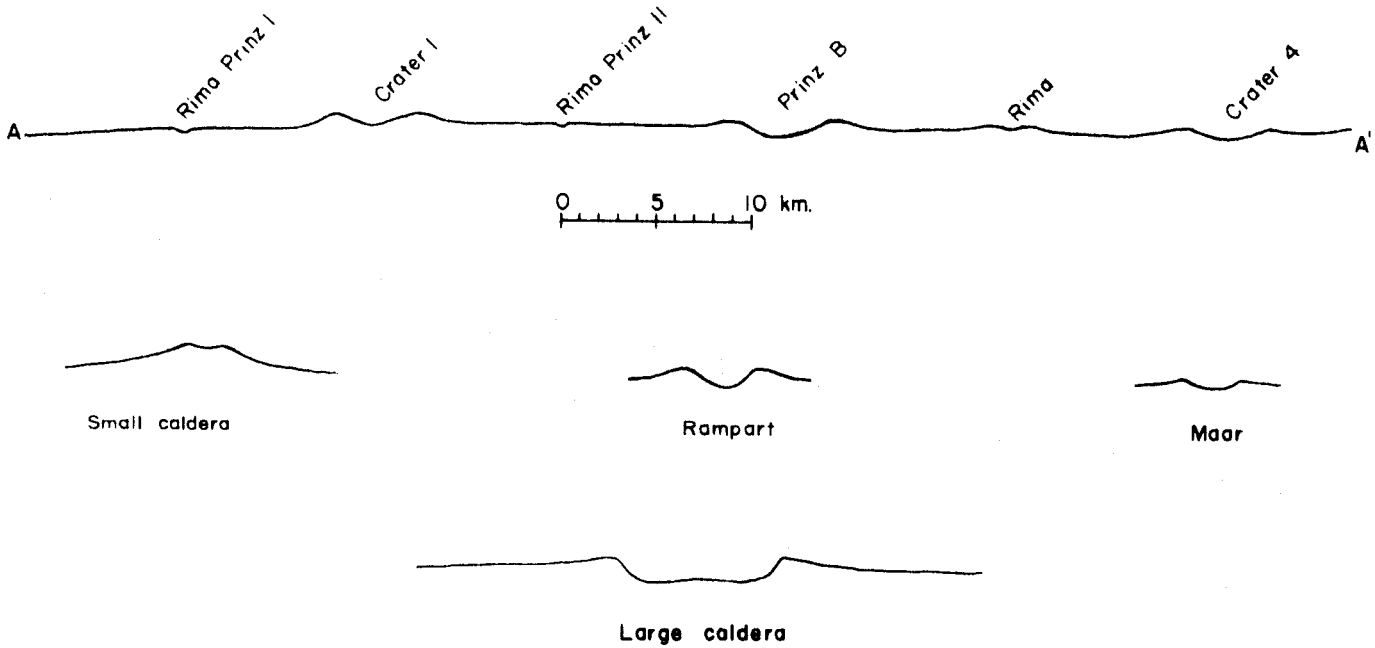

Figure 3. Comparison between lunar craters near the Harbinger Mountains and selected terrestrial craters. Line of Section across volcanic complex corresponds to line marked A-A' in figure 2. Vertical and horizontal scales are equal.

from the flank crater and onto the nearby mare for a distance of about 50 km (figs. 1 and 2). Another feature of the first type of association is an elliptical hill about 10 km wide and 15 km long (centered on 26°20'N and 44°W) with an associated craterlet chain along its north and northeast flanks connecting with Rima Prinz I. Rima Prinz I may be traced north from the chain of craterlets onto the mare along a sinuous course for about 65 km.

A crater 21 km due west of Prinz B, at 26°50'N and 40°W, represents the second type of morphologic association (fig. 2, crater 1; and fig. 1). This crater is about 4 km across and 400 to 500 m deep. No resolvable rimae are associated with this crater. Two arcuate ridges immediately to the north of this crater, however, possibly represent a breached crater. The rim crest of the crater rises 500 to 900 m above the surrounding terrain. The crater is about 300 m deep.

The third morphologic association is represented by craters 4 and 6 (fig. 2). Crater 6 is about 7 km across and 600 m deep. A rima composed of coalesced elongate craters may be traced northward 15 km from this crater. The surrounding terrain is a relatively flat plateau. Small mounds occur parallel to the rima and around the crater. Crater 4 is about 3½ km across and about 300 m deep. A rima may be traced 37 km north of crater 4. This rima has a regular zigzag pattern (figs. 1 and 2), the individual elements of which trend N 30°W and N 30°E in an area north

of the crater Aristarchus (Moore, 1964, p. 42). Telescopic observations and inspection of lunar photographs reveal irregular bulges along the northern third of the rima. This rima may be composed of a chain of coalesced craters that cannot be fully resolved.

The fourth morphologic association is represented by two isolated rimae on the mare (fig. 2, crater 7). These features are small and, as seen through the telescope, apparently have no associated craters.

Possible terrestrial analogs

The morphologic associations of craters on the apices and flanks of hills with long rimae, rimae composed of chain craterlets, and craters connected with rimae, strongly suggest that these features are volcanic. Linear features such as chain craters, troughs cut by nuées ardentes, and fissures are commonly associated with terrestrial volcanoes. Although some of the craters in one group near the Harbinger Mountains may resemble impact craters, they also resemble ring-wall or rampart maars (Rittman, 1962, p. 114-115), and the long rimae connected with these craters suggest that an impact origin is unlikely.

Individual craters in the complex appear to have had simple histories. They do not resemble stratovolcanoes, or shield volcanoes which, on earth, are built up of a complex sequence of flows and pyroclastic deposits. Craters along profile A-A' may be compared with several forms of terrestrial

volcanoes in figure 3. Crater Lake, Oregon (Williams, 1942, p. 64) is the model for one large caldera; Brokeoff Volcano (Williams, 1932, p. 245) for the small caldera; Hverfjall crater, Iceland (Rittman, 1962, p. 141) is the model for the rampart maar and the profile for the maar is based on Rittman (1962, p. 114). The easternmost crater along profile A-A' (figs. 2 and 3, crater 4) is similar to the normal maar but Prinz B and crater 1 (figs. 2 and 3) are more closely comparable with the rampart or ring-wall type of maar (Rittman, 1962, p. 114). These last two craters are similar in form to the Hverfjall rampart crater in northeast Iceland (Rittman, 1962, p. 141) and certain small explosion craters of the Mono Craters area, California (Cotton, 1944, p. 173).

The lunar craters are as much a 5 km in diameter. Because of the low acceleration of gravity of the Moon's surface we might expect simple lunar craters to be two and possibly three times larger than their terrestrial counterparts. Other factors that may contribute to make lunar craters larger than their terrestrial counterparts have been discussed by Green (1962, p. 175-179).

Crater 6 (fig. 2) resembles a caldera with a flat floor and relatively low walls. It is slightly smaller than the large caldera (Crater Lake, Oregon) illustrated in figure 3, but resembles it in form.

The arcuate rima along the flank of the hill near crater 5 (figs. 1 and 2) is clearly a crater chain. The trend of the crater chain appears

to be controlled by the hill to the south. This hill may be a constructional volcanic feature, such as a volcanic pile. A crater occurs at the junction of the crater chain and Rima Prinz I (fig. 1); it is possible that Rima Prinz I may also be a crater chain.

The rima that zigzags northward from crater 4 is also a chain of craters over at least the last third of its length. Parallelism between the zigzag pattern of this rima and the lineaments in the nearby uplands north of Aristarchus suggests that underlying structures control its form. Thus, not all sinuous rimae may be due to erosion by nuées ardentes as suggested by Cameron (1964).

A straight rima extending northward from crater 6 appears to be a series of elongate craters, which are subparallel to the N 30°W direction of lineaments north of Aristarchus. The trace of this rima may also be controlled by underlying structures.

Conclusions

Hills with apical or flank craters, the craters with associated rimae, and the isolated rimae just west of the Harbinger Mountains, appear to represent a volcanic complex on the Moon. The craters are closely comparable to terrestrial volcanic features, such as maars, rampart or ring-wall maars, and calderas. The rimae, including the sinuous ones, are probably, in part, a series of craterlets whose positions were controlled by underlying structures.

References

Cameron, W. S., 1964, An interpretation of Schröter's Valley and other sinuous rilles: Jour. Geophys. Research, v. 69, no. 12, p. 2423-2430.

Cotton, C. A., 1944, Volcanoes as landscape forms: Christchurch, N. Z., Whitcombe and Tombs, 416 p.

Green, Jack, 1962, The geosciences applied to lunar exploration, in Kopal, Zdenek, and Mikhailov, Z. K., eds., The Moon--Symposium no. 14 of the International Astronomical Union: New York, Academic Press, p. 169-257.

Moore, H. J., 1964, The geology of the Aristarchus Quadrangle of the Moon: U.S. Geol. Survey, Astrogeologic studies annual progress report, August 25, 1962 to July 1, 1963, pt. A, p. 33-45.

Rittman, Alfred, 1962, Volcanoes and their activity, translated from the second German edition by E. A. Vincent: New York, Interscience, 305 p.

Williams, Howell, 1932, Geology of Lassen Volcanic National Park: Calif. Univ. Dept. Geol. Sci. Bull., v. 21, p. 195-385.

Williams, Howell, 1942, The geology of Crater Lake National Park, Oregon: Carnegie Inst. Wash. Pub. 540, 162 p.

IMPACT-INDUCED VOLCANISM

by M. H. Carr

Introduction

Observations of cratered central peaks within the large craters in the Timocharis region (Carr, 1964) led to this investigation of the possibility that volcanism might be induced by impact. Impact energy alone is insufficient to produce extensive volcanism, but lowering of the thermal conductivity of the lunar crust by brecciation below an impact crater, easy access of magma through the breccia lens, and the presence of an impact-induced thermal anomaly near the lunar surface may all tend to induce volcanism in an impact region.

Distribution of heat produced by impact

On the assumption of an impact origin for the crater, the temperature regime around the crater Timocharis immediately subsequent to impact may be evaluated from the shock theory. For a lunar crater, assuming fourth root scaling:

$$E = 10^{23.1} D^4 \quad \text{(Chabai and Hankins, 1960)},$$

where E is the energy in ergs and D is the diameter.

For Timocharis:

$$D = 34 \text{ km}$$

$$E = 10^{23.1} (34)^4$$

$$= 1.68 \times 10^{29} \text{ ergs}$$

$$= 4 \times 10^{21} \text{ cal.}$$

From shock wave theory Gault and Heitowit (1963) derived the following equation for computing irreversible waste heat during shock compression:

$$E_w = 1/2\ u_p^2 \left\{ 1\text{-}2 \left[\frac{a}{bu_p} + \left(\frac{a}{bu_p} \right)^2 \log \frac{a}{a+bu_p} \right] \right\} \qquad (1)$$

where E_w is the waste heat, u_p is the particle velocity, and $u_s = a+bu_p$ where u_s is the shock wave velocity. Assuming that Timocharis formed by an impact in which both the target and projectile had a Hugoniot similar to basalt, and assuming that the shock pressure decayed as the fourth power (Chabai and Hankins, 1960) of the distance from the path of penetration of the projectile, then the above equation can be solved: (a = 2.60, b = 1.62 for basalt (Lombard, 1961)). The solution may be used to obtain the distribution of heat as a function of the distance from the center of gravity of energy release by assuming spherical propagation of the shock. Heat produced by viscous dissipation of kinetic energy behind the shock will be ignored (see Shoemaker and others, 1963).

To determine the heat distribution as a function of distance from

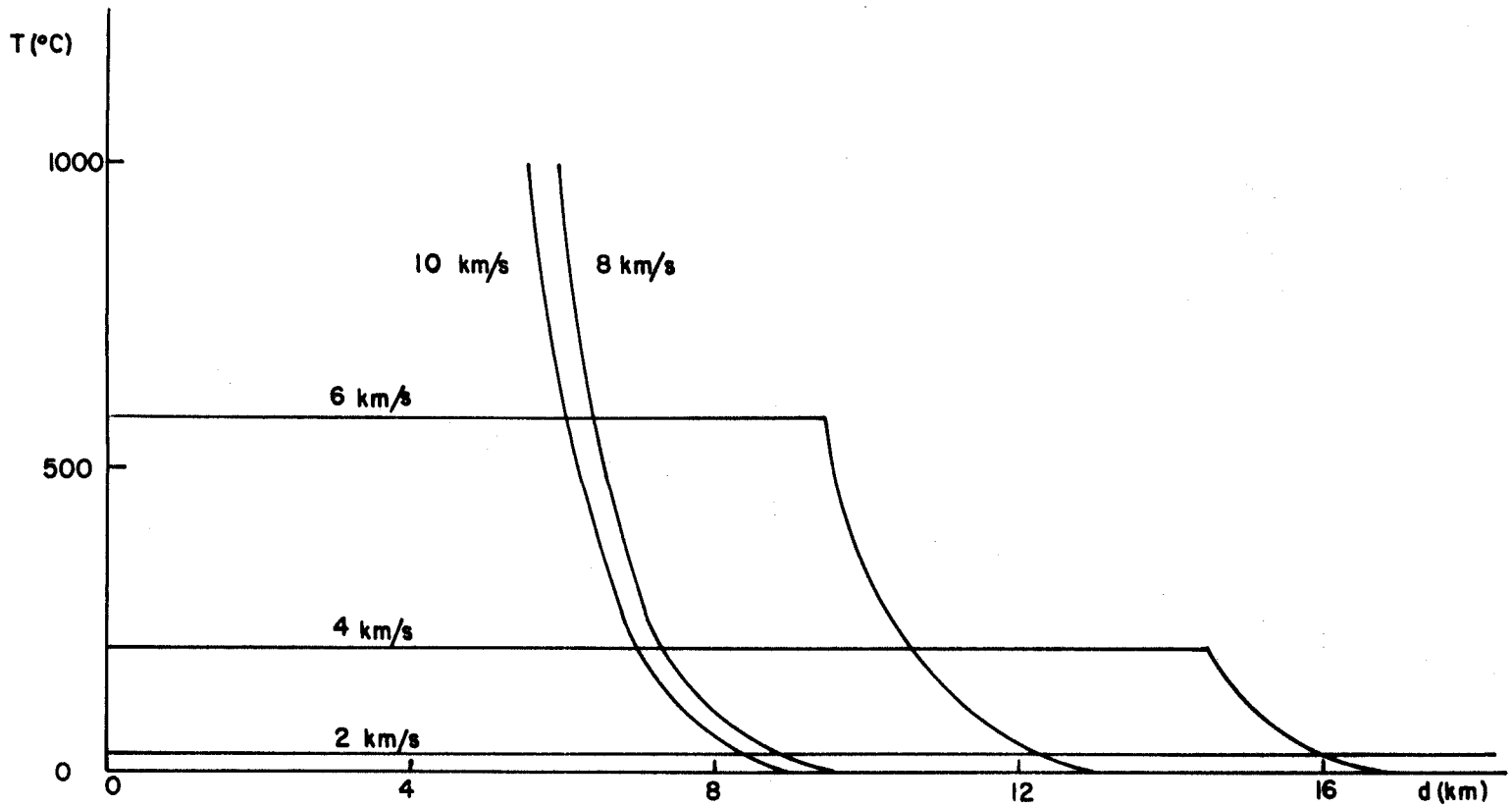

Figure 1. Calculated temperatures (T) below Timocharis as a function of distance below an original surface along a line passing through the center of the crater. Temperature profiles are given for different impact velocities.

the original lunar surface on this model, the depth of the center of gravity of energy release must be computed. Again, assuming basalt Hugoniots for both projectile and target, the particle velocities and shock wave velocities can be determined for a given impact velocity. The partition of energy between target and projectile will be taken as completed when the shock wave generated by impact has reached the back side of the projectile. On this basis the time taken for energy partition is $\frac{2r}{u_s}$, where r is the radius of the projectile and u_s is the shock wave velocity. During this time the interface between unshocked projectile and shocked projectile will have moved a distance $\frac{2r}{u_s}(v-u_s)$, where v is the impact velocity. Then the depth of the center of gravity of energy release below the original surface is

$$\frac{2r}{u_s}\left(v-u_s\right) - \frac{2rp_o}{p}.$$

The solution to equation 1 may now be transposed into a form giving the heat distribution as a function of distance from the lunar surface. In figure 1 the heat distribution is expressed as temperature, having taken 1 cal/gm/°C for the specific heat of the lunar crust. Fusion temperatures are reached only for impact velocities greater than 8 km/sec. At an impact velocity of 8 km/sec sufficient heat is available to melt 50 km^3 of rock, taking the latent heat of fusion as 300 cal/gm. At a

velocity of 10 km/sec, 45 km^3 may be melted, with heat left over for vaporization of some of the material. The nature of the partition of heat between fusion and vaporization is not known. Much of the fused material will be ejected during impact.

For impact velocities greater than 8 km/sec, sufficient fused material is available to form the central peak of Timocharis (10 km^3). The high albedo of the central peak (Carr, 1964), however, suggests that the central peak formed later than the crater. It is instructive, therefore, to consider what effect the impact had on the subsequent thermal history of the crater.

Thermal history of craters after impact

The presence of possible volcanic features, such as domes and crater chains, apparently unrelated to impact, suggests that the thermal gradient was close to the minimum melting point gradient at some depth within the Moon at the time of formation of these features. Impact could affect the normal thermal gradient in the following ways:

(1) The gradient will become steeper beneath the crater as a consequence of reduced thermal conductivity due to brecciation.

(2) Transient elevation of the isotherms below a large crater will result from the presence of a transient heat source near the surface.

(3) Rise in temperature near the surface caused by shock heating

will cause a transient lowering of the thermal conductivity in the heated material.

(4) The fusion temperatures of the materials below the crater will be lowered because of the release of pressure by ejection of material from the crater.

The effect of each of these mechanisms will be considered individually. By analogy with Meteor Crater (Shoemaker, 1960 and 1963) and the Holleford, Brent, and Deep Bay craters (Innes, 1961), Timocharis should be underlain by a breccia lens extending to a depth of approximately 7 km below the crater rim. The breccia underlying the Brent crater has a higher porosity, lower density (Innes, 1961) and lower thermal conductivity than the surrounding unbrecciated materials. Similarly, Timocharis should be underlain by a zone of low conductivity. If the principal mode of heat transfer is diffusion, then the effect of decreasing the conductivity will be to increase the thermal gradient below the crater. In other words, the equilibrium temperature below the crater will rise (fig. 2).

The high temperature created near the surface by impact will have the effect of an insulating layer, causing temperatures below the anomaly to rise. The energy required will be derived both from the high temperature anomaly above and from lunar internal heat. The depth to which the heat anomaly will be felt, and the magnitude of the subsequent temperature elevations will depend on the duration of the high temperature anomaly

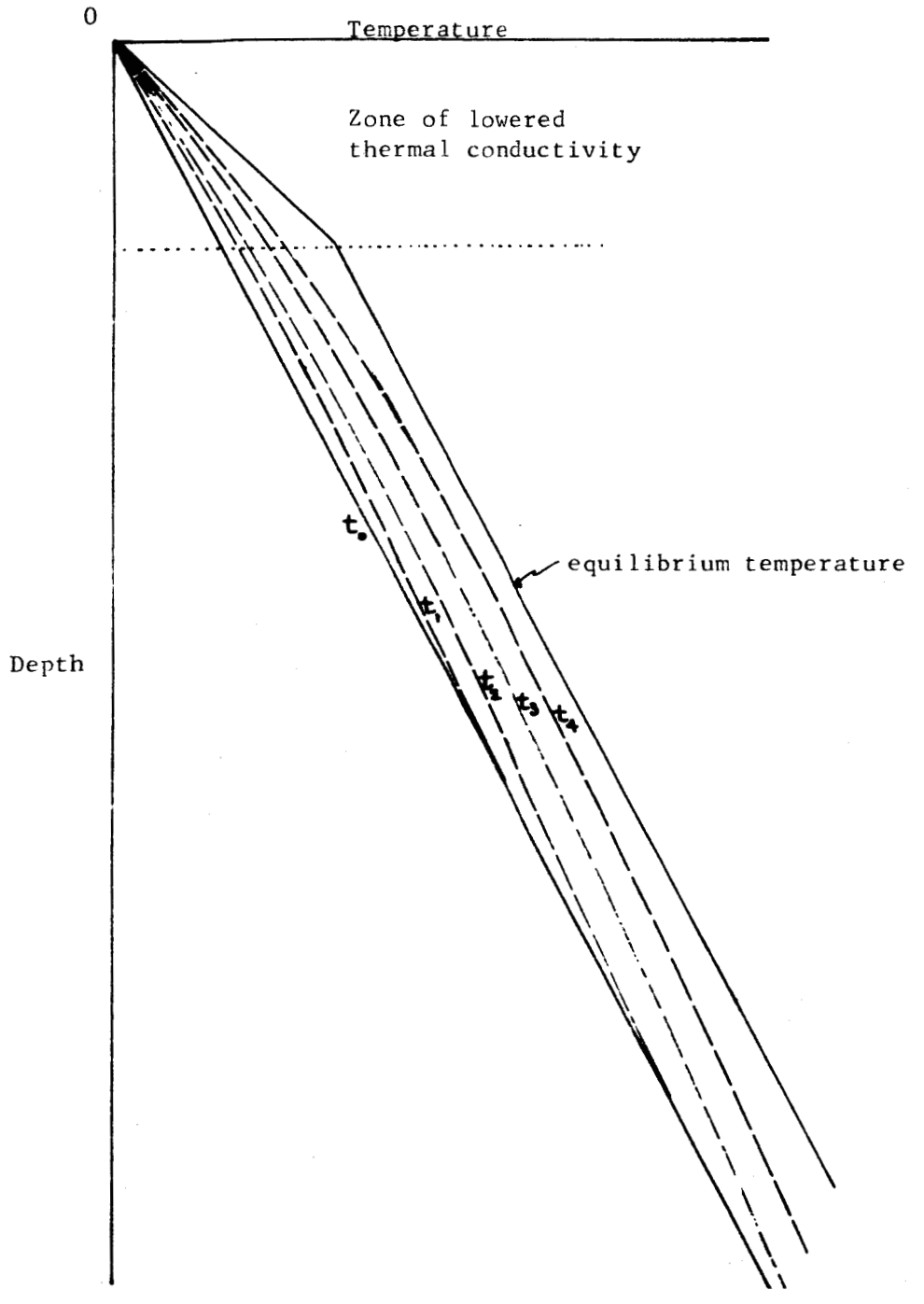

Figure 2. Schematic diagram showing the changes in temperature caused by a lowering of the thermal conductivity near the surface. t_o represents the temperature profile before impact. t_1, t_2, etc. represent temperature profiles at successive times after impact.

at the surface and on the magnitude of the thermal gradient. Estimates may be made of the length of time the anomaly will persist. As a first very crude approximation we can assume that after impact, a uniform temperature of 1000°C extends to 4 km below Timocharis, and below this the temperature is initially at zero. In the real case, the initial temperature decreases exponentially downward. The effect of the simplifying assumption will be to increase the estimate of time required for a given rise of temperature at depth perhaps by more than an order of magnitude.

From the theory of heat flow (Ingersoll and others, 1948),

$$T = \frac{T_o}{\pi}\left[\int_{-x\upsilon}^{(\ell-x)\upsilon} e^{-\beta^2}\,d\beta - \int_{x\upsilon}^{(\ell+x)\upsilon} e^{-\beta^2}\,d\beta\right],$$

where T is the temperature at the distance x from the surface; T_o is the initial temperature (1000°C); ℓ is the thickness of the original high temperature zone (4 km); $\upsilon = 1/2\ \alpha t$, where t is time and α is diffusivity (0.012). According to this model, at a depth of 2 km from the surface, the temperature will fall to 600°C in 9000 years; to 200°C in 40,000 years; and to 80°C in 90,000 years. At a depth of 8 km the temperature will rise over 100°C in 40,000 years above the existing gradient. During the period of cooling of the near surface anomaly, the lunar interior is essentially insulated from the surface so that the heat flow from the

interior of the Moon will supplement the temperature rise below the breccia lens due to diffusion of heat downward from the anomaly. This supplementation will, of course, be partially offset by the divergence of the lines of heat flow around the anomaly. Figure 3 shows schematically the expected temperature variations after impact, taking into account the thermal gradient.

Thermal insulation at the surface caused by temperature elevation may be further enhanced by a decrease in conductivity caused by rise in temperature. Lubimova (1958) showed that below temperatures at which radiative heat transfer becomes important (close to melting), thermal conductivity varies inversely with temperature. Because of this effect, McBirney (1963) suggested transient thermal instability could result in the Earth. The conditions for thermal instability are a rise in temperature at the surface over a zone of low conductivity, the exact conditions which should prevail under an impact crater. According to McBirney, the transient instability would persist until the temperatures in the high temperature zone rose to the fusion temperature. The effectiveness of this mechanism is in doubt, because experimental observations have not indicated an appreciable lowering of thermal conductivity with increasing temperature (Birch and others, 1942). If real, this mechanism could explain volcanism induced by impact.

One further effect that may lead to melting beneath an impact crater

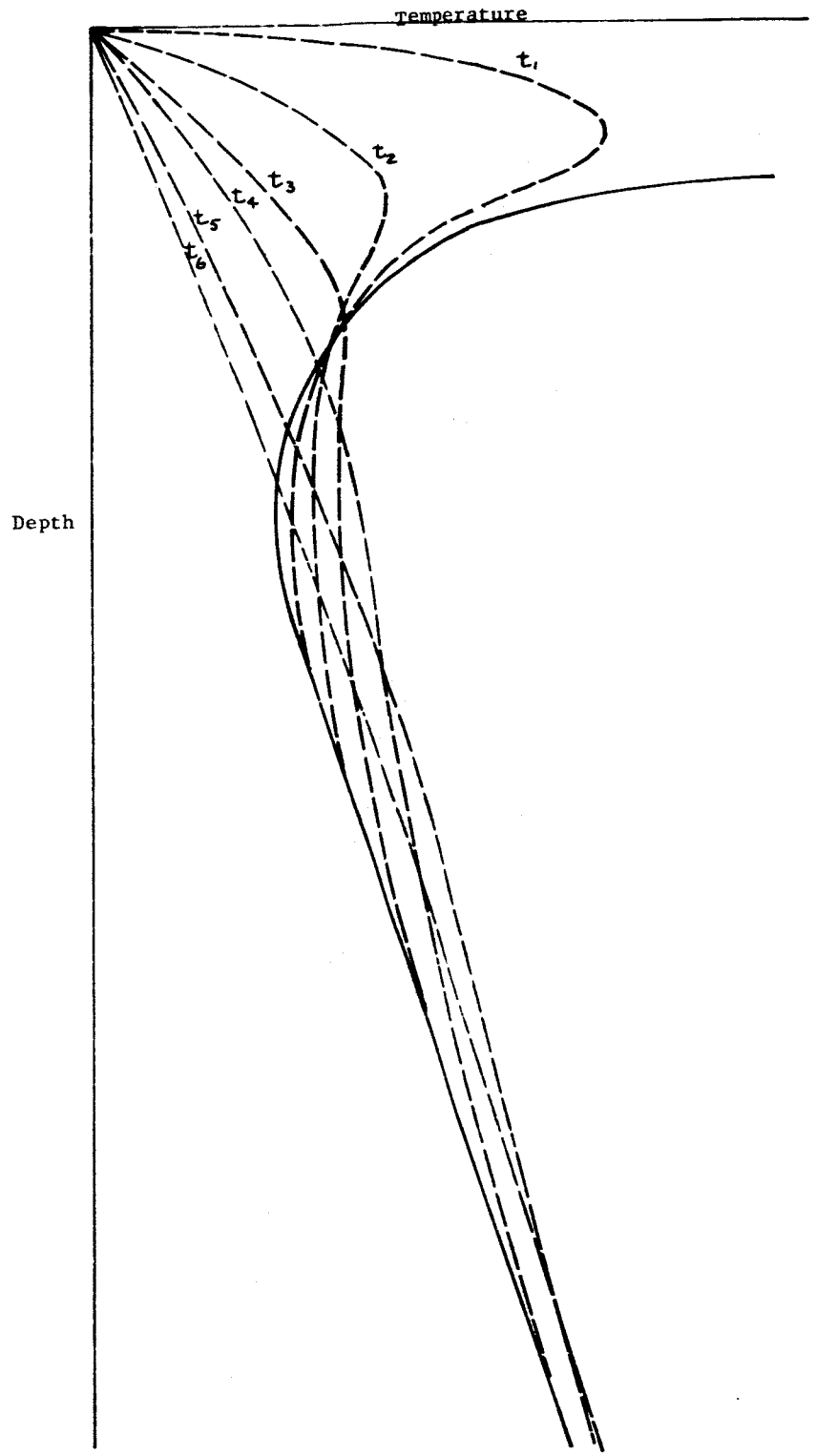

Figure 3. Schematic diagram showing expected temperature changes after impact. t_1, t_2, etc. represent temperature profiles at successive times. Solid line represents temperature profile immediately after impact.

is the lowering of the melting point of rock materials by the release of compressional stress (Uffen, 1959). Material is ejected from a crater during impact and the crater floor lies below the level of the original surface. Thus, the lithostatic pressure below the crater will decrease. For Timocharis this could lead to a change in melting temperature of only a few degrees and so the mechanism is thought to have a negligible effect on volcanism.

Of the four mechanisms which could lead to a rise in the temperature below an impact crater, only the presence of a heat source near the surface and the lowering of thermal conductivity are considered significant for craters the size of Timocharis. Without knowing the thermal gradient in the Moon, the depth at which melting would occur as a result of these effects cannot be calculated. For high velocities of impact (greater than 6 km/sec) the high temperature source near the surface is probably the dominant cause of a temperature rise at depths below an impact crater. For lower velocities of impact, the lowering of thermal conductivity by brecciation may be more important than the transient thermal anomaly.

Assuming the temperature rise at depth is sufficient to cause melting, then a different process for heat transfer would operate after melting. Mass transport would then be more effective than diffusion. This transport may be of volatiles or of the magma itself rising to the

surface. Whichever the transport mechanism, the highly porous breccia lens would provide an avenue through which transport could be rapid. Thus, subsequent volcanism might be expected above the breccia lens in the crater, as is suspected in the case of Timocharis.

Effect of impact on thermal history of Mare Imbrium

This theory of magma generation and volcanism has broad implications concerning the history of the Moon. If the Mare Imbrium basin was formed by impact, then a high temperature anomaly should have existed close to the lunar surface for an extended period of time. The time during which the heat anomaly persisted at the surface can be computed following the same line of reasoning as that used above for Timocharis. The diameter of the inner ring of peaks of the Mare Imbrium may be taken as the diameter of the original crater. Minimum times for cooling from an assumed 1000°C at a depth of 60 km are 25 million years to 600°C, 100 million years to 200°C, and 230 million years to 100°C. Thus, for an extended period of time the interior of the Moon was effectively insulated from the surface in the Imbrian region. During this period, increase in temperature at depth must have resulted. This may well have led to extensive fusion in the lunar interior. Once fusion occurred, rapid egress of the magma to the surface would be possible because of the extensive fracturing caused by the Imbrian event (which is expressed at the surface

as the Imbrian sculpture). The time between impact and melting depends on the original thermal gradient. This time may easily have been as long as a billion years. This mechanism would explain the apparent time gap between the formation of the Mare Imbrium basin and its filling with mare material (Shoemaker, 1962, p. 350; Shoemaker and Hackman, 1962, p. 299).

The thermal history of the Moon could be profoundly affected by the insulating effect of impact. The formation of large impact basins would result in low internal heat losses for long periods in the Moon's history. These could lead to much higher temperatures within the Moon than would be anticipated without considering the effects of impact.

Conclusions

(1) Shock heating during impact is insufficient to produce extensive volcanism on the Moon.

(2) The formation of an impact crater reduces the local thermal conductivity and increases the temperature at the surface. These two effects will result in a later rise of temperature at depth, and could bring about melting at depth and subsequent volcanism.

References

Birch, Francis, Shairer, J. F., and Spicer, H. C., 1942, Handbook of physical constants: Geol. Soc. America Spec. Paper 36, 325 p.

References--Continued

Carr, M. H., 1964, The geology of the Timocharis Quadrangle: U.S. Geol. Survey, Astrogeologic studies annual progress report, August 25, 1962 to July 1, 1963, pt. A, p. 9-23.

Chabai, A. J., and Hankins, D. M., 1960, Gravity scaling laws for explosion craters: U.S. Atomic Energy Comm., SC-4541 (RR), 18 p.

Gault, D. E., and Heitowit, E. D., 1963, The partition of energy for hypervelocity impact craters formed in rock: Symposium on hypervelocity impact, 6th, Proc., v. 2, pt. 2, p. 419-457.

Ingersoll, L. R., Zobel, O. J., and Ingersoll, A. C., 1948, Heat conduction: New York, McGraw-Hill, p. 276.

Innes, M. J. S., 1961, The use of gravity methods to study the underground structure and impact energy of meteoritic craters: Jour. Geophys. Research, v. 66, no. 7, p. 2225-2239.

Lombard, D. B., 1961, The Hugoniot equation of state of rocks: U.S. Atomic Energy Comm., UCRL-6311, 28 p.

Lubimova, H. A., 1958, Thermal history of the earth with consideration of the variable thermal conductivity of its mantle: Geophys. Jour., v. 2, p. 115-134.

McBirney, A. R., 1963, Conductivity variations and terrestrial heat flow distribution: Jour. Geophys. Research, v. 68, no. 23, p. 6323-6329.

References--Continued

Shoemaker, E. M., 1960, Penetration mechanics of high velocity meteorites, illustrated by Meteor Crater, Arizona: Internat. Geol. Cong., 21st, Copenhagen 1960, Rept., pt. 18, p. 418-434.

Shoemaker, E. M., 1962, Interpretation of lunar craters, in Kopal, Zdenek, ed., Physics and astronomy of the Moon: New York, Academic Press, p. 283-359.

Shoemaker, E. M., 1963, Impact mechanics at Meteor Crater, Arizona, in Middlehurst, Barbara, and Kuiper, G. P., eds., The Moon, meteorites, and comets--The solar system, vol. IV: Chicago, Univ. of Chicago Press, p. 301-336.

Shoemaker, E. M., Gault, D. E., Moore, H. J., and Lugn, R. V., 1963, Hypervelocity impact of steel into Coconino sandstone: Am. Jour. Sci., v. 261, no. 7, p. 668-682.

Shoemaker, E. M., and Hackman, R. J., 1962, Stratigraphic basis for a lunar time scale, in Kopal, Zdenek, and Mikhailov, Z. K., eds., The Moon--Symposium no. 14 of the International Astronomical Union: New York, Academic Press, p. 289-300.

Uffen, R. J., 1959, On the origin of rock magma: Jour. Geophys. Research, v. 64, no. 1, p. 117-122.

INFRARED EMISSION FROM THE ILLUMINATED MOON

by Kenneth Watson

Introduction

Present knowledge of the lunar surface is based almost entirely on observations of the emission and reflection of radiation. The pioneer work of Pettit and Nicholson (1930) on the 8 to 14μ emission of the illuminated Moon and of the Moon during a total eclipse provided the first evidence that the surface materials are in a finely divided or porous state. The strong back-scattering of visible light from the lunar surface (Barabashev, 1923; Markov, 1924; Fedoretz, 1952; and van Diggelen, 1959) implies a surface layer with a very open structure. Theoretical studies of the infrared emission and the visible light reflection from the lunar surface, however, have tended to develop along independent lines with only qualitative discussions of their application to each other. It is the purpose of this report to examine the implications of the visible lunar photometric function on the infrared emission of the illuminated Moon.

Infrared emission of the illuminated Moon

Pettit and Nicholson (1930) observed that the infrared emission of the limb of the Moon near zero phase angle along the lunar equator

exceeds that which would be expected from a Lambert emitter. Pettit and Nicholson have proposed that their equatorial observations approximately fit a 2/3 power of the cosine of the brightness longitude:

$$E = E_o \cos^{2/3} (\beta - \beta_o),$$

where

β = lunar longitude;

λ = lunar latitude;

E = observed emission from the point $\lambda = o, \beta$;

β_o = longitude of the subsolar point; and

E_o = observed emission from the subsolar point,

$\lambda = o, \beta = \beta_o$.

As the absorbed energy at any point on the Moon's surface is proportional to the co-albedo, it is clear that this experimental fit ignores variations in normal albedo. Pettit and Nicholson suggested that the departure from Lambert emission is due entirely to the fact that at full Moon no shadows are seen, so that only illuminated surfaces contribute to the infrared emission. They discuss this phenomenon in terms of lunar mountains and valleys, but it is clear that the average slopes at this scale (McCauley, unpublished communication) are much too low to produce appreciable excess infrared emission of the limb. If, on the other hand, the scale of roughness is less than a few centimeters, then reradiation

between surfaces which are illuminated or shadowed tends to produce a uniform emission which is Lambertian in character. In fact, Pettit and Nicholson point out that small depressions will have enhanced emission toward the selenographic zenith and diminished emission toward the horizon. Neither the roughness on a scale greater than a kilometer nor roughness on a scale below a few centimeters appears to provide an adequate explanation of the observed excess infrared emission at the limb.

In an attempt to discover the causes of excess infrared emission at the limb, an investigation was undertaken of the variation of the total reflectivity of an element of the lunar surface as a function of the angle of incidence of the solar radiation. A greater understanding of the lunar infrared emission should result if a comparison is made between the observed infrared emission and the theoretical infrared emission from a surface which obeys the visible lunar photometric function.

The visible light reflection from the Moon.--Various theoretical models have been proposed to explain the large backscattering component of the Moon's reflectivity: the geometrical surface models examined include grooves (Barabashev, 1923), spherical domes (Schönberg, 1925), hemi-ellipsoidal cups (Bennett, 1938; van Diggelen, 1959), and "fairy castles" (Hapke, 1963). For the purposes of this study, the Hapke model was selected for the theoretical computations of the total reflectivity because it probably best fits the observations of Fedoretz (1952), and

van Diggelen (1959). It is important to note that, although the surface models for infrared emission and visible reflection must be consistent, the effective depths to which these must apply are quite different. The extension of models based solely on visible light photometric properties to any depths below a few dust-size grains is not justified.

Derivation of the total reflectivity of a surface element from the differential scattering law.--The relationship between the angles of incidence (i), reflection (ϵ), local phase (α), and azimuth (μ), where $\underline{n}$ is the vector normal to the surface element are illustrated in figure 1. The phase angle is measured in the plane containing the incident and reflected rays, and the azimuth is measured in the plane of the surface element. From elementary vector analysis it can be shown that:

$$\cos \alpha = \sin i \sin \epsilon \cos \mu + \cos i \cos \epsilon. \qquad (1)$$

Now we shall define dI to be the intensity of the reflected light per unit area, which is received from a surface element of area dA, at a reflection angle ϵ, for unit intensity light incident on dA at an angle i. Then the total reflectivity R(i), defined as the fraction of the incident light which is reflected from the surface, is given by:

$$R(i) = 2 \int_{\epsilon=o}^{\pi/2} \int_{\mu=o}^{\pi} \frac{\sin \epsilon}{\cos i} \, dI d\epsilon d\mu \qquad (2)$$

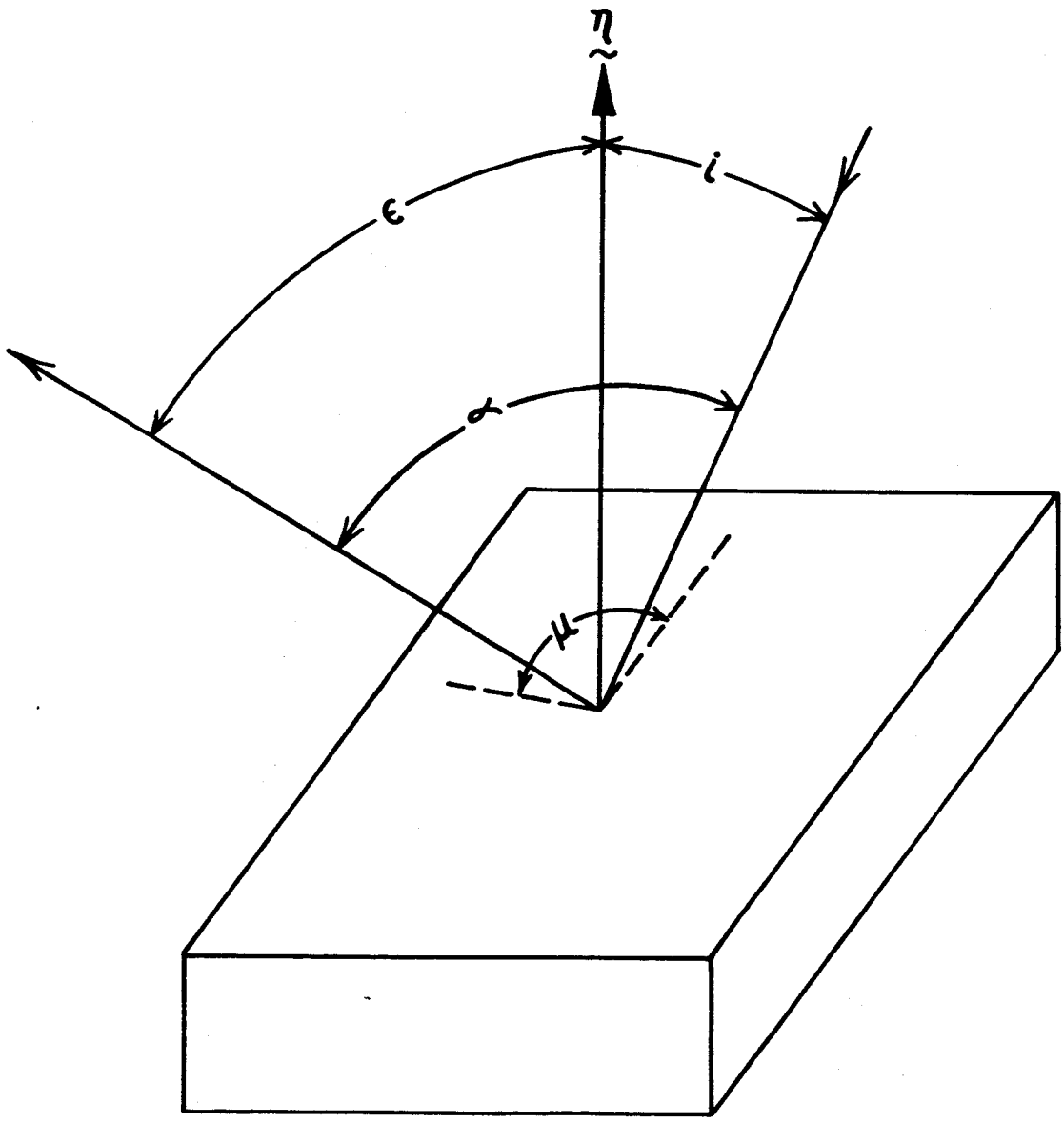

Figure 1. Angles defined for surface element.

We shall further define E(i) as the energy absorbed at the surface element dA, and it is simply the difference between the incident and reflected energies:

$$E(i) = (1 - R(i)) \cos i. \qquad (3)$$

During the following discussion we shall use the subscript H when referring to the Hapke photometric model and the subscript L when referring to the Lambert photometric model.

From Hapke (1963, p. 4577, equation (10))

$$I(i,\epsilon,\alpha) = E_o \alpha d\omega \frac{2}{3\pi} b \cdot \frac{1}{1+\cos \epsilon/\cos i} \cdot \frac{\sin \alpha + (\pi-\alpha)\cos \alpha}{\pi} \cdot B(\alpha,g),$$

where $\frac{2b}{3}$ = normal albedo (p. 4582, equation (12))

$$B(\alpha,g) = 2 - \frac{\tan \alpha}{2g} (1-e^{-g/\tan \alpha})(3-e^{-g/\tan \alpha}), \text{ when } \alpha \leqslant \frac{\pi}{2} \text{ and}$$

$$B(\alpha,g) = 1, \text{ when } \alpha \geqslant \frac{\pi}{2}.$$

g = a numerical constant ranging from 0.4 to 0.8 which Hapke relates to the degree of compaction of the surface;

E_o = flux of energy in the direction of incidence;

α = area of the detector;

$d\omega$ = solid angle of the acceptance cone of the detector=dA cos ϵ.

Now dI in equation (2) of this report is related to Hapke's I by:

$$dI = \frac{I}{E_o \alpha dA}. \tag{4}$$

Defining K_H to be the normal albedo, we obtain from (4) and (2):

$$R_H(i) = 2 \int_{\epsilon=o}^{\pi/2} \int_{\mu=o}^{\pi} K_H \frac{\sin \epsilon \cos \epsilon}{\cos i + \cos \epsilon} \cdot \frac{\sin \alpha + (\pi-\alpha)\cos \alpha}{\pi} B(\alpha,g) d\epsilon d\mu \tag{5}$$

where

$$\alpha = \alpha(i,\epsilon,\mu) \text{ as given in equation (1).}$$

From equation (3)

$$E_H(i) = (1-R_H(i)) \cos i. \tag{6}$$

For a Lambert reflector (see for example Hapke, 1963, p. 4582 and the previous analysis)

$$dI_L = \frac{\cos i \cos \epsilon}{\pi}, \tag{7}$$

$$\text{and } \therefore R_L(i) = 1. \tag{8}$$

Thus we obtain the obvious result that a perfectly diffuse reflector

reflects all the energy incident on it. It has been general practice, when discussing the lunar infrared emission, to use a photometric model, thus "almost a Lambert reflector," that is, a body which obeys the Lambert differential reflection law but absorbs some of the incident energy. This model is similar to the gray body introduced for convenience in radiation physics. For this case then,

$$dI_L = K_L \frac{\cos i \cos \epsilon}{\pi}, \tag{9}$$

where K_L is equivalent to a normal albedo.

Thus, $$R_L(i) = K_L \tag{10}$$

and $$E_L(i) = (1-K_L) \cos i. \tag{11}$$

The total reflectivity for the Hapke model and the Lambert model are plotted as a function of the angle of incidence in figure 2. The results for the Hapke model were computed by numerical integration of equation (5) on an IBM 7094 computer. For convenience, the total reflectivities are both made equal to unity at zero incidence. The increase in total reflectivity with increasing angle of incidence for the Hapke model (fig. 2) implies that the total energy absorbed must also decrease. This would lead to a dark limb in the infrared emission. The normalized absorbed energy for the Hapke and Lambert models are plotted against

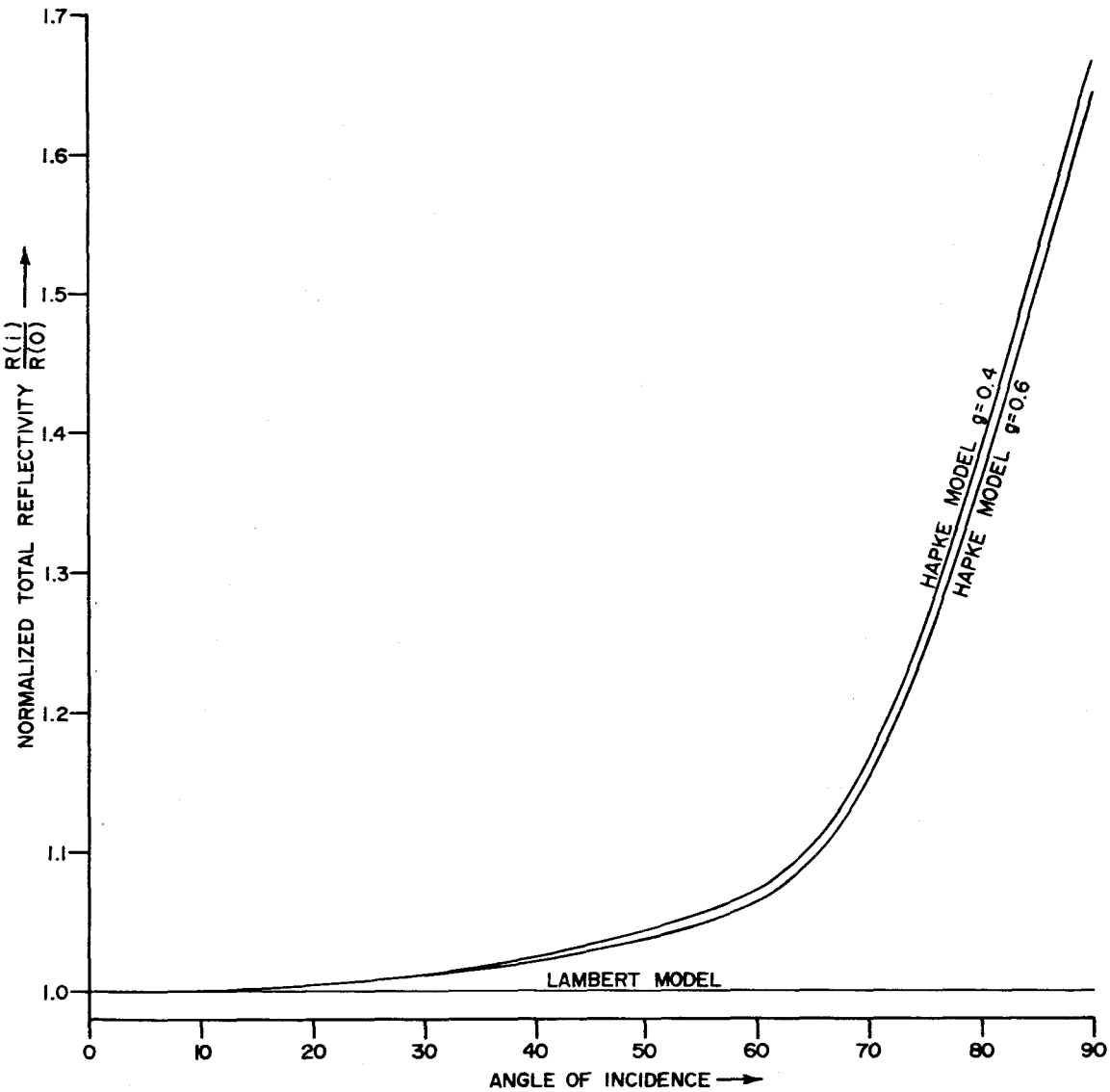

Figure 2. Normalized total reflectivity as a function of angle of incidence.

Pettit and Nicholson's observations of the infrared emission in figure 3. It can be seen that the variation in total visible reflectivity, as a function of angle of incidence, does not provide an adequate explanation of the observed lunar infrared emission.

Conclusions

Previous explanations by Pettit and Nicholson, of their 1930 infrared observations, imply significantly steeper slopes, at a scale greater than a kilometer, than exist on the Moon. The total visible reflectivity of the lunar surface, computed from Hapke's model, increases as the angle of incidence increases, thus implying a limb darker than that expected for a Lambert reflector. Thus neither the model of Pettit and Nicholson nor that of Hapke is adequate to explain the observed infrared emission of the limb. Two possible explanations of the observations are: (1) the roughness on a scale between a centimeter and a meter is sufficient to produce the necessary shadowing or (2) the emission from a lunar surface element is non Lambertian in distribution. Finite transparency of grains on the surface cannot explain the observations as the temperature gradients at the two limbs are reversed. The resulting emission would be greater at the sunset limb than at the sunrise limb. Further studies utilizing slope distributions as observed both from the Ranger photographs and from occultation studies will examine the effect of small scale

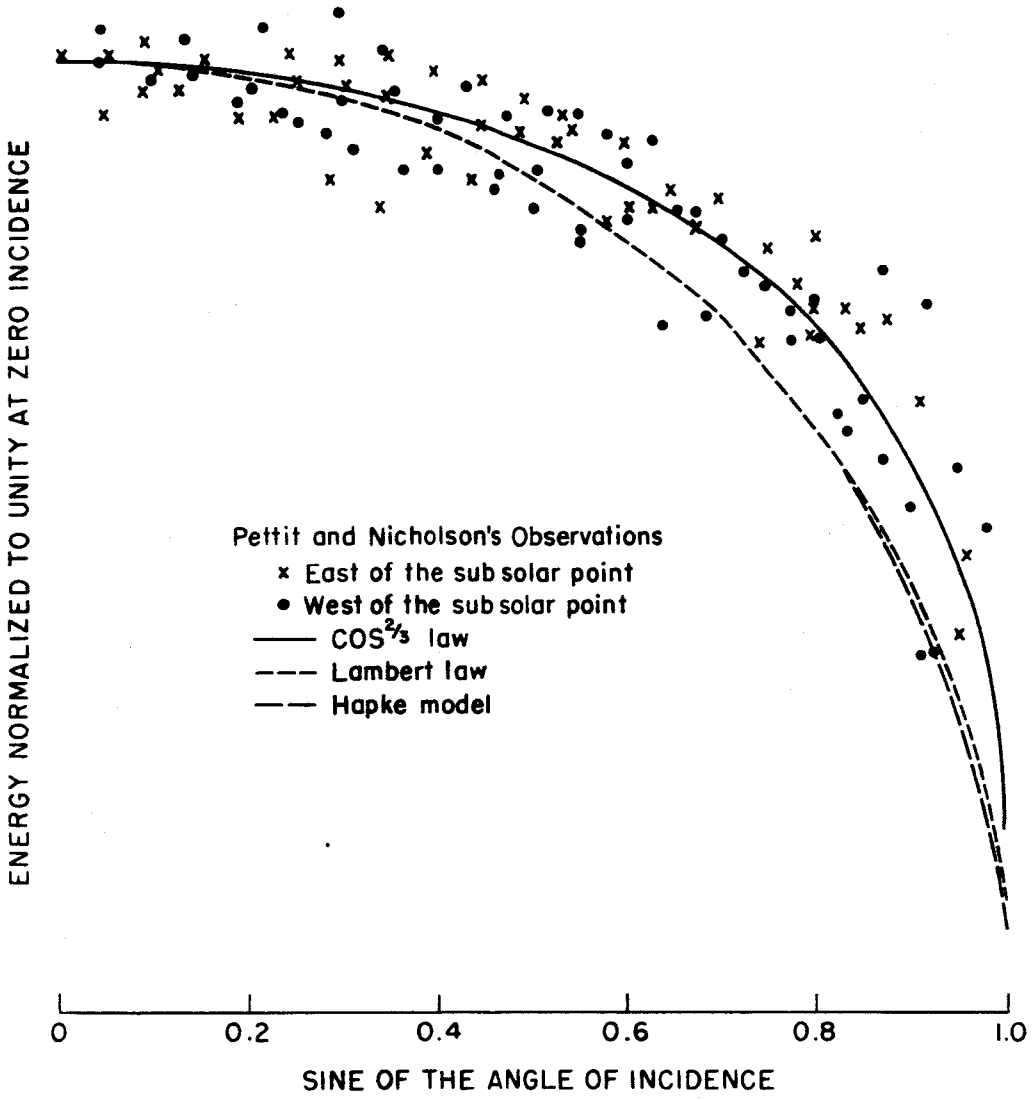

Figure 3. Computed absorbed energy as a function of sine of angle of incidence compared with Pettit and Nicholson's infrared observations of emitted energy.

roughness on the lunar infrared emission. It is possible that the observed low infrared emission at the limb may be related to the high spatial density of secondary craters on the lunar surface.

References

Barabashev, N. P., 1923, Bestimmung der Erdalbedo und des Reflexionsgesetzes für die Oberflache der Mondmeere--Theorie der Rillen: Astron. Nachr., v. 217, p. 445-452.

Bennett, A. L., 1938, A photovisual investigation of the brightness of 59 areas on the Moon: Astrophys. Jour., v. 88, p. 1-26.

Diggelen, J. van, 1959, Photometric properties of lunar crater floors: Utrecht Observ. Recherches Astron., v. 14, no. 2, 114 p.

Fedoretz, V. A., 1952, Photographic photometry of the lunar surface [in Russian]: Kharkov Univ. Astron. Observ. Trudy, v. 2, p. 49-172.

Hapke, Bruce, 1963, A theoretical photometric function for the lunar surface: Jour. Geophys. Research, v. 68, p. 4571-4586.

Markov, A. V., 1924, Les particularités dans la réflexion de la lumière par la surface de la lune: Astron. Nachr., v. 221, p. 65-78.

Pettit, Edison, and Nicholson, S. B., 1930, Lunar radiation and temperatures: Astrophys. Jour., v. 71, p. 102-135.

Schönberg, Erich, 1925, Untersuchungen zur Theorie der Beleuchtung des Mondes auf Grund photometrischer Messungen: Soc. Sci. Fennicae Acta, v. 50, p. 1-70.

A SYSTEMATIC PROGRAM OF PHOTOELECTRIC AND PHOTOGRAPHIC PHOTOMETRY OF THE MOON

by H. A. Pohn

The determination of many characteristics of the lunar surface are based on measurements of the local photometric phase function of the Moon. For example, the insolation function used to compute the heat flow for comparison of theoretical models with infrared observations assumes a known photometric function for the lunar surface (Watson, unpublished doctorial thesis, California Institute of Technology). Microdensitometric measurements of existing lunar plates for determination of slopes and analysis of terrain requires that the plate be calibrated and the normal albedo mapped (Wilhelms, 1964; McCauley, unpublished communication). The optimum design and adjustment of cameras on unmanned lunar spacecraft must be based on the measured phase function of the intended target area on the Moon. To meet these and other needs of lunar geologic investigations, an extensive program of precise photographic and photoelectric photometry has been undertaken by the Geological Survey. The results of this program will be used to prepare a photoelectrically calibrated photographic atlas of the Moon.

The techniques of extracting photometrically accurate photoelectric and photographic information about the Moon from telescopic observations

date back only to the mid-1930's. Rougier (1933) made the first observations of the integrated brightness of the lunar disk as a function of phase. Most of the usable information about the surface brightness of the Moon has been gathered by photographic means, notably by Fedoretz (1952), and later augmented by van Diggelen (1959). Until recently, however, low reliability of photomultiplier tubes, nonlinear response of photographic emulsions, and nonuniform exposure and development of photographic emulsions prevented accurate photoelectric and photographic measurements. The photoelectric observations of lunar color indices (van den Bergh, 1962) and eclipse observations by Barbier (1961) represent notable advances in photometric observations of the Moon.

In order to insure the most precise photographic measurement possible it is necessary to reduce the sources of error in photographic systems. Experimentation by the author has shown that standard commercial focal plane shutters typically exhibit nonuniform shutter travel, producing variations of exposure exceeding 100 percent. The highest quality spectroscopic emulsions have a variation of plate response of $\pm$ 3 percent of the mean plate density, and commercial plate processing equipment leads to variation of development within individual plates of 10 to 20 percent from the mean plate response.

For these reasons it was decided to depart from commercial systems and to design an entirely different, integrated, photographic system.

Early in 1963, the design of a photometric camera was begun at the California Institute of Technology by the author, with the cooperation of Robert Wildey, and James Westphal, for use at the 20-inch telescope at Palomar Mountain in California. The camera completed by the Geological Survey, has less than 1 percent variation in shutter speed for speeds of 1/25 of a second and slower. This improvement was accomplished by use of a high torque motor to pull a set of adjustable slits which run on mated teflon ways. A larger and more accurate camera will be built for use on both the 30-inch telescope of the Geological Survey and the 24-inch telescope of Arizona State College, both located at Flagstaff, Arizona. Several plate processing systems are presently under investigation, including the Mount Wilson rotating rocker and the nitrogen burst system developed by Eastman Kodak. Processing by each system produces internal variations in plate response of about 3 percent of mean plate density, and further tests are needed before a proper evaluation can be made.

Preliminary photoelectric observations by Wildey and Pohn have been under way for the past 2 years using the Mount Wilson 60-inch reflector and the Palomar 20-inch reflector. The standard observing program for a given night begins with the photoelectric observation of a number of standard stars, UBV color indices of which are determined using the system established by Johnson and Morgan (1953). These observations provide corrections for various color changes caused by atmospheric extinction.

Photoelectric scans are then made across selected regions of the Moon to establish standard reference areas. Next, photographs are taken in the visible, blue and ultraviolet regions of the spectrum. The lunar surface brightness in these colors then is calibrated by the photoelectric observations. Finally, the selected regions are again scanned and the standard stars remeasured to provide residual corrections for changes in the atmospheric extinction. In fiscal year 1965, this observing program will be conducted using the new photoelectric photometer and the new photometric camera constructed for use at Flagstaff, Arizona for an entire lunation. The procedure will be repeated over 3 or 4 lunations separated by several months.

The photoelectric scans will be used to calibrate scans across the photographic plates made with a microphotometer. By this means the plates can be used to determine the phase functions for small areas on the Moon approaching in diameter the resolution of the plates. This data can, in turn, be used to calibrate existing lunar plates. In addition the information will be used to construct a photoelectrically calibrated, photographic atlas for phase angles ranging from -140 to +140°. This atlas will contain plates in three colors taken with a spacing of approximately 5° phase angle between photographs. Each photograph will be intercalibrated with step wedges and photoelectric tracings.

References

Barbier, Daniel, 1961, Photometry of lunar eclipses, in Kuiper, G. P., and Middlehurst, B. M., eds., Planets and satellites--Vol. III of The solar system: Chicago, Univ. of Chicago Press, p. 249-271.

Bergh, Sidney van den, 1962, The color of the Moon: Astron. Jour., v. 67, no. 2, p. 147-150.

Diggelen, J. van, 1959, Photometric properties of lunar crater floors: Utrecht Observ. Recherches Astron., v. 14, no. 2, 114 p.

Fedoretz, V. A., 1952, Photographic photometry of the lunar surface [in Russian]: Kharkov Univ. Astron. Observ. Trudy, v. 2, p. 49-172; also Kharkov Univ. Uchenye Zapiski, v. 42, p. 49-172.

Johnson, H. L., and Morgan, W. W., 1953, Fundamental stellar photometry for standards of spectral type on the revised system of the Yerkes spectral atlas: Astrophys. Jour., v. 117, no. 3, p. 313-352.

Rougier, Gilbert, 1933, Photométrie photoélectrique globale de la lune: Strasbourg Observ. Annales, v. 2, no. 3, p. 203-339.

Wilhelms, D. E., 1964, A photometric technique for measurement of lunar slopes: U.S. Geol. Survey, Astrogeologic studies annual progress report, August 25, 1962 to July 1, 1963, pt. D, p. 1-12.

INITIATION OF A PROGRAM OF LUNAR POLARIMETRY

by D. E. Wilhelms

A Lyot visual polarimeter has been mounted for measurements of the Moon on the 12-inch refractor of Lick Observatory, Mt. Hamilton, California. The degree of polarization of light reflected from the Moon and the orientation of the plane of polarization is being measured at small intervals of phase angle for each lunar geologic unit, beginning in areas in which the geology already has been mapped. The purpose of the program is to obtain the polarization properties to aid in the discrimination and identification of lunar geologic units.

The values of maximum polarization, which are obtained near the quarter phases, are of particular interest. In addition, points of crossover between positive and negative polarization, which occurs about two days before and after full moon, will be studied carefully. Previous workers disagree as to whether the crossover occurs instantly or gradually. The data on polarization will be compared with photometric data to provide a more complete picture of the optical properties and fine-scale structure of the lunar surface.

Preliminary results indicate that polarization can be measured for areas 8 km in diameter on the lunar surface under conditions of good seeing with the instruments employed.

DESCRIPTION OF AN EXTENSIVE HUMMOCKY DEPOSIT AROUND THE HUMORUM BASIN

by S. R. Titley and R. E. Eggleton

In a study of the distribution of a regional deposit around Mare Imbrium, Eggleton and Marshall (1962) noted several areas of hummocky material near Mare Humorum. These areas and others in the southern part of the Moon were interpreted as outlying exposures of the regional deposit related to Mare Imbrium now called the Fra Mauro Formation (Eggleton, 1964). Correlation of the hummocky material in these outlying areas with the Fra Mauro was based on similarities in topography and normal albedo and on its wide distribution. Recent studies of the distribution of the Fra Mauro indicate that it is more limited in extent than previously believed and that some of the outlying hummocky materials are part of other geologic units of regional extent.

Recent mapping of the Mare Humorum Quadrangle (Titley, Marshall, and McCauley, 1964), the Pitatus Quadrangle (Titley, 1964) and the Montes Riphaeus Quadrangle (Eggleton, 1964) has led to recognition of a regional deposit of hummocky material near Mare Humorum. At one time this unit was probably exposed almost continuously around Mare Humorum; it occurs now as isolated exposures because it is partly covered by younger crater rim deposits and by mare material.

The exposures of hummocky material extend some 500 km from the edge of the Humorum Basin (fig. 1). Not all of the exposures shown have been accurately mapped. Except for two extensive tongues of the hummocky material that extend northwest and southeast from the Humorum

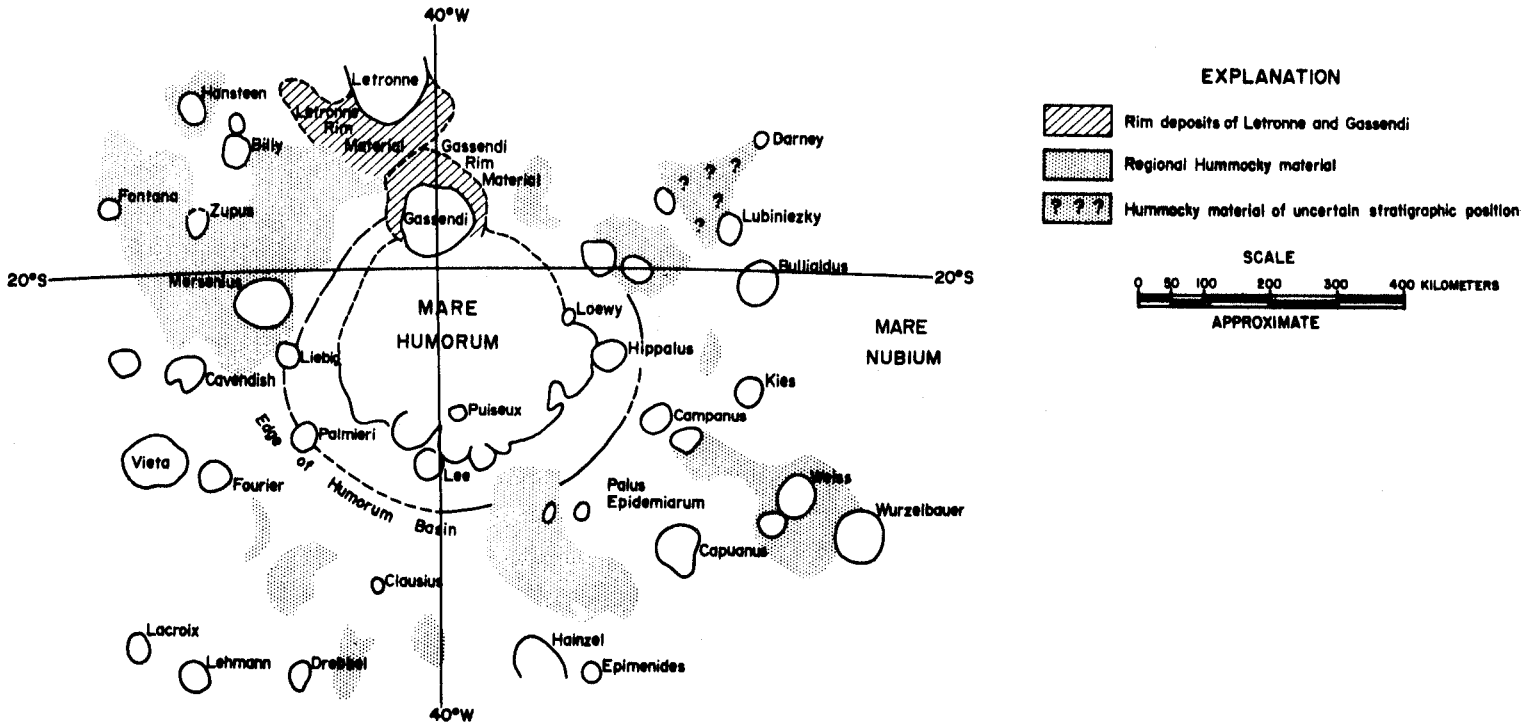

Figure 1. Sketch map of the region around Mare Humorum showing the distribution of hummocky regional deposit.

rim crest, all exposures are apparently parts of a once continuous or nearly continuous annular band.

The best exposure of the hummocky material, which may be taken as a type area, lies between latitudes 46 and 26°S and longitudes 42 and 58°W (IAU convention). In this area, the hummocky material makes up an elongate patch some 300 km long surrounding the crater Mersenius and extending toward Cavendish and northwest to Fontana; the rim materials of these craters apparently are superimposed on the hummocky regional unit. It overlies the rim and floor materials of Zupus and passes under the Letronne rim material. On the western edge of the patch, the hummocky material is in distinct contact with material showing a very fine topographic texture.

The topographic texture of the hummocky material in the type area is similar to that found in other exposures. Rounded or angular ridges and valleys 2 to 10 km in length are the dominant land forms. Relief is uniformly on the order of 100 to 300 m. Valley widths range from the limit of telescopic resolution to around 3 or 4 km. Albedo is about the same as that described for the Fra Mauro Formation (Eggleton, 1964).

South of the Humorum Basin, the hummocky material is present in isolated patches near Fourier, between Clausius and Drebbel and northwest of Mee. It extends in a belt 100 km wide along the southwest and south sides of Palus Epidemiarum and in another belt along the southwest edge of Mare Nubium. A few isolated patches have been recognized and mapped along the west edge of Mare Nubium in the Pitatus and Mare Humorum

Quadrangles. Northeast of the Humorum Basin, in the region southwest of Darney and probably in patches northeast of Darney and east of Darney J not yet mapped, the smooth facies of the Fra Mauro Formation may overlie the hummocky material around Mare Humorum.

Characteristic lineaments, marked by alignment of ridges and valleys, are present in all exposures of the hummocky material. The lineaments are both concentric to and radial to the Humorum Basin and the best developed are those nearest Mare Humorum, on the highlands south of Palus Epidemiarum and along the southwest edge of Mare Nubium. Length of individual lineaments averages about 10 km.

The Humorum Basin may be considered an analogue of the Imbrium Basin. Its diameter is 400 km; that of the inner Imbrium Basin is 670 km. Regional hummocky material extends as much as 500 km from the edge of the Humorum Basin, whereas the hummocky Fra Mauro extends 700 to 1100 km beyond the edge of the inner Imbrium Basin. Thus, the distribution is comparable with the distribution of the Fra Mauro Formation when scaled according to the relative size of the basins. We also consider the regional hummocky unit around the Humorum Basin to be an extensive ejecta blanket of material ejected from the basin.

References

Eggleton, R. E., and C. H. Marshall, 1962, Notes on the Apenninian Series and pre-Imbrian stratigraphy in the vicinity of Mare Humorum and Mare Nubium: U. S. Geol. Survey, Astrogeologic studies semiannual progress report, February 26, 1961 to August 24, 1961, p. 132-137.

Eggleton, R. E., 1964, Preliminary geology of the Riphaeus Quadrangle of the Moon and definition of the Fra Mauro Formation: U. S. Geol. Survey, Astrogeologic studies annual progress report, August 25, 1962 to July 1, 1963, pt. A, p. 46-62.

Hartmann, W. K., and G. P. Kuiper, 1962, Concentric structures surrounding lunar basins: Arizona Univ. Lunar and Planetary Lab. Comm., v. 1, no. 12, p. 51-66.

Titley, S. R., 1964, Stratigraphic and structural relationships in the Pitatus Quadrangle and adjacent parts of the Moon: this report.

Titley, S. R., Marshall, C. H., and McCauley, J. F., 1964, Preliminary geologic map of the Mare Humorum Quadrangle of the Moon: U. S. Geol. Survey, Astrogeologic studies annual progress report, August 25, 1962 to July 1, 1963, supp., pt. A.

STRATIGRAPHIC AND STRUCTURAL RELATIONSHIPS IN THE PITATUS QUADRANGLE AND ADJACENT PARTS OF THE MOON

by S. R. Titley

Introduction

A detailed study of the stratigraphy in the Pitatus Quadrangle and adjoining Mare Humorum Quadrangle suggests the history of this region involves a complex sequence of events that includes basin formation, regional deposition, and later tectonic activity. This report briefly discusses the features of the Pitatus Quadrangle; full interpretation of these features must await more extended observations.

Regional setting

The major geologic features of the Pitatus Quadrangle are related to two large ajoining basins on the southwest limb of the Moon occupied by Mare Humorum and Mare Nubium. Eastward facing scarps and structures that delimit the western semi-circumference of the Nubium Basin are superimposed upon the older circumferential Humorum structures and stratigraphic units.

Preliminary mapping has been completed in three adjoining regions about the Pitatus Quadrangle. This mapping includes the Letronne (Marshall, 1963), Montes Riphaeus (Eggleton, 1964) and Mare Humorum (Titley, 1964) Quadrangles. These studies have resulted in further definition and recognition of the Imbrian System in regions north and northwest of Mare Nubium (Eggleton, 1964, Marshall, 1963) and

recognition of the Imbrian-pre-Imbrian Humorum Group on the western edge of the Pitatus Quadrangle.

On the northern edge of the Pitatus Quadrangle, Procellarum Group material in Mare Nubium extends continuously to the Riphaeus Mountain region. On its eastern edge, the quadrangle is bounded by Procellarum Group mare material that extends eastward beyond the mapped area for a distance of about 150 km.

Stratigraphy

Stratigraphic units exposed range from pre-Imbrian to Copernican. Imbrian units include the Fra Mauro Formation, crater rim materials of the Archimedian Series, and mare material of the Procellarum Group. The Procellarum Group of Imbrian age is exposed dominantly in the eastern one-half of the region. The Humorum Group of Imbrian-pre-Imbrian age is exposed in the western third of the region; a new regional unit of the Humorum Group has been recognized in the Pitatus Quadrangle (Titley and Eggleton, this report). Some of the older crater rim materials have been correlated with the Gassendi Group, and the rim materials of other craters such as Pitatus and Wolf have been designated as Imbrian-pre-Imbrian in age for lack of evidence for correlation with either the Archimedian Series or the Gassendi Group.

Pre-Humorum Group strata

The oldest stratigraphic units previously described in the Pitatus Quadrangle are those of the Humorum Group. In the south-

eastern part of the quadrangle, however, older and as yet uncorrelated materials are present. They have been mapped tentatively as Imbrian-pre-Imbrian. These old rocks make up a varied terrain that ranges from the mountainous escarpments about Mare Humorum on the west to the bench and craters on the south to isolated mountain ranges scattered across Mare Nubium.

Unclassified Imbrian-pre-Imbrian regional material

Unclassified regional material of pre-Procellarum Group age has been mapped in the eastern half of the quadrangle where it has not been possible to identify either Humorum Group or Apenninian Series units. North of Pitatus, near the center of Mare Nubium are exposures of old upland material surrounded by mare material. The rim material of the craters Wolf, Opelt, and Gould, and exposures near Nicollet ψ and θ are typical. Most of this material is characterized by a relatively smooth terrain that has low relief, a high density of small craters 2 to 4 km in diameter, discontinuous ridges and valleys, and scarps and plains. Upland (terra) with these characteristics extends well south and east of the mapped area. The origin and stratigraphic position of this material is obscure, but in its topographic characteristics, small crater density, and linear rille distribution, it is similar to the smooth bench material peripheral to Mare Humorum.

Humorum Group

The Humorum Group has been described from exposures surrounding Mare Humorum (Titley, 1964). Humorum Bench and Rim units present

on the eastern semi-circumference of Mare Humorum are exposed in the western one-third of the Pitatus Quadrangle. In addition to these two units, a regional deposit in the Humorum Group occurs in the Pitatus Quadrangle (Titley and Eggleton, this report).

The regional deposit is exposed in isolated patches that extend for about 500 km radially from the rim of the Humorum Basin. In its typical facies, the regional unit is nearly identical to the coarse Fra Mauro, but in the Pitatus Quadrangle the Humorum Group regional unit can be distinguished from the Fra Mauro because only the fine facies of Fra Mauro is present. The telescopic characteristics of the Humorum Group regional deposit are a moderate albedo and a uniformly hummocky topography comprising rounded to angular hills 2 to 5 km across, and ridges, valleys, and small subdued craters.

The regional unit is distinguished from the Humorum Rim unit by its lower albedo and by more subdued and even relief. It is distinguished from the Humorum Bench unit by a considerably wider distribution and a characteristically more rugged topographic development. In its type area, the regional unit is intermediate in topographic characteristics between the comparatively smooth and cratered, mare-like surface of the bench unit and the rugged mountainous terrain of the rim unit. Tentatively, the regional unit is considered to be the older because the rim unit has a slightly higher albedo which suggests that it may represent a facies of the regional unit with interspersed Copernican slope material.

The bench unit is probably the youngest of the three units composing the Humorum Group.

In the Pitatus Quadrangle the relationships between the regional unit of the Humorum Group and the Fra Mauro Formation are not clear, but there is some suggestion that the Fra Mauro overlaps the coarser material typical of the Humorum regional unit. This uncertain relationship is best observed in the region west and north of the crater Lubiniezky, where there is an albedo contrast between the two deposits.

Imbrian System

Apenninian Series.--The fine facies of the Fra Mauro Formation has been mapped along the northern border of the Pitatus Quadrangle. Although Eggleton (1964) has mapped extensive exposures of this formation in the Riphaeus Quadrangle to the north, it appears to be absent over most of the Pitatus Quadrangle; it has been questionably mapped in the upland area north of Bullialdus W.

Archimedian Series.--Numerous pre-Procellarum Group craters Archimedian or Gassendian in age, are present in the Pitatus Quadrangle. A number of them occur on the upland; a few are exposed as nearly completely inundated craters in the mare. Most of these craters have Copernican slope material on their interior walls; all are floored with Procellarum material; and their rims and walls show varying degrees of modification, ranging from apparent collapse and

foundering within Pitatus, to the cratering about Mercator, to the comparatively fresh appearance of the rim about Campanus. These features characterize Archimedian craters, but a definable relationship to Apenninian rocks is lacking so that correlation to the Archimedian Series cannot be unambiguously made. Several of the craters of possible Archimedian age are fairly large, having diameters of 35 to 40 km. Campanus, Mercator, Weiss and Gould are examples. Smaller craters of possible Archimedian age include Konig and Weiss E; these have diameters of about 10 to 15 km. Some craters, for example Mercator, Agatharchides P, and Weiss, are correlated with the Gassendi Group on the basis of superposition on Humorum Group materials. Others, such as Pitatus, Opelt and Gould cannot be correlated at this time; relationships to known stratigraphic units are lacking.

Procellarum Group material makes up the surface of Mare Nubium. It exhibits ridges and rilles, scarps, depressions, domes, and contrasts in reflectivity. It exhibits a varied surface, in contrast to material in Mare Humorum, which is comparatively smooth and modified only by a series of nearly concentric mare ridges on its eastern edge.

Procellarum material in Mare Nubium has a higher albedo but otherwise is similar to Procellarum material elsewhere. A striking feature of the mare surface is the existence of marked variations in albedo, some of which are related to superposition of rays from Tycho. The most pronounced albedo variation in the quadrangle occurs as a

bright, horseshoe-shaped region, about 150 km across, that opens southward toward the crater Wolf. The contrast in tone is distinquishable at practically all angles of illumination of the surface. The density of superimposed craters appears to be fairly uniform on both light and dark areas.

The smoothness of the mare surface is interrupted by abundant linear ridges, which cross the mare areas as unbroken features. Smooth Procellarum-covered, roughly circular ridges, which are interpreted to represent buried crater rims, and a few rilles, also modify the surface. Many of the linear ridges are about 15 km apart; many appear to be circumferential to the Eratosthenian crater Bullialdus. A group of "braided" ridges, which diverge toward the east, and the embayment of Thebit, can be interpreted to overlie a large pre-Procellarum basin, because the characteristics of these ridges, which lie southeast and east of the crater Nicollet, are very like the braided mare ridges on the east side of Mare Humorum. Elsewhere, Procellarum material appears to be thin, only partially obscuring the character of the subjacent topography. Single, roughly circular ridges which probably represent buried craters, commonly have a rim diameter of about 15 km. In some cases crater rims are only partly buried, such as in the craters Gould, Opelt and Kies.

Ridge and crater complexes that may be a type of mare dome occur at a few places. They are elongate, rather than circular or elliptical, and commonly contain small craters at the high point of their form.

Mare ridges of this type are either associated with a crater located in an area of positive relief, or appear to be part of lines of broken crater chains, the craters of which have diameters on the order of 2 to 3 km. Examples of such ridges are found at Gould Z; the elongate ridge about 15 km west of Opelt; the northward plunging ridge line 5 km northwest of Kies; and a ridge and crater complex that lies about 5 km north of Hesiodus X.

Eratosthenian and Copernican Systems

Craters and stratigraphic units of Eratosthenian and Copernican age are present on both mare and upland. The materials include units associated with the large Eratosthenian crater Bullialdus in the center of the mare, with lesser craters of the same system, and with younger deposits associated with Copernican craters such as Agatharchides A. Young material also is associated with the extensive north-trending ray system that is radial to the crater Tycho, 250 km south of Pitatus. This ray material is particularly prominent in parts of Mare Nubium.

The most imposing topographic feature in the quadrangle is the Eratosthenian crater Bullialdus. This large crater, about 55 km in rim diameter, has a large, asymmetrical crater rim deposit that has an average diameter of about 120 km. This crater rim deposit is similar to the rim deposit of Copernicus, having marked changes in slope from crater rim to the toe of the deposit, numerous radial ridges, and a family of satellitic craters. An extremely faint

ray pattern has been discerned by telescopic observation, but mapping of it is incomplete.

Carr (1964) has documented differences in character between the rims of secondary craters of Eratosthenian and Copernican age. Preliminary work in the Pitatus Quadrangle has shown that rims of satellitic craters range from sharp to very subdued. Elongate craters, possibly derived from Tycho, are present along the south edge of Mare Nubium, and similar craters are present about Bullialdus. In the area between the two craters which would presumably contain craters satellitic to both Tycho and Bullialdus, a distinction as to origin has been difficult to make. It is suggested that the variation in sharpness of probable satellitic craters may be a reflection of both the nature of material in which the crater is developed as well as the origin (and thus age) of such objects.

Structure

Structural features in the quadrangle are of three main types: ridges in Mare Nubium, which have been discussed in the section on the Imbrian Series, a set of major rille systems on the west edge of the mare; and upland structure. Of these, the most informative in regard to information on geologic history are the structural relations observed in rille systems and the uplands on the west edge of the mare.

Two intersecting rille systems are present in the Campanus-Agatharchides region. The most pronounced and well developed of the

two sets is circumferential to Mare Humorum; the other set is circumferential to Mare Nubium. Both sets of rilles are developed mainly in Procellarum material, but very locally the rilles transect upland. Their geometric distribution and their regional continuity indicate that rilles are probably related to basin structures. Rilles inferred to be related to Mare Humorum for the most part are offset and broken by rilles inferred to be related to Mare Nubium. Such relationships are seen along Rima Happallus II and IV. Additionally, the rilles that appear related to Mare Nubium transect on both the north and south borders of the quadrangle. Rilles related to Mare Nubium are thus apparently the younger.

Structural and stratigraphic information in the Pitatus and Mare Humorum Quadrangles indicate that emplacement of mare material with associated events had a complex history that involved subsidence, filling, and adjustment, followed by cyclical repetition of the sequence.

Upland structures about Mare Nubium are characterized by a structural "grain" and by numerous basin-associated scarps. The most pronounced of the scarps is one that bounds the upland and Mare Nubium in the southwest part of the quadrangle. The upland here includes Humorum Group units. The major scarp is largely unbroken, and includes a part of the basin circumference that is nearly 300 km in length. Other scarps concentric to the basin are located near Bullialdus W and Agatharchides L. Structural lineations in the

uplands, with the exception of the region southeast of Pitatus, contain consistent radial or circumferential trends with respect to the Humorum and Nubium basins.

Summary

1. Characteristics of Procellarum material in Mare Nubium indicate that in the central part mare material is fairly shallow, filling an old upland-like topography. On the east side of the Pitatus Quadrangle, braided ridges in the Procellarum suggest filling of a single large basin that had a diameter of about 250 km.

2. Structural adjustments and perhaps some filling of the Nubium basin postdates structural adjustment and perhaps the filling of the Humorum Basin.

3. A regional deposit is present that is composed of material derived from the Humorum Basin. It apparently predates the Fra Mauro Formation.

References

Carr, M. H., 1964, The geology of the Timocharis Quadrangle: U. S. Geol. Survey, Astrogeologic studies annual progress report, August 25, 1962 to July 1, 1963, Part A, p. 9-22.

Eggleton, R. E., 1964, Preliminary geology of the Riphaeus Quadrangle of the Moon and definition of the Fra Mauro Formation: U. S. Geol. Survey, Astrogeologic studies annual progress report, August 25, 1962 to July 1, 1963, Part A, p. 46-63.

Marshall, C. H., 1963, Geologic map and sections of the Letronne region of the Moon: U. S. Geol. Survey Map I-385.

Titley, S. R., 1964, A summary of the geology of the Mare Humorum Quadrangle of the Moon: U. S. Geol. Survey, Astrogeologic studies annual progress report, August 25, 1962 to July 1, 1963, Part A, p. 64-73.

A PRELIMINARY REPORT ON THE ROLE OF ISOSTATIC REBOUND IN THE GEOLOGIC DEVELOPMENT OF THE LUNAR CRATER PTOLEMAEUS

by Harold Masursky

Introduction

Near the center of the subterrestrial hemisphere of the Moon is the crater Ptolemaeus, 93 miles in diameter (fig. 1). Its broad, shallow form has led British workers to call it a ringed plain (Fielder, 1961) and Russian workers to call it a circus (Bakharev, 1939). The rim of the large crater is highly irregular, offset, and dimpled by many smaller craters (fig. 2).

Geologic mapping of the Ptolemaeus quadrangle has provided the basis for reconstructing the geologic development of this large feature. This reconstruction may serve as a guide to the origin of the many similar large, shallow craters on the Moon. The purpose of this paper is to show a mechanism--isostatic rebound--by which the present form of Ptolemaeus could have developed if its original form was like that of the young crater Copernicus. Copernicus is inferred to be of impact origin by analogy with young terrestrial craters like Meteor Crater, Arizona. The sequence of events leading to the present form of Ptolemaeus has been inferred by comparison with the lunar craters Taruntius and Gassendi and with several old, large, shallow terrestrial craters recently described in the Canadian Shield.

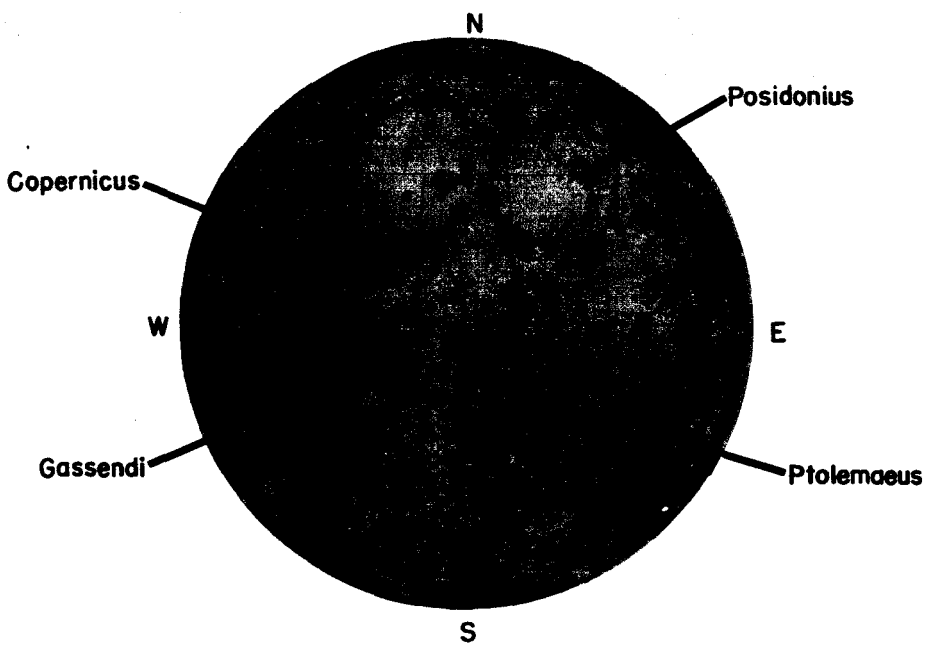

Figure 1. Index map of the moon showing location of craters discussed in the text.

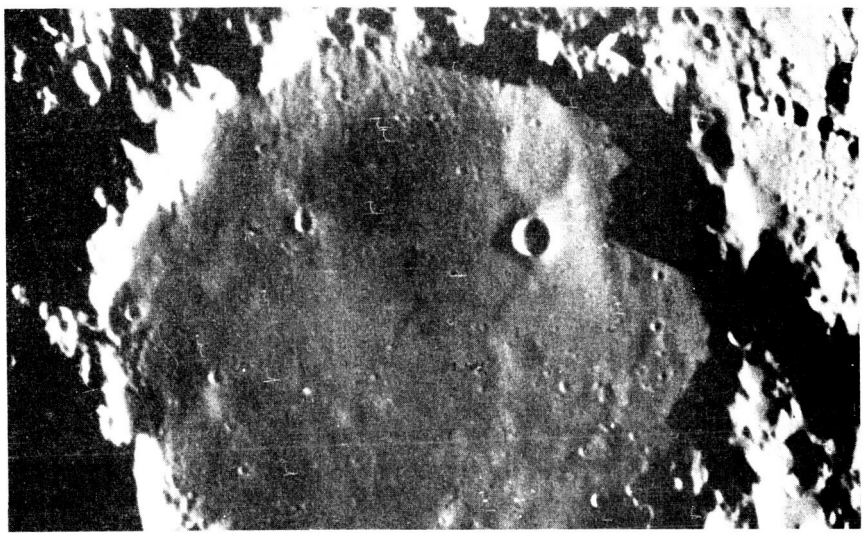

Figure 2. Lunar crater Ptolemaeus, about 93 miles in diameter. The low and greatly distorted rim and shallow depth indicate a complex post-formation history. Fresh, sharp craters and partially buried ones are on the floor. Note also radial ridges and aligned secondary craters caused by ejecta from the crater Herschel that lies on the northern rim of Ptolemaeus. (Photograph by Dollfus; 24-in. refractor, Observatory of the University of Toulouse, Pic du Midi, France.)

This work is based, in great part, on observations at the 36-inch and 12-inch refracting telescopes at Lick Observatory and the 60-inch McMath Solar Telescope at Kitt Peak National Observatory, on examination of telescopic photographs published in the Photographic Lunar Atlas (Kuiper, 1960) and unpublished photographs from G. H. Herbig, Lick Observatory, Roger Lynds, Kitt Peak National Observatory, and Zdenek Kopal, Observatory of the University of Toulouse.

Geology of Ptolemaeus

Ptolemaeus is about 5000 feet deep and its rim is raised 1500 to 3000 feet above the surrounding country. The crater is polygonal and its walls are offset in many places by trenches and ridges; the offsets are interpreted to be faults with both horizontal and vertical displacement. Many lines of small craters, both on the floor of Ptolemaeus and in the surrounding upland, are interpreted to be chains of volcanic craters.

Ptolemaeus is blanketed by regional material of the Apenninian Series of Imbrian age presumably derived from the Imbrium basin but also from many local sources. The covering layer includes the Frau Mauro Formation, which is believed to be a deposit of ejecta from Mare Imbrium, and local deposits like that from the crater Herschel of both pre- and post-Apenninian age. Buried under the regional material on the floor of Ptolemaeus are many small pre-Imbrian craters, whose presence is revealed by shallow depressions in the overlying layer. Ptolemaeus is thus older than the floor filling and the buried pre-Imbrian craters. Rim material and lines of secondary craters associated with the crater Herschel of Archimedian or Eratosthenian age are superposed on the northern rim of Ptolemaeus.

Origin of craters of the Copernicus type

The geologic study of terrestrial craters has been the key to interpretation of lunar craters. Criteria that lead to making the crucial distinction between an impact crater and a volcanic crater of the maar type can be set up by comparing two craters of the same size. After critical morphologic characteristics of recent craters have been determined, the original morphology of old and greatly modified craters can be inferred by unravelling the subsequent modifications.

Meteor Crater, Arizona, 4000 feet in diameter, is the best studied terrestrial impact crater (Gilbert, 1893; Barringer, 1905; Nininger, 1953; Shoemaker, 1963; Chao, Shoemaker, and Madsen, 1960). The geologic relations in the wall rocks and surrounding rim deposits, the presence of meteoritic iron and dense shock-metamorphosed forms of silica (coesite and stishovite) are strong evidence for an impact origin. The general crater form--the floor lower than the level of the surrounding country, the raised inner rim, and surrounding hummocky rim deposits--can be seen in figure 3. The polygonal shape, according to Shoemaker (1962), is due to the presence of pre-existing joints and faults in the country rock.

Lunar Crater, Nevada (Marshall, C. H., 1962, written communication), shown in a vertical photograph, is a volcanic crater of the maar type (fig. 4). It is about 4000 feet in diameter and has a rim about 100 feet higher than the surrounding country; it is superficially nearly a twin to Meteor Crater, Arizona. The surrounding rim is tuff composed of volcanic ejecta of new basaltic material and xenolithic fragments of subjacent

Figure 3. Oblique aerial photograph of Meteor Crater, Arizona. The crater is about 4,000 feet in diameter and 600 feet deep; its rim is about 120 feet high. Meteoric debris and shock-metamorphosed minerals (coesite, stishovite) indicate an impact origin. The polygonal shape is due to a pre-existing joint pattern.

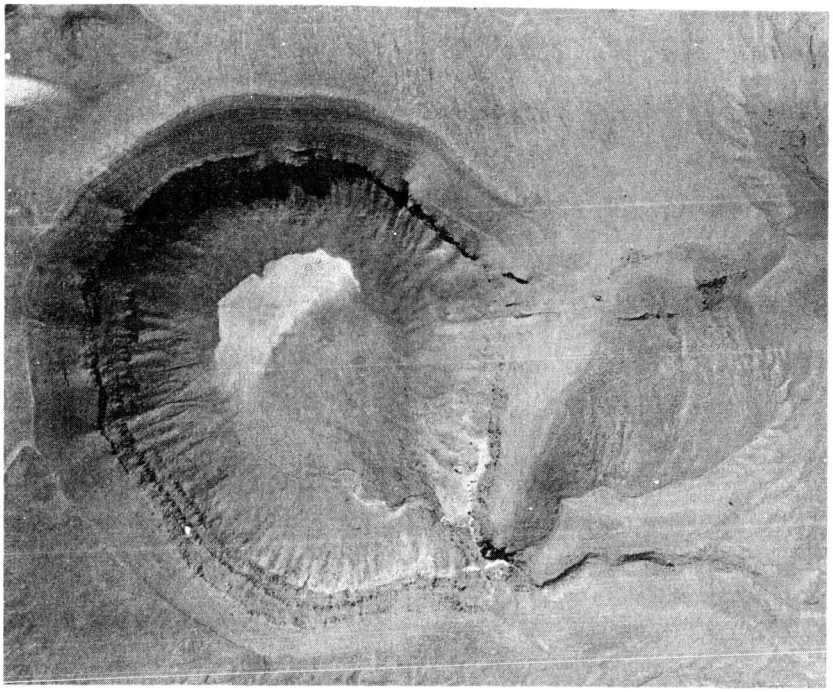

Figure 4. Vertical aerial photograph of Lunar Crater, Nevada. It is surrounded by a tuff ring formed by violent degassing. Crater diameter is about 4000 feet; its raised rim consists of alternating thin layers of volcanic debris, newly erupted basalt, and comminuted country rock.

volcanic rocks. The thin-bedded ejecta deposits dip away from the crater, as do similar deposits in the Navajo country, Arizona, described by Shoemaker (1957). The smooth outer slopes of the rim, formed by deposits of ejecta entrained by the escaping volcanic gasses, contrast sharply with the morphology of the hummocky ejecta from shock-produced craters.

The detonation of a nuclear device produces a shock wave and a crater much like that produced by hypervelocity impact (Shoemaker, 1962; Baldwin, 1963). The Sedan Crater (fig. 5), 1300 feet in diameter, was produced by the underground detonation of a nuclear device; it is closely similar to Meteor Crater. In addition, secondary craters in raylike patterns are also present, whereas there are none at Meteor Crater. High-speed films of the explosion show the generation of the shock wave, upheaval of a dome of ejected material to form the hummocky rim deposits, and the breakthrough of jets of material that impact on the rim and beyond to produce the secondary craters. (Film available from Lawrence Radiation Laboratory, Livermore, California.) It is inferred that Meteor Crater originally had a well-developed secondary crater field that has been destroyed by erosion.

Forms of large terrestrial impact craters

Several large meteorite craters in the Canadian Shield (fig. 6) recently described by Beals and others (Beals, Ferguson, and Landau, 1956; Beals, 1958; and Beals, Innes, and Rottenberg, 1960) shed important light on the problem of crater modification by isostatic rebound.

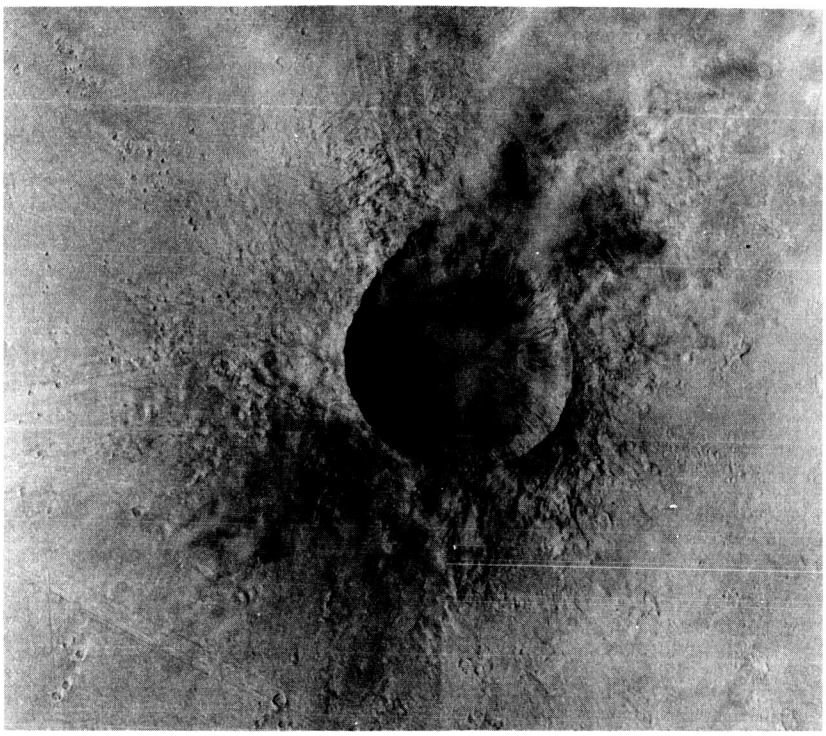

Figure 5. Vertical aerial photograph of Sedan Crater, Nevada, formed by the subsurface burst of a nuclear device. Its diameter is 1300 feet. In general morphology, it is similar to Meteor Crater, Arizona, but it has a well developed field of small secondary craters, which have been destroyed by erosion at Meteor Crater. (Courtesy of Lawrence Radiation Laboratory.)

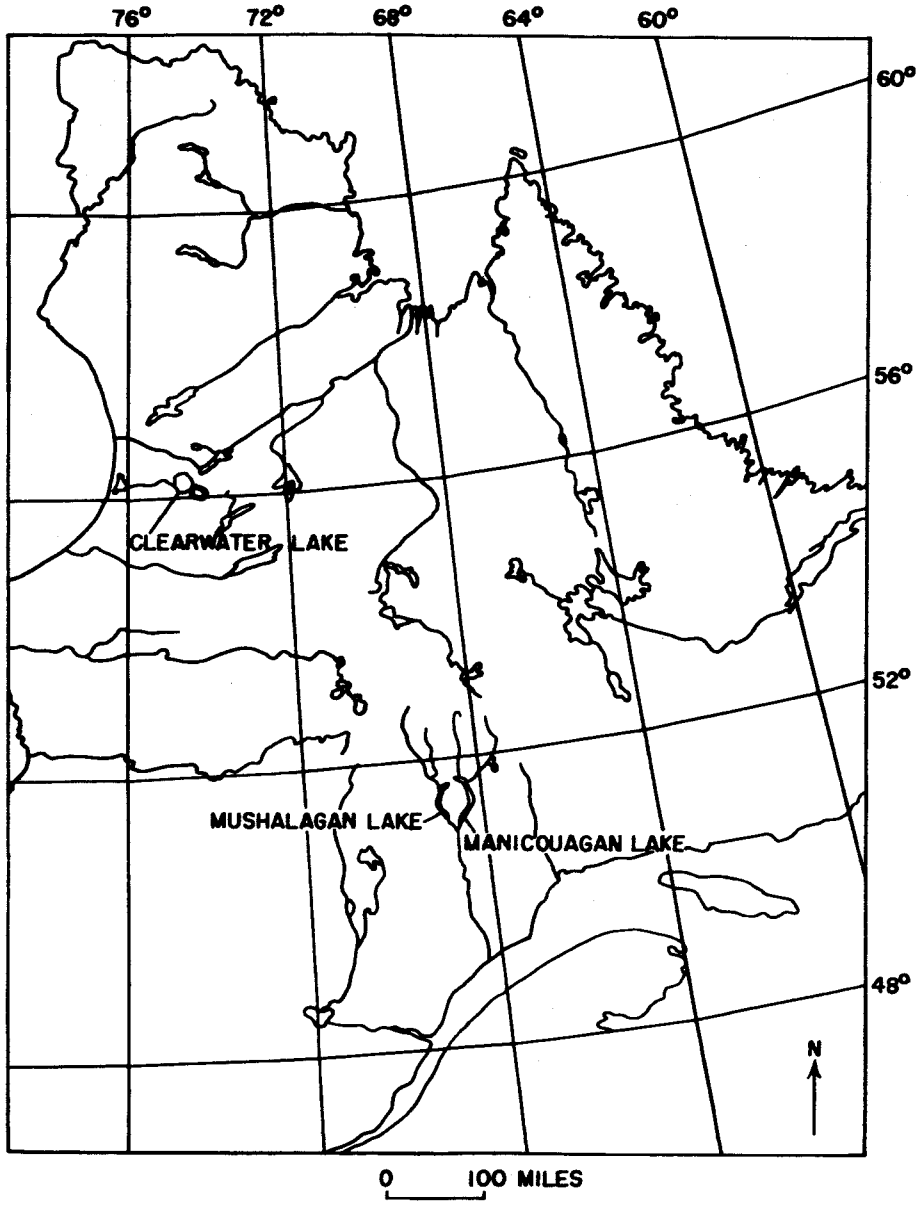

Figure 6. Index map of eastern Canada showing location of Clearwater and Manicouagan-Mushalagan Lakes.

Clearwater Lake.--West Clearwater Lake, Quebec (fig. 7) a crater lying within the crystalline terrain of the Canadian Shield, reportedly contains flat-lying Ordovician sediments. It is 20 miles in diameter, about 1200 feet deep (including 300 feet of water), and has a rim about 500 feet above the general level of the surrounding country. The crater has been studied by Beals, Innes and Rottenberg (1960), and by Shoemaker and Dence (1963, written communication). Both investigations led to the conclusion that the crater is of meteoritic origin. Kranck and Sinclair (1963), and Currie (1964), however, studied the island ring and central peak and concluded that they were of volcanic origin.

A photomicrograph of a rock from the "central peak" (Kranck and Sinclair, 1963, p.25, plate V.B) is described as pyroxene and feldspar that is "fused" to glass. The texture and mineralogy of this rock, however, match a shock-metamorphosed gabbro described by Milton and De Carli (1963). Feldspar glasses of this type are not known in terrestrial volcanic rocks. The available evidence from the field mapping, drilling, gravity surveys, and petrography supports the impact origin.

The present morphology of the crater, especially its low ratio of depth to diameter, indicates considerable modification in form since its origin. This modification is interpreted to be primarily the result of isostatic rebound of the floor.

Lake Manicouagan.--Lake Manicouagan, Quebec, another very large terrestrial crater within the Canadian Shield, has been described by Rose (1954); Berard (1962); Currie (1964); and Dence and Manton (1964,

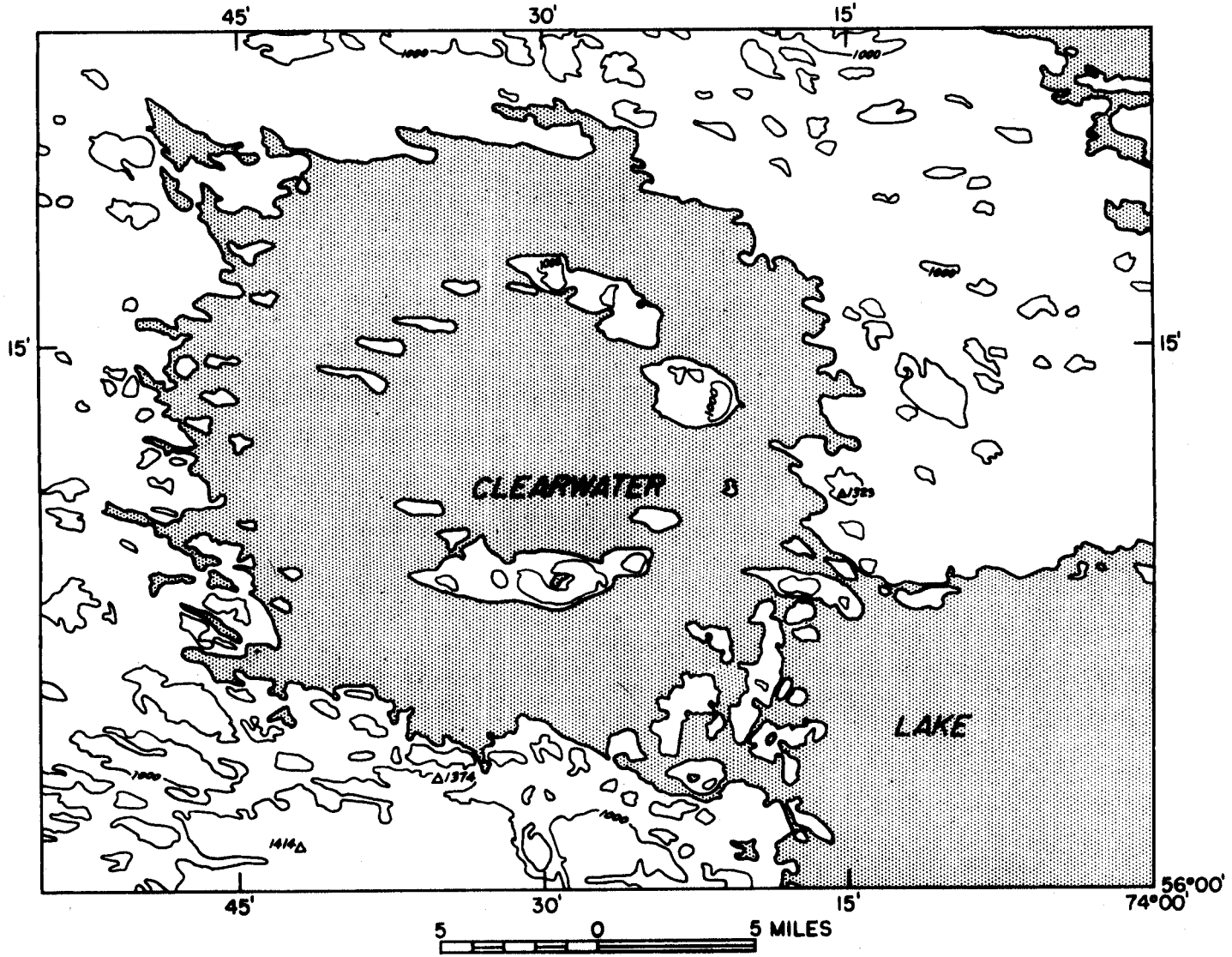

Figure 7. Sketch of Clearwater Lake, New Quebec, 20 miles in diameter. The central peak, island arc, and low rim are believed to be the result of alteration of the original crater. (Map modified from the Clearwater, Quebec, Provisional Map, 1:250,000, Department of Mines and Technical Surveys, Canada, 1962.)

written communication). The structure consists of a crater 40 miles in diameter (fig. 8) with a raised rim about 1000 feet higher than the surrounding country. The lakes are about 1100 feet deep. The central plateau is 700 feet above the present level of the lakes, and the central peak rises 1500 feet above the plateau.

Although Rose, Berard and Currie tend strongly to interpret the surface rocks as volcanics, Dence and Manton have identified them as suevite-like, shock-metamorphosed rocks and have reported shatter cones in the central peak area (Mont de Babel).

Interpretation of the crater as an impact structure rests on the unpublished information by Dence and Manton, who interpret the "volcanic rocks" as impactite and thus similar to those of the Ries Basin, Germany (Shoemaker and Chao, 1960). Geophysical work suggests that the floor consists of an isostatically raised block of very complex lithology.

Forms of large lunar craters

Copernicus.--The lunar crater that most closely resembles Meteor Crater and the Sedan crater, except for the difference in size, is Copernicus (fig. 9), which on the basis of extensive stratigraphic evidence is one of the youngest major lunar craters (Shoemaker, 1962; Baldwin, 1963). It is about 56 miles in diameter, with a raised interior rim and surrounding hummocky deposits that change outward into radial ridges. A well-developed field of secondary craters is present, along with rays and loops marked by additional secondaries that are at or below the limit of resolution.

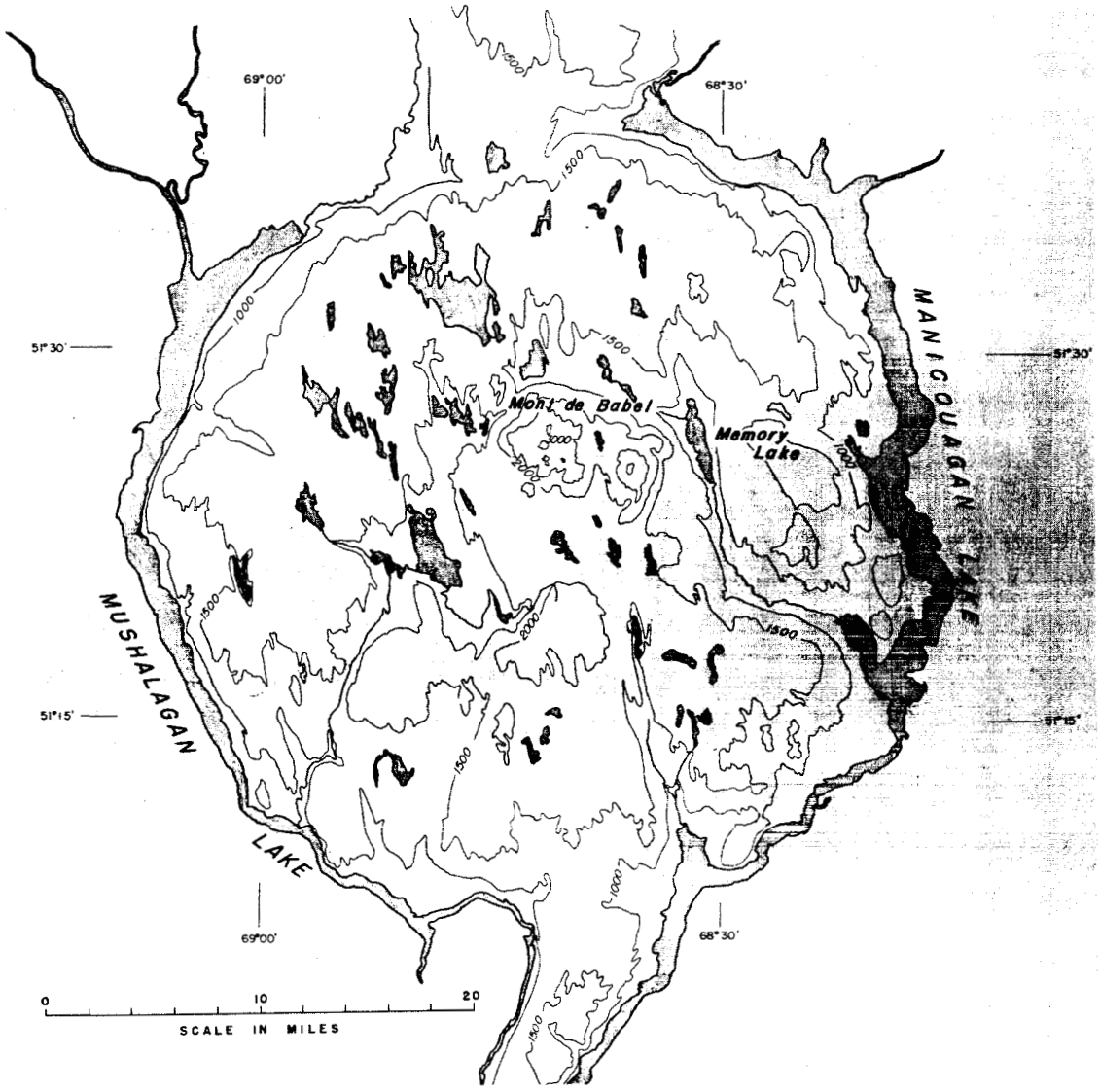

Figure 8. Sketch map of Manicouagan-Mushalagan Lakes, which define a structure about 40 miles in diameter. The low rim is 500 to 1000 feet above the surrounding country; lakes are nearly 1100 feet deep; central plateau and central peak (Mont de Babel) display the form of an isostatically resprung crater. (Modified from Manicouagan-Mushalagan Lakes Map, Dominion Observatory Drafting Office, November 1963.)

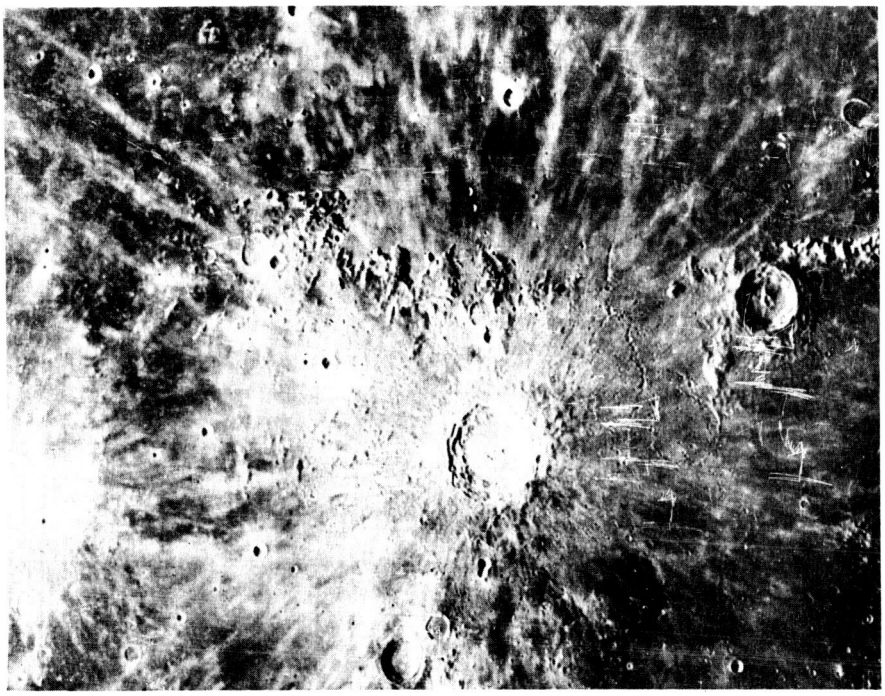

Figure 9. Lunar crater Copernicus, about 56 miles in diameter. Crater shape, raised rim, hummocky terrain grading outward to radial ridges, secondary craters, and rays indicate probable impact origin. Note central peaks and slump terraces on inner rim. (Mt. Wilson Observatory photograph.)

Taruntius.--The lunar crater Taruntius (fig. 10) is 35 miles in diameter and seems to be analagous in general form to the West Clearwater Lake crater. It shows the uplifted central plateau with a preserved central peak, the island ring, and the inward-facing crater rim. If this crater were flooded to the same proportional depth, its morphology would exactly match that of West Clearwater Lake.

According to Henry Moore (1964, oral communication), the ratio between terrestrial and lunar crustal structures used in scaling hypervelocity impact models is 1:1.6. On the basis of this scale ratio, Clearwater Lake on the Earth, 20 miles in diameter, and Taruntius on the Moon, 35 miles in diameter, are comparable.

Gassendi.--The lunar crater Gassendi (fig. 11) at the north end of the Humorum Basin (Titley, 1964; Titley, McCauley, and Marshall, 1964) is about 75 miles in diameter, has a narrow, low rim about 4000 feet above the surrounding country, and is about 5000 feet deep. A crescent-shaped body of mare material occupies the southern end of the crater and with a central peak cluster rises about 3600 feet above a central plateau, or 1400 feet below the rim.

Although Gassendi is nearly twice as large as the Manicouagan structure, it has a striking morphologic similarity. Its present shallow form may be the result of isostatic rebound of the floor rather than of filling by now buried mare material.

Posidonius.--The contrast between two craters of almost the same size but of different age--the young, post-mare Copernicus and the older pre-mare

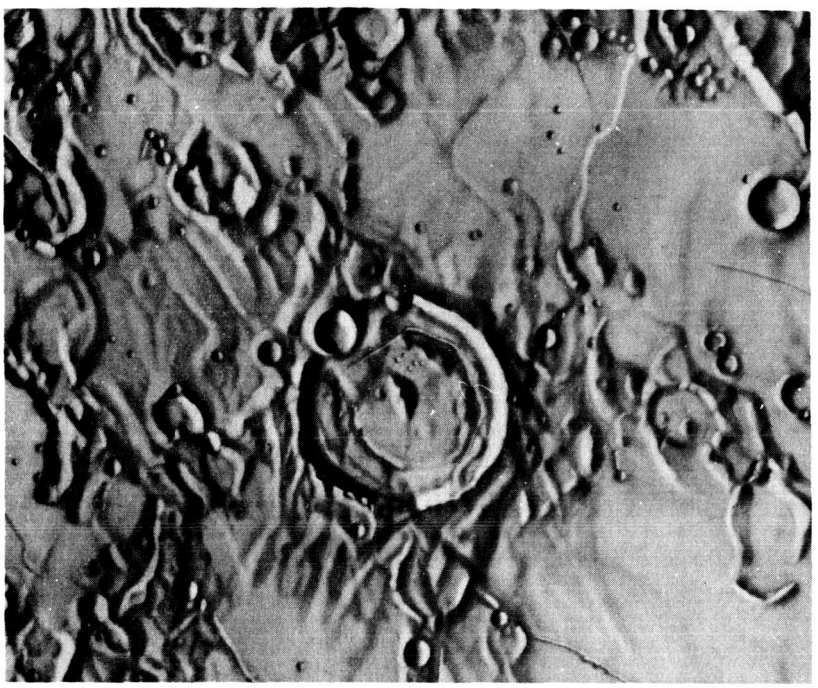

Figure 10. Lunar crater Taruntius, 35 miles in diameter. If this structure were flooded with water to near the top of the central peaks, it would closely resemble Clearwater Lake with its central peak, island ring, and crater rim. (U. S. Air Force Aeronautical Chart, LAC 61.)

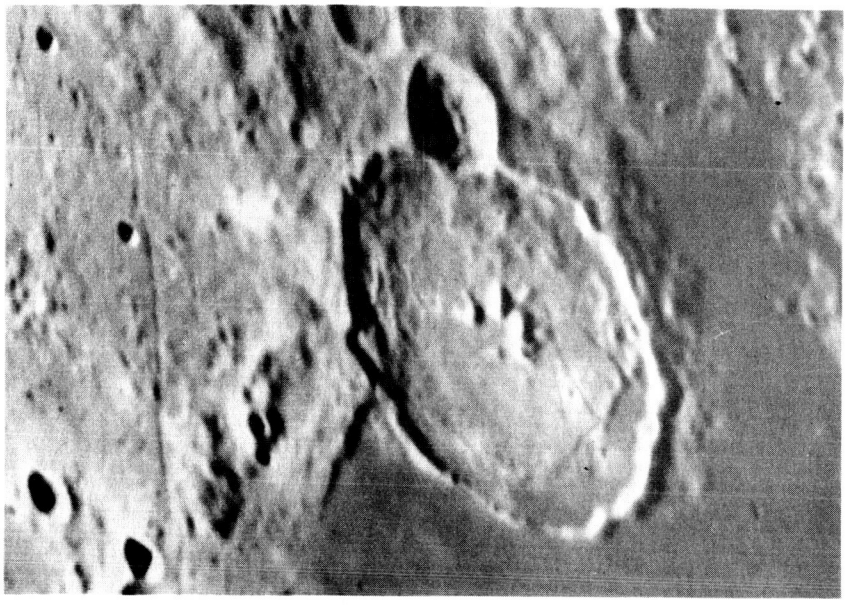

Figure 11. Lunar crater Gassendi, about 70 miles in diameter. Plateau-like floor with its central peak and small rim indicate isostatic adjustment flooding by mare material of the crescent-shaped trough inside the rim. (Lick Observatory, photograph.)

Posidonius--is shown in figures 12a and 12b. Copernicus, 56 miles in diameter, displays a cup-shaped crater form, a prominent rim, a flat floor, and small central peaks. Posidonius, 63 miles in diameter, has a much narrower rim, a central plateau with small central peaks, and mare-filled crescentic lowlands inside the rim. The critical features are the central peaks. If the diminution in depth of Posidonius were due to infilling, the central peaks would be covered. As they are not, even though the crater is probably less than half as deep as it was originally, the shallow depth must be due to rebound of the crater floor.

Comparison of Ptolemaeus with other craters

Craters of the Copernicus type are in distinct contrast to the broad, shallow, flat-floored crater Ptolemaeus (fig. 13). Ptolemaeus has a barely discernible raised rim, an extensive, relatively flat floor with many craters--some fresh, others partially buried--and no surrounding secondary craters or recognizable hummocky ejecta blanket. Extrapolation from younger craters suggests that an unmodified impact crater the size of Ptolemaeus should be on the order of 26,000 feet deep and have a rim 4300 feet above the surrounding country, hummocky rim deposits extending outward for at least one crater diameter, and a pronounced field of secondary craters.

Previous hypotheses.--The discordance between the present form of the crater and the inferred original form results from a change in depth and the destruction of the original rim morphology. Three theories have been advanced to account for the shallowness of this large lunar crater.

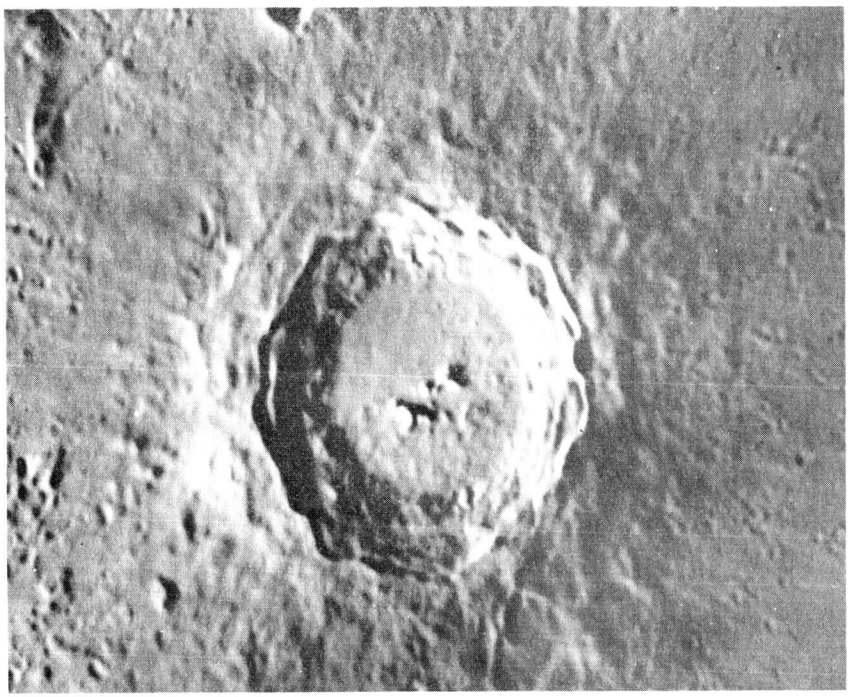

Figure 12a. Lunar crater Copernicus, 56 miles in diameter, is about 11,000 feet deep; rim is about 5000 feet high, and central peaks are about 1200 feet high. (Photograph by G. H. Herbig; 120-in. telescope, Lick Observatory.)

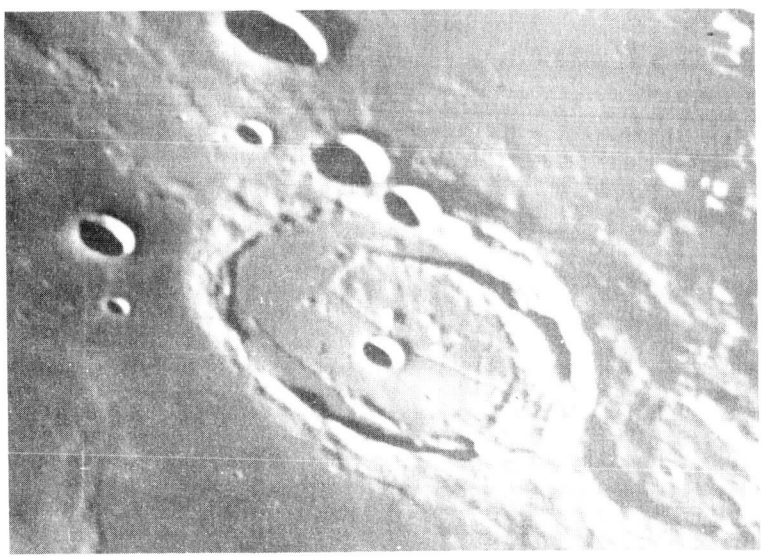

Figure 12b. Lunar crater Posidonius, more than 60 miles in diameter. Type of resprung floor is intermediate between that of Taruntius and that of Gassendi. (Photograph by G. H. Herbig; 120-in. telescope, Lick Observatory.)

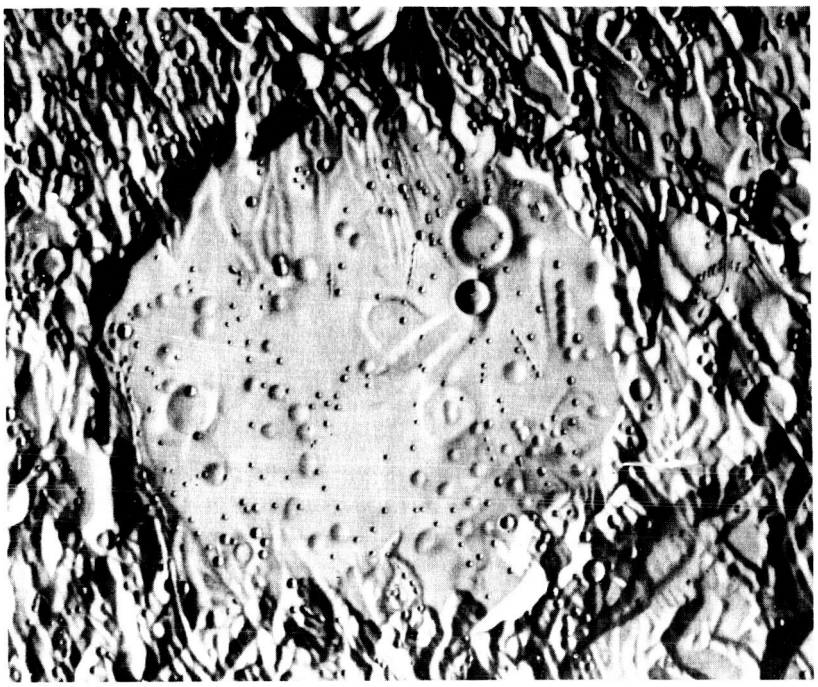

Figure 13. Shaded relief map of crater Ptolemaeus. The degraded rim, cut by through-going faults created after formation of the crater, is well shown. (Drawing from U. S. Air Force, Aeronautical Chart, LAC 77.)

Gilvarry (1964) showed that a nuclear crater formed beneath a shallow layer of water in the Pacific had a depth-to-diameter ratio similar to that of lunar craters of the Ptolemaeus type. He then concluded that similar lunar craters may have originated by impact into ephemeral lunar seas. This thesis can be rejected because most of the shallow craters referred to by Gilvarry are shallow because they have been filled with later sediments. In addition, no evidence for water-generated erosion (wave-cut cliffs, etc.) or sedimentation (beaches, bars, etc.) has been observed. Shoemaker and Hackman (1962), on the other hand, have described craters like Archimedes that are shallow because they have been partially filled with mare material after their formation (fig. 14). Eggleton and Marshall (1962), have used this explanation to account for the shallowness of a number of large lunar craters, including Ptolemaeus, the floors of which are covered by pre-mare regional material, presumably derived from the Imbrian Basin and perhaps partly by an even earlier generation of mare material. This thesis does not account for the loss of the crater rim or the preservation of structure characteristics of the crater floor and the central peaks in shallow craters such as Taruntius, Gassendi and Posidonius.

Dietz (1961), Danes (1962), and Baldwin (1963) have proposed quite a different mechanism that may explain the geometry of these craters--that postformational isostatic adjustment results in crater modification and shallowing. This process appears to operate at a regular rate, so that the amount of rebound for a particular crater may be useful as a

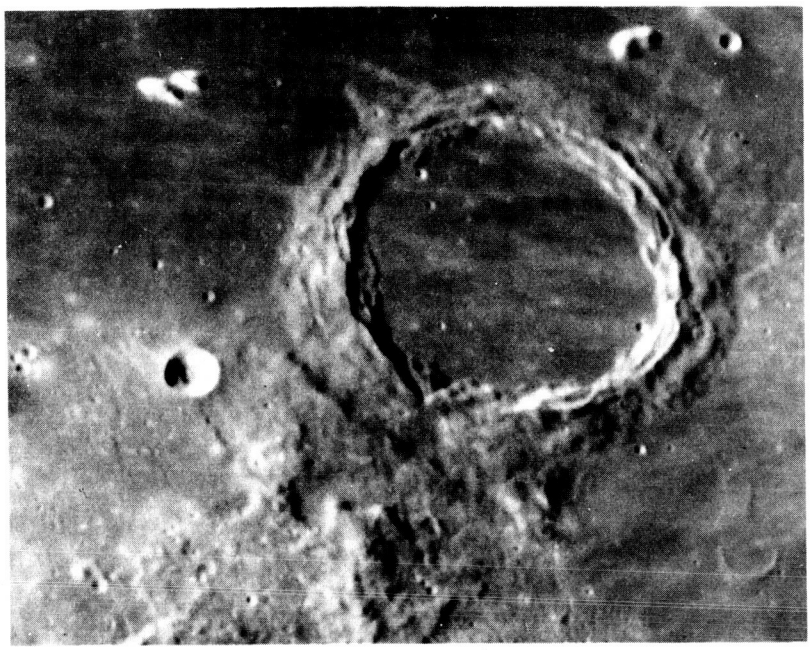

Figure 14. Lunar crater Archimedes, about 50 miles in diameter. Crater is filled and field of secondary craters on the Apennine Bench is overlain by postformation mare material. Note slumping of crater walls and reduced size of crater rim. (Photograph by G. H. Herbig; 120-in. telescope, Lick Observatory.)

general age index. There appear to be all gradations in form between craters of the Copernicus type and the Ptolemaeus type on the lunar surface.

Theory of viscous flow and isostatic rebound of craters

Z. F. Danes (1962) has analyzed the behavior of an idealized model of the crater Copernicus, assuming a single-layer condition and materials that behave as viscous fluids. He presents the cross section of Copernicus (fig. 15) and traces through the readjustment of the crust.

Of particular interest in the sequence of profiles is the double bulge in the uplifted floor and the depression in the crater rim under the load of the overlying ejecta blanket. The profile of the rim in this analysis is very similar to those of the rims of Posidonius, Archimedes and Gassendi, whereas the form of the floor resembles the crater Taruntius. This suggests that the degradation of the rim (fig. 16) of an old crater like Ptolemaeus is the result of subsidence of the surface beneath the weight of the rim material.

Danes, however, has neglected the presence of the central peak, although this may be the best measure of the amount of residual stress that the crust is capable of supporting. He also neglects the brittleness of the upper layers as evidenced by the numerous linear anastomosing rilles seen on the floors of craters of this type, and the fact that craters of the size of Gassendi have fractured at the edges of the floor rather than bending as indicated in the model, which together suggest that the upper layers of the lunar crust yield to stress by fracturing in addition to flexure.

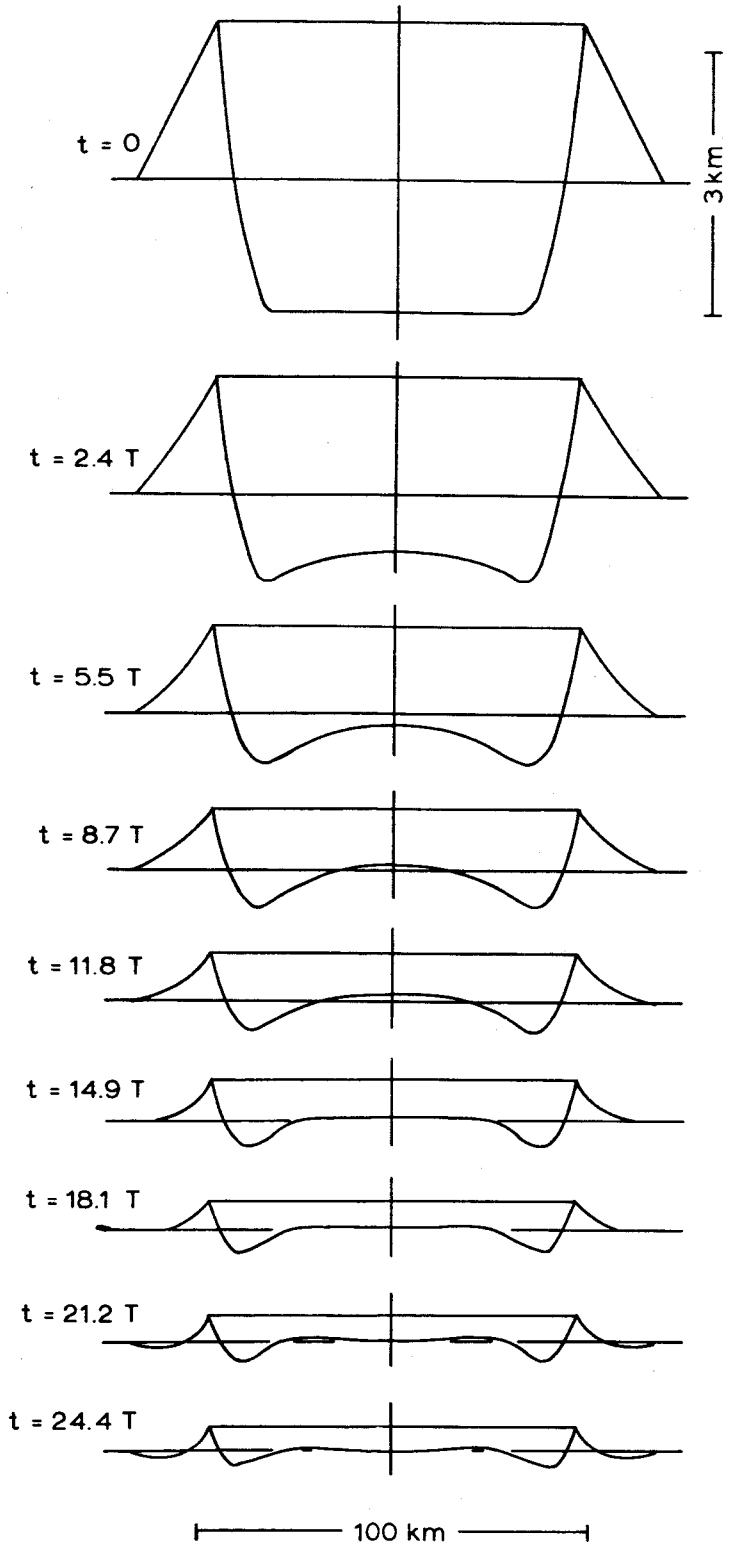

Figure 15. Profiles showing isostatic compensation of lunar crater Copernicus. Note raising of crater floor and depression of rim. (From Danes, Z. F., 1962.)

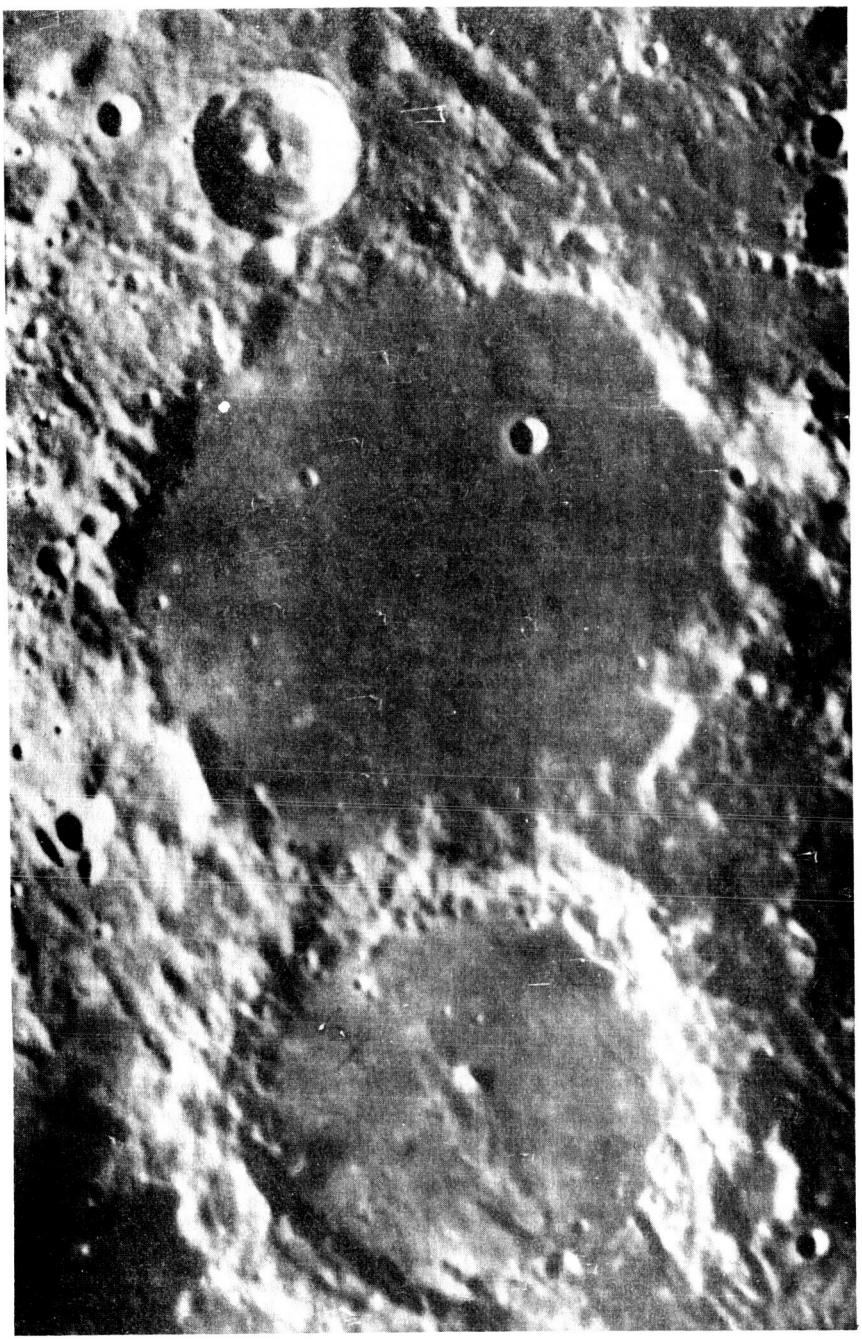

Figure 16. Craters Ptolemaeus and Alphonsus. On the floor of Alphonsus is an anastomosing network of rilles with dark halo craters at intersections. The rilles are characteristic of uplifted crater floors. The volcanic ejecta contribute to the blanket on the floors of both craters.

A further deficiency of the Danes model is that the final configuration of lunar craters seems to be scale dependent. Craters below about 10 miles in diameter do not appear to rebound isostatically. At the Clearwater-Taruntius scale (20 miles terrestrial, 35 miles lunar), a smoothly curved, double-arched configuration develops, as in the Danes model. At the Manicouagan-Gassendi scale (40 miles terrestrial, 75 miles lunar), the central plateau breaks free along bounding faults, and the whole center rises. Danes is presently cooperating with the author on a more complex model that will incorporate some of the observations discussed in this report.

Geologic history of Ptolemaeus

Immediately after formation, slumping of material from the walls onto the floor of Ptolemaeus probably contributed to its partial filling, as in the Sedan nuclear crater (fig. 5). The interior walls of Copernicus (fig. 9) and numerous other young craters have many large slump terraces. It is possible that slumping may also occur on the outer slopes of the rims and flanks of lunar craters, further contributing to the overall degradation in form. The form of the rim of Archimedes (fig. 14) suggests this process.

The polygonal form of Ptolemaeus was influenced by pre-existing fault patterns. The east and west sides of the crater, however, also coincide with subsequently active tectonic directions, particularly the "Imbrian sculpture," which is a complex system of lineaments radial to

Mare Imbrium. These originally were described by Gilbert (1893) as grooving by ejecta, but were later interpreted as faults by Suess (1909).

The prominent development of the "sculpture" in this part of the Moon is due to reinforcement of the pre-existing tectonic structures by the deformation accompanying the formation of the Imbrian Basin. Chain craters along fault lines parallel to the Imbrian sculpture are present both on the floor and rim of Ptolemaeus. A partially buried line of chain craters lies along the foot of the western wall of the crater; these must be earlier than some of the floor-filling material. Another series of chain craters lies along the southwestern edge of the crater, cross cutting both the rim and floor deposits. The "Straight Wall," just southwest of the map area appears to be a fault parallel to the same structural trend and later than the surrounding mare material. It is therefore clear that the structural history of this area is complex and that structural deformation has occurred both before and at several times after formation of the crater. The faults offset the crater wall and cut the rims into blocks, so that the original shape is obscured.

Radiating ridges and lines of secondary craters derived from Herschel are present at the north end of the floor (fig. 2); these indicate that subsequent impact has also contributed to the filling process. Each of the many small craters on the floor has spread a similar blanket of ejecta, and by this combination of erosion--i.e., crater formation and redistribution of the ejecta blanket--the surface is gradually churned. Evidence for this process can be seen very well in figure 2, which shows

all stages of craters from the freshest to the most obscure "ghosts." With the lack of atmosphere, this process of erosion and sedimentation will continue down to the smallest crater, as shown by Carr (1964) in the Imbrian Basin and in the final pictures taken by Ranger VII.

A terrestrial example that appears applicable is the effect of extensive artillery bombardment at Verdun during World War I. Trenches were blasted and filled, redug and reburied many times. This extreme churning of the surface layer must be equivalent, in general, to the process on the lunar surface, down to the micro scale, as the result of meteoritic impact.

An additional sedimentation process, whose effect is difficult to evaluate, is seen in figure 16, where the dark halo craters that are interpreted as dark volcanic ejecta occur along rilles in the crater Alphonsus. It is also possible that large amounts of disseminated volcanic ejecta and gases may still be emerging (Kozyrev, 1962) from this group of vents, but their abundance cannot now be estimated.

References

Bakharev, A., 1939, Observations of the lunar circus Gassendi: Vses. Astron.-Geod. Obshchestvo Byull., no. 1, p. 22-25.

Baldwin, R. B., 1963, The measure of the Moon: Chicago, Univ. of Chicago Press, 488 p.

Barringer, D. M., 1905, Coon Mountain and its crater: Natl. Acad. Sci. Washington Proc., v. 57, p. 861-881.

Beals, C. S., 1958, Fossil meteorite craters: Sci. American, v. 199, no. 1, p. 32-39.

Beals, C. S., Ferguson, G. M., and Landau, A., 1956, A search for analogies between lunar and terrestrial topography on photographs of the Canadian Shield: Royal Astron. Soc. Canada Jour., v. 50, no. 5, p. 203-211.

Beals, C. S., Innes, M. J. S., and Rottenberg, J. A., 1960, The search for fossil meteorite craters: Current Sci., v. 29, p. 205-218, 249-262.

Berard, Jean, 1962, Summary geological investigation of the area bordering Manicouagan and Mouchalagane lakes, Saguenay County: Quebec Dept. Nat. Resources Prelim. Rept. no. 489, 14 p.

Carr, M. H., 1964, The geology of the Timocharis quadrangle: U. S. Geol. Survey, Astrogeologic studies annual progress report, August 25, 1962 to July 1, 1963, pt. A, p. 9-22.

Chao, E. C. T., Shoemaker, E. M., and Madsen, B. M., 1960, First natural occurrence of coesite: Science, v. 132, no. 3421, p. 220-222.

Currie, K. L., 1964, On the origin of some 'recent' craters on the Canadian Shield: Meteoritics, v. 2, no. 2, p. 93-110.

Danes, Z. F., 1962, Isostatic compensation of lunar craters: Tacoma, Wash., Univ. of Puget Sound Research Inst. RIR-GP-62-1, 11 p.

Dietz, R. S., 1961, Vredefort Ring structure--meteorite impact scar?: Jour. Geology, v. 69, p. 499-516.

Eggleton, R. E., and Marshall, C. H., 1962, Pre-Imbrian history of the lunar surface [abs.]: Am. Geophys. Union Trans., v. 43, no. 4, p. 464.

Fielder, Gilbert, 1961, Structure of the Moon's surface: London, Pergamon Press, 266 p.

Gilbert, 1893, The Moon's face, a study of the origin of its features: Philos. Soc. Washington Bull., v. 12, p. 241-292.

Gilvarry, J. J., 1964, Evidence for the pristine presence of a lunar hydrosphere: Astron. Soc. Pacific Pub., v. 76, no. 451, p. 245-253.

Kozyrev, N. A., 1962, Physical observations of the lunar surface, in Kopal, Zdenek, ed., Physics and astronomy of the Moon: New York, Academic Press, p. 361-383.

Kranck, S. H., and Sinclair, G. W., 1963, Clearwater Lake, New Quebec: Canada Geol. Survey Bull. 100, 25 p.

Kuiper, G. P., ed., 1960, Photographic lunar atlas: Chicago, Univ. of Chicago Press.

Milton, D. J., and De Carli, P. S., 1963, Maskelynite--Formation by explosive shock: Science, v. 140, no. 3567, p. 670-671.

Nininger, H. H., 1953, Symmetries and asymmetries in Barringer Crater: Earth Sci. Digest, v.7, no. 1, p. 17-19.

Rose, E. P., 1954, Manicouagan Lake-Mushalagan Lake area, Quebec: Canada Geol. Survey Prelim. Map 55-2.

Shoemaker, E. M., 1957, Primary structures of maar ruins and their bearing on the origin of Kilbourne Hole and Zuni Salt Lake, New Mexico [abs.]: Geol. Soc. America Bull., v. 68, no. 12, pt. 2, p. 1846.

Shoemaker, E. M., 1962, Interpretation of lunar craters, in Kopal, Zdenek, ed., Physics and astronomy of the Moon: New York, Academic Press, p. 283-359.

Shoemaker, E. M., 1963, Impact mechanics at Meteor Crater, Arizona, in Middlehurst, B. M., and Kuiper, G. P., eds., The Moon, meteorites and comets--The solar system, vol. IV: Chicago, Univ. of Chicago Press, p. 301-336.

Shoemaker, E. M., and Chao, E. T. C., 1960, New evidence for the impact origin of the Ries Basin, Bavaria, Germany: Jour. Geophys. Research, v. 66, no. 10, p. 3371-3378.

Shoemaker, E. M., and Hackman, R. J., 1962, Stratigraphic basis for a lunar time scale, in Kopal, Zdenek, and Mikhailov, Z. K., eds., The Moon--Symposium no. 14 of the International Astronomical Union: New York, Academic Press, p. 289-300.

Suess, Edward, 1909, The face of the Earth, vol. IV, translated from the German: Oxford, Clarendon Press, 673 p.

Titley, S. R., 1964, A summary of the geology of the Mare Humorum quadrangle of the Moon: U. S. Geol. Survey, Astrogeologic studies annual progress report, August 25, 1962 to July 1, 1963, pt. A, p. 64-73.

Titley, S. R., McCauley, J. F., and Marshall, C. H., 1964, Preliminary geologic map of the Mare Humorum quadrangle: U. S. Geol. Survey, Astrogeologic studies annual progress report, August 25, 1962 to July 1, 1963, pt. A, Suppl.